THE UNIVERSITY OF TEXAS AT AUSTIN
CENTER FOR TRANSPORTATION RESEARCH

TECHNICAL REPORT 0-6854-1
TxDOT PROJECT NUMBER 0-6854

Evaluating the Use of Nanomaterials to Enhance Properties of Asphalt Binders and Mixtures

Center for Transportation Research
Angelo Filonzi
Indu Venu Sabaraya
Ramez Hajj
Dipesh Das
Dr. Navid B. Saleh
Dr. Amit Bhasin

The University of Texas Rio Grande Valley
Dr. Enad Mahmoud

February 2017; Published September 2018

http://library.ctr.utexas.edu/ctr-publications/0-6854-1.pdf

Technical Report Documentation Page

1. Report No. FHWA/TX-17/0-6854-1	2. Government Accession No.	3. Recipient's Catalog No.
4. Title and Subtitle Evaluating the Use of Nanomaterials to Enhance Properties of Asphalt Binders and Mixtures (FHWA 0-6854-1)		5. Report Date February 2017; Published September 2018 6. Performing Organization Code
7. Author(s) CTR: Angelo Filonzi, Indu Venu Sabaraya, Ramez Hajj, Dipesh Das, Dr. Navid B. Saleh, Dr. Amit Bhasin The University of Texas Rio Grande Valley: Dr. Enad Mahmoud		8. Performing Organization Report No. 0-6854-1
9. Performing Organization Name and Address Center for Transportation Research The University of Texas at Austin 1616 Guadalupe St., Suite 4.202 Austin, TX 78701		10. Work Unit No. (TRAIS) 11. Contract or Grant No. 0-6854
12. Sponsoring Agency Name and Address Texas Department of Transportation Research and Technology Implementation Office P.O. Box 5080 Austin, TX 78763-5080		13. Type of Report and Period Covered Technical Report February 2015–February 2017 14. Sponsoring Agency Code
15. Supplementary Notes Project performed in cooperation with the Texas Department of Transportation and the Federal Highway Administration.		

16. Abstract

Traditional polymer modified binders are typically used to achieve a target performance grade (PG) and also to enhance resistance of the binder to distresses such as rutting, fatigue cracking, and low-temperature cracking. Conventional modifiers used with asphalt binders are often expensive and are not very effective to improve the low-temperature properties. Recent advances in nanotechnology have allowed for development of novel materials that can be tailored to deliver improvements in both high and low-temperature properties of the modified composite. Several existing studies have shown an improvement in the high-temperature properties of asphalt binders due to the addition of nanomaterials. The main objectives of this study were to evaluate a number of different nanomaterials in terms of their ability to (i) disperse effectively in the asphalt binder at a nanometer length scale (as opposed to forming micrometer sized or larger agglomerates), (ii) provide beneficial effects in terms of high-, intermediate-, and low-temperature properties (or at least benefits in a certain temperature range without compromising the properties in other ranges), and (iii) provide a cost-effective solution to modify asphalt binders.

Initially the study was focused on the use of carbon nanotubes. However, owing to the cost of these nanomaterials and based on a review of the literature, the study was expanded to include other nanomaterials. These were nanosilica, nanoclay, nanoalumina, and nanoglass. In an effort to improve dispersion, nanosilica was also surface functionalized using two different agents. Several techniques were used to evaluate the mixing conditions required to fully disperse nanomaterials as well as assess the extent of dispersion of these nanomaterials. Direct observations using SEM, AFM, and mechanical tests, complemented by indirect observations in reference solvents, show that in most cases nanomaterials do not disperse as nanometer sized particles but rather form agglomerates that are several micrometers in size. Under such circumstances, the benefits of using nanomaterials are rather limited. Amongst the nanomaterials used in this study, nanoglass was the only material that had maximum dispersion approaching a nanometer length scale, was cost-effective, and demonstrated improvement in mechanical properties as observed using the binder, mortar, and mixture tests. This study also presented procedures to rapidly evaluate whether dispersion can be achieved by the nanomaterials in an asphalt binder as a screening tool before subscribing to the use of such materials for material property enhancement.

17. Key Words	18. Distribution Statement
nanomaterials, polymer modified binder, nanosilica, nanoclay, nanoalumina, nanoglass, carbon nanotubes	No restrictions. This document is available to the public through the National Technical Information Service, Springfield, Virginia 22161; www.ntis.gov.

19. Security Classif. (of report)	20. Security Classif. (of this page)	21. No. of pages	22. Price
Unclassified	Unclassified	126	

Form DOT F 1700.7 (8-72) Reproduction of completed page authorized

Center for Transportation Research
The University of Texas at Austin
3925 W. Braker Lane
Austin, TX 78759

http://ctr.utexas.edu/

THE UNIVERSITY OF TEXAS AT AUSTIN
CENTER FOR TRANSPORTATION RESEARCH

Evaluating the Use of Nanomaterials to Enhance Properties of Asphalt Binders and Mixtures

Center for Transportation Research
Angelo Filonzi
Indu Venu Sabaraya
Ramez Hajj
Dipesh Das
Dr. Navid B. Saleh
Dr. Amit Bhasin

The University of Texas Rio Grande Valley
Dr. Enad Mahmoud

CTR Technical Report:	0-6854-1
Report Date:	February 2017; Published September 2018
Project:	0-6854
Project Title:	Engineering the Properties of Asphalt Mixtures Using Carbon Nanotubes
Sponsoring Agency:	Texas Department of Transportation
Performing Agency:	Center for Transportation Research at The University of Texas at Austin

Project performed in cooperation with the Texas Department of Transportation and the Federal Highway Administration.

Disclaimers

Author's Disclaimer: The contents of this report reflect the views of the authors, who are responsible for the facts and the accuracy of the data presented herein. The contents do not necessarily reflect the official view or policies of the Federal Highway Administration or the Texas Department of Transportation (TxDOT). This report does not constitute a standard, specification, or regulation.

Patent Disclaimer: There was no invention or discovery conceived or first actually reduced to practice in the course of or under this contract, including any art, method, process, machine manufacture, design or composition of matter, or any new useful improvement thereof, or any variety of plant, which is or may be patentable under the patent laws of the United States of America or any foreign country.

Engineering Disclaimer

NOT INTENDED FOR CONSTRUCTION, BIDDING, OR PERMIT PURPOSES.

Project Engineer: Navid Saleh
P. E. Designation: Research Supervisor

Acknowledgments

The authors express appreciation to the TxDOT Project Director, Wade Odell, and members of the Project Monitoring Committee. The authors would also like to acknowledge the university students and staff who assisted in this project.

Products

Product P1, Learning Materials to Promote Use of CNT Modified Binders, is provided as an appendix (page 95).

EXECUTIVE SUMMARY

The main objectives of this study were to evaluate a number of different nanomaterials in terms of their ability to (i) disperse effectively in the asphalt binder at a nanometer length scale (as opposed to forming micrometer sized agglomerates), (ii) provide beneficial effects in terms of high-, intermediate-, and low- temperature properties (or at least benefits in a certain temperature range without compromising the properties in other ranges), and (iii) provide a cost-effective solution to modify asphalt binders. The nanomaterials included in this study were (i) nanosilica, (ii) nanoclay, (iii) nanoalumina, and (iv) nanoglass. In addition, two surface modified variations of nanosilica were also prepared with two different chemical compounds (Tetraethyl orthosilicate (TEOS) and Trimethoxymethylsilane (TMMS)): (i) TEOS-nanosilica and (ii) TMMS-nanosilica.

The first Task of this project was to conduct a thorough review of the literature to determine the current knowledge related to the use of nanomaterials in asphalt binders. The key findings from this review were as follows:

- Most studies showed improvement in the high-temperature properties of asphalt binders modified using nanomaterials. However, it is unclear whether the intermediate- or low-temperature properties remained the same or were compromised due to such modifications.
- There was a lack of information in the existing literature about the dispersion of nanomaterials in asphalt binders. In other words, it was unclear whether the nanomaterials were acting as nanometer sized particles creating local strengthening or as micrometer sized agglomerates, in which case such particles were acting akin to active or inert fillers.
- The literature review was also used to identify the most common nanomaterials experimented for use with asphalt binders and the typical ranges of concentrations for these nanomaterials.
- Finally, the literature review was also used to identify the physicochemical nature of the asphalt binders and solvents at room temperatures that can be used to study dispersion of nanomaterials under idealized conditions.

Tasks 2 and 3 of this project focused on identifying the most effective set of dispersants (medium to carry and distribute the nanomaterials) and/or functionality that will result in effective dispersion of nanomaterials in the asphalt binder as well as the extent of dispersion achieved in the asphalt binder. Task 2 considered the use of flux oil, kerosene, and water (via foamed asphalt production) as potential mediums or carriers to initially dis-

perse nanomaterials in the form of a concentrate, which could then be added to the asphalt binder to achieve effective dispersion. However, each one of these three mediums were found not to be feasible for the given nanomaterials and typical target concentrations. The most effective means of adding and dispersing nanomaterials in asphalt binders was determined to be direct mixing using a high-shear mixer. The extent of dispersion was assessed through a combination of mechanical performance tests, atomic force microscopy (AFM), and scanning electron microscopy (SEM) with samples of modified asphalt binders after different duration of mixing. However, the dark color of the binder and poor dispersion made it challenging to adequately evaluate the extent of dispersion of the nanomaterials in the binder. Finally, the nanomaterials were dispersed in solvents that represent a similar chemical environment as the asphalt binder. These solvents have a very low viscosity at room temperatures. State of dispersion of the nanomaterials in the solvents was analyzed with a dynamic light scattering apparatus, which evaluated the range of hydrodynamic radii over time for each of the samples. Results show that with a couple of exceptions, most nanomaterials formed agglomerates that were several micrometers in size, even under such idealized conditions.

Tasks 4 and 5 evaluated the performance characteristics of asphalt binders, mortars, and mixtures modified using different nanomaterials, i.e., the most promising candidates from binder testing were used for evaluation with mortars, and the most promising of these were validated with full asphalt mixture testing.

The analysis showed that, binders modified using nanoglass exhibited the most significant improvement in the high-temperature properties as evaluated using the $G^*/\sin\delta$ parameter under unaged and short-term aged conditions as well as the J_{nr} parameter from the multiple stress creep recovery test (MSCR). Specifically, while other nanomaterials achieved a high-temperature grade change of 1-2 °C, the use of nanoglass achieved a high-temperature grade change of 7-9 °C. A poker chip test was used to evaluate the tensile strength of the unmodified and nanomaterial modified asphalt binder. Results showed that nanoalumina and nanoglass had the most substantial improvement (40 and 80% improvement for unaged condition, respectively) in the tensile strength of the asphalt binders as evaluted at intermediate temperatures. An evaluation of the binder properties at low-temperatures using the bending beam rheometer (BBR) showed that most of the nanomaterials had minimal effects on the low temperature performance of the asphalt binders. Some increased the magnitude of the low temperature true grade by less than 2 °C, while others actually caused a decrease in such gradation. Specifically, nanoglass did not cause

any problem with regards to low temperature performance, although its observed benefits were not noteworthy. Surface energy theory and measurements were employed to assess the influence of the nanomaterials on the moisture damage resistance of moidified binders with several different types of aggregates. Results showed that in many cases addition of nanomaterials made the binders slightly more moisture susceptible compared to the control binders, although the overall reduction was not below the acceptable thresholds established in previous studies. Finally, based on a review of mortar and mixture performance (rutting and cracking), it was observed that nanoglass was the most promising candidate in terms of improving mixture performance.

TABLE OF CONTENTS

LIST OF FIGURES

LIST OF TABLES

CHAPTER 1. INTRODUCTION

1.1 INTRODUCTION

Asphalt mixture is the most commonly used material for pavement construction in the United States, where nearly 94% of the roadways in the country are paved with this material. Asphalt mixtures typically comprise 90 to 95% mineral aggregates "glued" together by the asphalt binder. The mechanical and engineering properties of the asphalt binder dictate the properties and performance of the mixtures. The durability of asphalt mixtures and resistance to distresses such as rutting, fatigue cracking, and low-temperature cracking is directly dependent on the properties of the asphalt binder. Particularly, the asphalt binder has a very important role in resisting distresses such as fatigue and thermal cracking.

Asphalt binders are produced directly from the refining of crude oil. In most cases the straight run asphalt binders do not meet the market demand for performance grade (PG) requirements for specific climatic and/or traffic conditions. These binders are further modified by cross-blending with other binders and/or modifying them using polymers (elastomers or plastomers) or chemical additives. Traditional polymer modified binders are typically used to achieve a target performance grade (PG) and also to enhance resistance of the binder to distresses such as rutting, fatigue cracking, and low-temperature cracking. Conventional modifiers used with asphalt binders are often expensive and in many cases these are not very effective to improve the low-temperature properties.

Recent advances in nanotechnology have allowed for development of novel materials that can be tailored to deliver improvements in both high and low-temperature properties of the modified asphalt. Asphalt properties can be improved by modifying microstructures of the binder where nano-modified binder can potentially offer significant improvement over the non-modified or conventionally modified binder properties.

Most binders used today in the state of Texas are modified using elastomers or plastomers. The cost of polymer-modified binders is typically higher than the cost of a straight-run or unmodified binders. This section presents a summary of a comprehensive literature review that was conducted with the objective of finding low cost nanomaterials that can effectively improve overall performance characteristics of the asphalt binder (i.e., resistance to fatigue and low-temperature cracking), and eventually be used to produce asphalt mixtures with significantly enhanced performance characteristics and durability. This section presents a summary of the use of nanomaterials in the construction industry as well as

in asphalt, their associated costs, gaps, and shortcomings in recent nano-modified asphalt binder research and a plan to overcome these problems.

1.2 NANOMATERIALS IN CONSTRUCTION

Engineered nanomaterials (ENMs), i.e., materials with one dimension in the size range of 1 to 100 nm, with unique properties are considered to be valuable in the construction industry as strength enhancers (Sobolev et al., 2006), durable additives, corrosion control (Ge and Gao, 2008), and crack prevention materials. ENMs have displayed a wide array of such properties and are used in many applications that include: antimicrobial coatings (Liu et al., 2008) with self-cleaning (Zhang et al., 2006) properties, photocatalytic abilities (Liu et al., 2008; Zhang et al., 2006) for environmental cleanup, energy-producing coated surfaces (Pillai et al., 2007), etc., and hence have been used as surface additives in the construction industry (Lee et al., 2010). The primary focus of capitalizing on these nano-material properties has been performance enhancement while reducing carbon footprint.

ENMs' inherent surface area to volume advantage, ability to tailor chemical functionalities, and unique photocatalytic and sorptive properties have made these attractive for use in construction industries. Nano-scale silica (SiO_2) (Jo et al., 2007), iron oxides (Fe_2O_3) (Nazari et al., 2010c), titania (TiO_2) (Nazari, 2011), alumina (Al_2O_3) (Nazari et al., 2010d), and lime ($CaCO_3$) (Liu et al., 2012) show effectiveness as compressive and flexural strength enhancers. Carbonaceous materials such as carbon nanotubes (CNTs) (Ma et al., 2009) and nanofibers (Gao et al., 2009) are used to increase durability, tensile strength, toughness, etc. These nano-additives' advantages emanate from inherent strength properties and enhanced chemical bonding abilities with construction materials' chemical moieties. The antimicrobial (Liu et al., 2008), greenhouse gas conversion (Kemp et al., 2013), and self cleaning (Zhang et al., 2006) properties of ENMs on the other hand enable their use in coatings for constructed surfaces. Nano-TiO_2's electron transfer abilities (Crudden et al., 2011) enable their use as antimicrobial coatings via photocatalysis. Nano-TiO_2, nano-CdS and carbon naopowders (Cao et al., 2011) are also being considered as greenhouse gas converters. Tables 1.1 and 1.2 show use of carbon based and metallic nanomaterials used in the construction industry and their potential property enhancement capabilities.

1.3 NANOMATERIALS IN ASPHALT BINDER

Research on the incorporation of nanomaterials in asphalt binders and mixtures has not been as extensive as those for cementitious materials; however, a small body of work in this area suggests that nanomaterials can be used to enhance the mechanical properties and resistance of asphalt binders to different distresses. Various asphalt properties have been tested upon ENM incorporation. The most important of those are adhesion, ductility, viscosity, friction, moisture susceptibility, temperature sensitivity, oxidation resistance, aging resistance, and subsequent rutting, and cracking resistance. This section presents a brief summary from the limited literature that is available on the use of nanomaterials with asphalt binders.

CNTs are the most researched nanomaterials for asphalt property enhancement. Incorporation of 1.5% by weight of CNTs:binder has been reported to enhance the adhesive properties of the asphalt binder than that of poly(styrene-butadiene-styrene) or SBS modified binders (Al-Adham and Arifuzzaman, 2014). The same amount of CNTs have also been reported to increase failure temperature, complex modulus, and elastic modulus and to improve rutting resistance of the short-term aged or rolling thin film oven (RTFO) binders (Xiao et al., 2010). Sub-nano-sized hydrated lime (SNHL) has been reported to improve tensile strength of asphalt by 8 to 10% for SNHL dosage of 20% by weight of the asphalt binder (Cheng et al., 2011). 5% by weight of nano hydrated lime (NHL) has also been reported to be improving asphalt rheological properties (Diab et al., 2013). Improved rheological properties, stiffness, and ageing resistance have been reported when 7% weight of nanoclay was added to the binder (Jahromi and Khodaii, 2009). In another article, incorporation of 4% weight of nanoclay have shown to increase binder shear moduli and direct tension moduli (You et al., 2011). A 4% weight of nanosilica:binder has been reported to enhance anti-aging property and rutting and fatigue cracking performance as well as to significantly improve the dynamic modulus, flow number, and rutting resistance of asphalt mixtures (Yao et al., 2013b).

A few shortcomings that were identified from these limited studies in the area of nanomaterials and asphalt binders are: (i) very little attention was paid to cost of the modified material versus the expected increase in performance life, (ii) optimizing the additive amount by improving dispersion was not considered, and (iii) in most cases the focus was on rutting resistance and not much on cracking resistance and even less so on the resistance to low-temperature cracking. It must be emphasized that the rutting resistance of the asphalt

mixture is related to both the binder properties as well as to the aggregate type and gradation. On the other hand, resistance to cracking (fatigue and low-temperature) is mostly dependent on the properties of the binder. Therefore, the benefits of binder modifications can be maximized by focusing on these factors.

1.4 COST OF NANOMATERIALS

For promoting commercial use of nanomaterials to modify binders, it is essential to take cost of these nanomaterials into account. If the nanomaterial dosage required to improve the binder properties significantly increases the cost of asphalt mixture, commercial application of these modifications will not be feasible. Tables 1.3, 1.4, and 1.5 give costs of different types of nanomaterials that can be used in asphalt binders. Table 1.3 compiles the cost of different types of CNTs as a function of their diameter and purity. Table 1.4 is a compilation of industrial grade CNT costs. The industrial grade CNTs are cheaper and less pure in quality. Table 1.5 presents cost of other nanomaterials that are used in the construction industry and can potentially be used in asphalt binders.

1.5 NANOMATERIAL DISPERSION IN ASPHALT

One of the major challenges of nanomaterial incorporation in materials relevant to the transportation industry is the difficulty in attaining a uniform dispersion of the added nanomaterial throughout the asphalt matrix (Khattak et al., 2012). Asphalt binder is a complex mixture of organic compounds. It becomes necessary to modify the surfaces of the nanomaterials based on inherent hydrophobicity or liophobicity of these molecules to distribute the nanomaterials evenly. Nanomaterials' parent inter-particle attraction forces including van der Waals dictates the extent of the uniformity within the matrix. The lack of uniform distribution of nanomaterials can lead to reduction of physico-chemical compatibility with the matrix. Without proper dispersion and attainment of interfacial adhesion between the nanomaterial and the matrix, the reinforcement of the matrix, i.e., in this case the asphalt binder, remains incomplete. High aggregation tendency of nanomaterials can cause material segregation. This can lead to formation of uneven microstructures, leaving spots for micro-crack initiation as well as microstructure distortion during aging (Fang et al., 2013). Controlling such degradation with uniform distribution of nanomaterials can enhance the compatibility, thermal stability, and anti-ageing properties of the binder mix. Several dispersion techniques have been reported in the literature for achieving a homogenous nano-

modified binder suspension. Asphalt binder is a viscous liquid even at typical (150 to 170 °C) transport and mixing temperatures. As an example, consider the viscosity of water at room temperature, which is approximately 0.001 Pa-s whereas, viscosity of a binder at mixing temperatures is about 150 times higher at 0.15 Pa-s. It is challenging to disperse nanomaterials directly into the binder even at mixing temperatures. To overcome this problem, one option that was reviewed was to disperse nanomaterials in another less viscous organic chemical. This dispersion can later be mixed with binder for a homogeneous incorporation of nanomaterials into the binder. For example, carbon nanofibers (CNFs) were sonicated in kerosene, used as a delivery vehicle to bitumen; such evenly dispersed CNFs improved viscoelastic and fatigue characteristics of the modified binder (Khattak et al., 2012). Further, nanoclay or nanosilica when modified with polymers, surfactants, or silane coupling agents to obtain an intercalated or exfoliated forms, have resulted in excellent rutting, fractures, and ageing resistance via crack bridging as well as preventing contacts of oxygen, water or organic solvents (You et al., 2011; Yao et al., 2013a, 2012). Similarly, nano-TiO2 coated with silane agents have shown to better disperse in bitumen providing enhanced ultra violet shielding effects (Liu et al., 2014). Recently, graphene oxides have been modified with anionic surfactants to provide organophilic groups to provide stronger adhesion to bitumen, resulted in better freeze-thawing resistance (Li and Zhang, 2015). However strength enhancement was not observed in such cases. In any case, the benefits of using a third medium (other than the binder and the nanomaterial) as a medium to facilitate dispersion must be carefully weighed against possible cost and safety issues. For example there is a cost component associated with the use of non-volatile dispersion agents such as paving flux oil. On the other hand, there is a safety concern with the use of dispersion mediums such as kerosene, which is highly combustible.

CNTs are the most researched nanomaterials for binder property enhancement. Achieving effective dispersion has been the primary area of concern. Dispersion of CNTs in binders is a challenging process due to their aggregation tendency. Strong van der Waals binding energies result in such aggregation propensity (Saleh et al., 2008, 2010). These strong forces originate from their polarizable extended -electron systems. When CNTs are added with a sufficiently high percentage to base asphalt binder, these can significantly affect rheological properties. CNTs provide enhancement of rutting resistance potential, resistance to thermal cracking and reduce susceptibility to oxidative aging. To ensure that CNTs are uniformly distributed in the matrix, these have to be effectively dispersed. Various methods have been employed to ensure effective dispersion of CNTs in asphalt matri-

ces.

Some studies (Santagata et al., 2012; Xiao et al., 2010) utilize a simple shear mixing technique to incorporate CNTs into the base bitumen, which is convenient in laboratory operations and is also easily scalable for hot mix asphalt plants. Features like low cost, simplicity and easy scalability makes this the most widely used approach to prepare mixtures. In this method, the CNTs are dispersed in the matrix using high shear and high temperatures of around 130 to 160 °C. Another method for dispersing CNTs in the asphalt matrix is the solution approach, with the use of ultrasonication (Kordkheili et al., 2015). Mechanical vibration generated by a sonicating probe transfers energy to the liquid medium and leads to the formation and collapse of microscopic bubbles (Zaib et al., 2012). This process creates shock waves, which disperses CNTs in the medium. Sonication time and energy are the two important parameters for this process. This will require external cooling to avoid the temperature increase during the sonication process. However, using high energy high shear mixing can exert tensile stress on the surface of the CNTs, which can result in the fracture of CNTs. Some studies have shown this to be relevant to sonication and confirmed breakage of CNTs during sonication (Gkikas et al., 2012; Huang and Terentjev, 2012).

To aid dispersion of the CNTs, surface treatment of these nanomaterials can be utilized. This process incorporates various functional moieties on the CNT surfaces. Acid etching (covalent) or surfactant modification (non-covalent), modify the compatibility of the CNTs with the binder (You et al., 2009). By using acid etching, CNT surfaces are modified by incorporation of functional groups on the surface. Functional groups like hydroxyl and carboxyl groups on CNT surfaces change the polarity of the CNTs and can result in alteration of binder interaction as compared to untreated CNTs. The electrostatic repulsion forces between the negatively charged functional groups can be utilized to disperse CNTs (Li et al., 2005). The use of surfactants in aqueous suspensions reduces the surface tension of water and uses the electrostatic/steric repulsions created by the polymeric surfactant molecules on the CNT surface to disperse the CNTs better. The surfactant type and concentration are important considerations (Metaxa et al., 2013). Composite approaches (e.g., sonication along with shear mixing) have also been undertaken (Khattak et al., 2012; Fakhim et al., 2015; Sun et al., 2014; Li et al., 2007; Han et al., 2009) to disperse nanomaterials in binders.

Table 1.1. Carbon based ENMs used in concrete

Material	Property enhancement tested	Reference
Multiwalled Carbon nanotubes	Mechanical durability; crack prevention; fluidity, Fracture prevention; tensile and compressive strength, self-healing concrete	Musso et al. (2009); Metaxa et al. (2009); Konsta-Gdoutos et al. (2010)
Graphene Oxide	Thermal Properties, durability, reduced early age thermal cracking	(Sedaghat et al., 2014)

1.6 SUMMARY

Nanomaterial incorporation in asphalt binders can potentially be revolutionary in terms of property enhancement and better recycling of asphalt. In spite of growing research in this sector, a facile way of homogenous nanomaterial incorporation in binder is yet to be achieved. Also, most of the studies have not taken the nanomaterial cost into account, which is the most important factor in practical use of the nano-modified binders. The focus of this research is to find a cost effective nanomaterial, which can effectively enhance the binder properties at low-temperature, improve recyclability, and can be incorporated homogenously into the binder to maximize the nanomaterial property in the matrix. Results and cost analysis indicated nanolime might be the best option for achieving the desired goals. However, upon completion of the first set of preliminary tests, all options were weighed in for the cost versus expected performance benefits. Finalist materials were discussed with the project monitoring committee before advancing to other tests for optimizing dosage and evaluating mixture performance.

Table 1.2. Metallic ENMs used in concrete

Material	Property enhancement tested	Reference
Nano SiO_2	Mechanical strength, scratch resistance, rapid formation of calcium-silica-hydrate (C-S-H) gel, refinement of pore structure and densification of interfacial transition zone, workability	Björnström et al. (2004); Quercia et al. (2012)
Nano Al_2O_3	Elastic modulus, compressive strength, initial mechanical strength	Nazari et al. (2010d); Li et al. (2006); Campillo et al. (2007); Nazari and Riahi (2011a)
Nano Fe_2O_3	Split tensile strength, flexural strength, decreased setting time	Nazari et al. (2010c,b)
Nano CuO	Acceleration of C-S-H gel formation, decreased compressive strength due to improper dispersion	Nazari and Riahi (2011c)
Nano ZrO_2	Split tensile strength, flexural strength, decreased setting time	Nazari et al. (2010a)
Nano ZnO_2	Flexural strength, improved C-S-H gel formation	Nazari and Riahi (2011b)
Nano TiO_2	Early C-S-H hydration rate, self-cleansing ability	Jayapalan et al. (2009)

Table 1.3. Cost of different types of multiwalled CNTs in USD

MWNT Prices	Multiwalled Carbon Nanotubes Prices (in Grams and Kilograms)						
	1 g	10 g	25 g	50 g	100 g	500 g	10 KG
Multi Walled Nanotubes 99wt% <20nm Prices	25	250	500	650	900	1500	call
Multi Walled Nanotubes 95wt% <8nm OD Prices	15	125	200	300	450	1,400	19,000
Multi Walled Nanotubes 95wt% 8-15nm OD Prices	10	75	150	250	400	1,250	17,000
Multi Walled Nanotubes 95wt% 10-20nm OD Prices	10	75	150	250	400	1,200	16,750
Multi Walled Nanotubes 95wt% 20-30nm OD Prices	8	60	100	175	210	550	7,000
Multi Walled Nanotubes 95wt% 30-50nm OD Prices	5	45	95	150	190	450	6,000
Multi Walled Nanotubes 95wt% >50nm OD Prices	5	45	95	150	190	450	6,000

Table 1.4. Cost of Industrial grade multiwalled CNTs

Industrial Grade Purified 90wt% Multiwalled Carbon Nanotubes Prices	1 KG	10 KGS	100 KGs	500 KGs	TON
Multiwalled Nanotubes 90wt% 10nm OD Prices SKU-030501	$450	$4,250	$38,500	$150,000	NA
Multiwalled Nanotubes 90wt% 10-30nm OD Prices SKU-030501	$390	$3,750	$25,000	$75,000	$125,000
Multiwalled Nanotubes 90wt% 20-40nm OD Prices SKU-030502	$300	$2,750	$20,000	$65,000	$95,000
Multiwalled Nanotubes 90wt% OH 10-30nm OD Prices SKU-03050201	$410	$3,950	$30,000	$80,000	$145,000
Multiwalled Nanotubes 90wt% OH 20-40nm OD Prices SKU-03050202	$400	$3,750	$25,000	$75,000	$125,000
Multiwalled Nanotubes 90wt% COOH 10-30nm ODPrices SKU-03050301	$410	$3,950	$30,000	$80,000	$145,000
Multiwalled Nanotubes 20-40nm OD Prices SKU-03050302	$400	$3,750	$25,000	$75,000	$125,000

Table 1.5. Cost of other nanomaterials

Nano material	Particle size (nm)	Length (micrometer)	SSA (m2/g)	Purity (%)	Price / 100g (US $)	Vendor
Carbon Nanofibers	200-600 (O.D.)	5-50	18	95	3000	US-Research Nanomaterials
SiO_2	15-20	–	170-200	99.5	58	US-Research Nanomaterials
Alpha-Al_2O_3	80	–	15	99+	55	US-Research Nanomaterials
TiO_2	10-25	–	200-240	>99	58	US-Research Nanomaterials
ZrO_2	40	–	20-40	>99	75	US-Research Nanomaterials
ZnO	18	–	40-70	>99	105	US-Research Nanomaterials
Fe_2O_3	30	–	20-60	>99.5	159	US-Research Nanomaterials
CuO	40	–	20	99	69	US-Research Nanomaterials

CHAPTER 2. SELECTION OF NANOMATERIALS AND CHOICE OF DISPERSING AGENTS

2.1 SCOPE

Nanomaterials have a very high specific surface area. Depending on the surface characteristics, these materials may not effectively disperse within the medium (i.e., asphalt binder in this case) but can form larger clusters that may be several micrometers in size. In such cases, these nanomaterials would act more as a traditional filler (aggregates finer than 75 micrometer in size) rather than an active modifier. Therefore it is important to ensure that the nanomaterials selected for use with asphalt binders can be effectively dispersed within the medium. In the context of this study, the term "effective dispersion" implies that the nanomaterial (i) does not form agglomerates that are several micrometers in size after mixing and blending with the binder, i.e., the maximum particle size of the nanomaterial is of the order of 5 µm to 10 µm or less.

The objectives of Tasks 2 and 3 of this study were to:

- Identify the most effective set of dispersants (medium to carry and distribute the nanomaterials) and/or functionality that will result in effective dispersion of nanomaterials in the asphalt binder **(TASK 2)**.
- Characterize the extent of dispersion achieved in the asphalt binder **(TASK 3)**.

This Chapter presents the work that was conducted to achieve the aforementioned objectives.

2.2 SELECTION OF NANOMATERIALS

Based on a review of the literature (discussed in the previous chapter), various nanomaterials were chosen as candidates for further evaluation. The initial primary objective of this project was to investigate carbon nanotubes (CNTs) as a nanomaterial modifier for asphalt binders. Because of the high price of carbon nanotubes ($450/kg), only a very small concentration of 0.1% by weight of the binder could be justified. Also, based on the inputs from the project monitoring committee, additional potentially lower cost nanomaterials were considered for evaluation in these tasks and in the remainder of the project. These nanomaterials were selected based on a review of the literature (Yao et al., 2013b; Jahromi and Khodaii, 2009). Four additional nanomaterials were selected, and each was evaluated

Table 2.1. Nanomaterials Added to Asphalt Binder

Nanomaterial	Low Percentage	High Percentage
Nanosilica	4%	6%
Nanoalumina	4%	6%
Nanoclay	2%	7%
Nanoglass	3%	6%

at two concentrations, the (higher and lower) concentrations that had been used in previous studies (Table 2.1).

The surface properties of the nanomaterials are critical in determining the performance and characteristics of these materials in their surrounding environment. Properties like electrostatic (from surface charge), steric (from polymeric surface coatings), and inherent van der Waals interactions determine the quality of dispersion in a nanoparticulate system. Based on preliminary results and costs, nanosilica was considered for further surface modification to enhance dispersion. The surface of nanosilica was chemically modified in order to achieve effective dispersion of the inorganic nanomaterials and to increase interfacial compatibility between the nanosilica and the asphalt binder. Organosilanes with epoxy or amino functional groups were utilized to enhance compatibility between the asphalt binder (matrix) and inorganic nanosilica surfaces (Basilissi et al., 2013). It was hypothesized that grafting organosilane coupling agents on the nanosilica surface can assist in improving the quality of dispersion of the nanosilica in the matrix, where the organic surface groups on these molecules can assist to favorably interact with the asphalt binder.

The functionalized silica particles were prepared using a modified Stober method. The chosen organosilanes, tetraethyl orthosilicate (TEOS) and trimethoxymethylsilane (TMMS), were separately added dropwise (2% by weight) to a mixture of nanosilica and methanol. This mixture was vigorously stirred overnight and the solvent mixture was subsequently evaporated to obtain a functionalized-silica product.

The two surface modified nanosilicas (TEOS- and TMMS-modified) were added to the list of nanomaterials. The final matrix of nanomaterials that were evaluted in this study are presented in Table 2.2.

Table 2.2. Final Matrix of Nanomaterials Added to Asphalt Binder

Nanomaterial	Low Percentage	High Percentage
Nanosilica	4%	6%
Nanoalumina	4%	6%
Nanoclay	2%	7%
Nanoglass	3%	6%
TEOS-modified Nanosilica	4%	N/A
TMMS-modified Nanosilica	4%	N/A

2.3 CHOICE OF DISPERSANT

As discussed earlier, one of the main challenges of using nanomaterials in asphalt binder is to properly disperse the nanoparticles throughout the binder. For this study, four dispersion mediums were considered: water, flux oil, kerosene, and direct dispersion of the nanoparticles in the binder. The following sections discuss the evaluation and disposition of each of these methods to deliver nanomaterials to the asphalt binder.

2.3.1 Water via foaming

One of the options to deliver the nanomaterials was to disperse the nanomaterials in water and then use this nanomaterial-water mix as a foaming agent to produce foamed asphalt binder. Note that foamed asphalt binder production is one of the most common methods of producing warm mix asphalt and is commonly used in the asphalt industry. In most cases, for the concentrations of nanomaterials that were being considered in this study, the water-nanoparticle concentrate would not properly flow, due to using almost, if not more than, as much nanomaterial as water in the solution. For example, the use of 5% nanomaterial by weight of asphalt binder would entail mixing the nanomaterial and water in a 62.5%-37.5% ratio by mass (for 3% water foamed asphalt). It would not be feasible to produce such a concentrate of nanomaterials in water and have it flow easily through the spray nozzles for the production of the foamed asphalt. For nanomaterials with very low concentrations (e.g., CNT used in 0.1% to 0.2% by weight of the binder), the use of the aforementioned method might be feasible. However, preliminary results have shown that the use of such low concentrations of CNT have no significant impact on the performance of the asphalt binder. For these reasons, the use of water as a dispersant (via the production of foamed asphalt) was ultimately discarded.

2.3.2 Flux oil

In order to ensure dispersion of nanoparticles in the asphalt binder, flux oil was also considered as a possible carrier or dispersant. The dispersion method involved mixing CNTs or other nanomaterials with flux oil, and then mixing that concentrate with asphalt binder in a high shear mixer for two hours. To serve as a basis for comparison, a composite of binder and flux oil alone (without any nanomaterial) was also mixed in the high shear mixer for two hours. The neat binder without any flux oil or nanomaterial was also used as a control for comparison purposes. The binder used was a PG 64-22 binder and the flux oil concentration was 10% by weight of the binder. Note that this percentage of flux oil was considered necessary to allow mixing other nanomaterials in concentrations of 5 to 10% by weight of the asphalt binder, which in turn would imply that naomaterial-flux oil concentrate would contain 30 to 50% by weight of the nanomaterial, which is a reasonable upper limit to produce such concentrations. The first nanomaterial used for this analysis was CNT with a target of 0.1% of the CNT by weight of the binder. Figure 2.1 shows a schematic of the materials tested for this purpose.

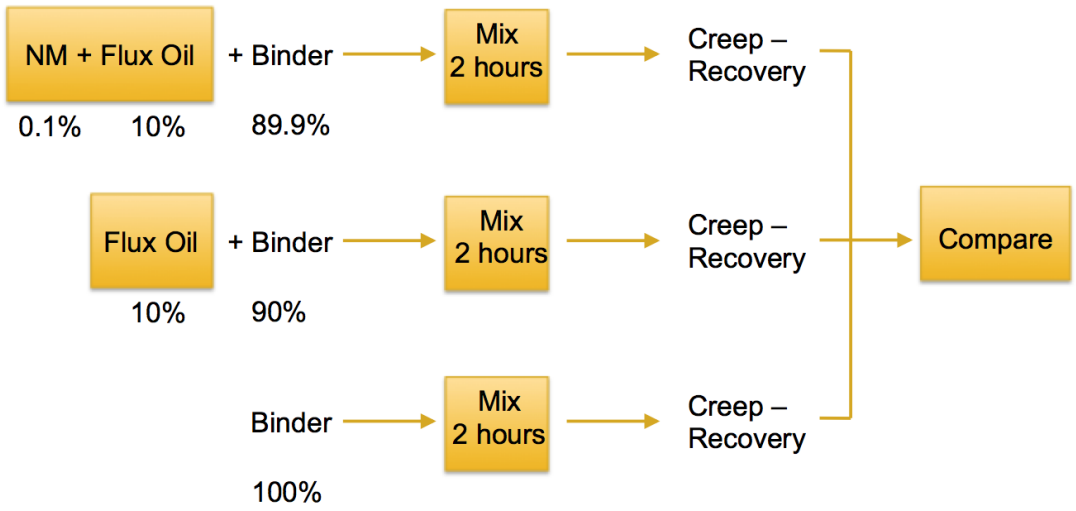

Figure 2.1. Schematic of Tests Performed to Determine Effects of Using Flux Oil as a Carrier or Dispersant

To evaluate the effects of using flux oil as a carrier or dispersant, the Multiple Stress Creep Recovery (MSCR) testing was performed on all three materials at a temperature of 64 °C. As expected, MSCR testing revealed that the binder had become less stiff upon the

addition of flux oil (Figure 2.2) and more prone to plastic deformation. The purpose of this testing was to establish the magnitude of such reduction in stiffness. As seen in the results, simply the addition of flux oil to the base binder (even at 10% by weight) increased the cumulative permanent strain by three times compared to the control binder. Moreover, the benefits of adding CNT to the binder via flux oil were negligible. The magnitude of softening of the binder was deemed unacceptable, so the use of a flux oil as a carrier was discarded. It is noted that different types and sources of flux oils will have a different impact on the binder performance. However, irrespective of the source and type, the flux oil selected to serve as a dispersant must have a similar (low) viscosity to enable dispersion and delivery of nanomaterials. Therefore, it is unlikely that the outcome would be different with different flux oils that are feasible candidates to serve as a dispersant.

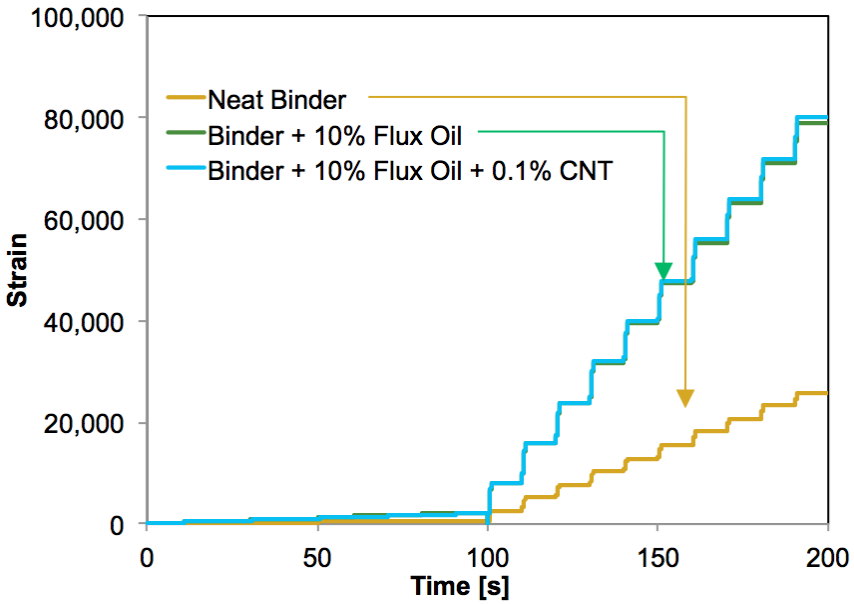

Figure 2.2. MSCR Results for Binder with and without Flux Oil

2.3.3 Kerosene

The third potential carrier or dispersant for the nanomaterials that was considered was kerosene. The choice of kerosene was based on: (i) its low viscosity at room temperature and consequently the ease with which nanomaterials could be dispersed in it at room temperatures and (ii) the low boiling point of kerosene which would make it possible to remove it from the binder-nanomaterial blend after dispersion. However, it was determined

that this method would not be suitable due to safety concerns. Specifically, kerosene has a low flash point (38 to 72 °C) and autoignition point (220 °C). Any mixing with asphalt binder will have to take place at temperatures higher than 150 °C, which is much higher than the flash point. The use of metal mixers and containers would risk the use of this carrier and approach to disperse nanomaterials in the asphalt binder. Therefore, kerosene was also ruled out as a potential carrier.

2.3.4 Direct mixing

As discussed above, flux oil, water, and kerosene were deemed unsuitable to safely serve as a medium to transport and disperse nanomaterials into the asphalt binder. Therefore, direct dispersion of the nanoparticles in the binder was deemed to be the most practical, cost effective, and safe approach. In this study, direct dispersion was achieved by blending the nanomaterials with the binder in the a high shear mixer at a temperature of 150 °C, and at 2400 rpm. At various time intervals, a sample of the binder/nanomaterial composite was taken so that the effects of dispersion for different duration of mixing time could be determined. The time intervals at which the material was sampled were as follows:

1. 15 minutes
2. 30 minutes
3. 1 hour
4. 2 hours
5. 3 hours

Figure 2.3 shows a schematic of this process. Four characterization methods were used to determine the effect of mixing time on blending. These methods are listed below and discussed in more detail in the following section.

1. Rheological Properties
2. Scanning Electron Microscopy (SEM)
3. Atomic Force Microscopy (AFM)
4. Dynamic Light Scattering (DLS)

2.4 DISPERSION OF NANOMATERIALS IN ASPHALT BINDER

2.4.1 Results based on rheology

Two rheological tests were performed in order to characterize the nanomaterial modified asphalt binder. The first test was a frequency-temperature sweep to construct the master

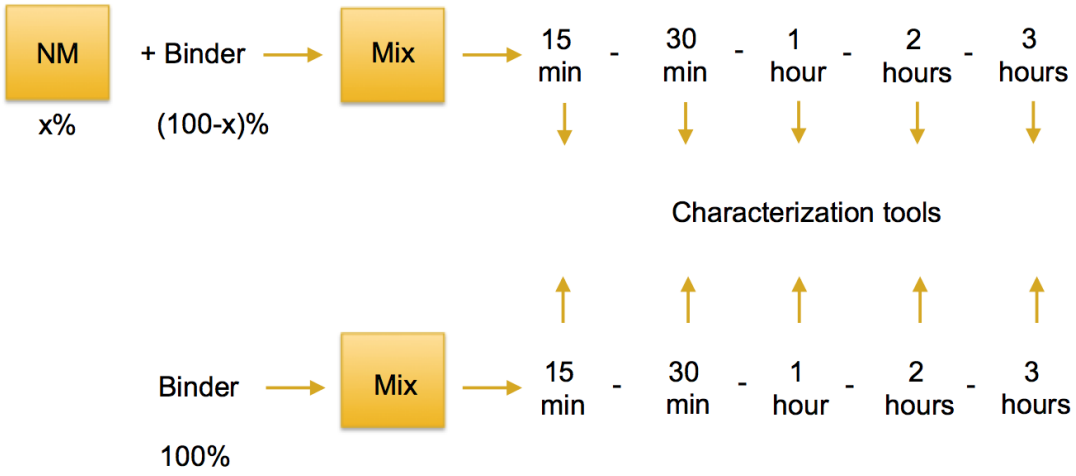

Figure 2.3. Schematic of Tests Performed to Determine Optimum Mixing Time

curve. Master curves represent the stiffness of the asphalt binder at different loading frequencies at a reference temperature. The range of frequencies used varied from 0.1 to 73 rad/s at a constant strain amplitude of 0.5%. The stiffness of the material is typically represented by a complex modulus (E^*) if the test is performed by using axial loads or by a complex shear modulus (G^*) if it is performed by using shear loads. For this study, the test was performed at three temperatures: 35 °C, 45 °C, and 55 °C, producing three curves relating loading frequency to complex shear modulus. By the time-temperature superposition principle, these curves can be shifted horizontally to align into one master curve at a specific temperature, referred to as the reference temperature. These lateral displacements or horizontal shifts correspond to the shift factors, which are specific to each temperature. Finally, the master curve was constructed at a reference temperature of 45 °C, the median of the three temperatures that was used for the test.

Figure 2.4 shows the master curves for the neat binder without any nanomaterial at each time interval. Figures 2.5, 2.6, 2.7, and 2.8 show the same curves for the binder modified with 4% nanosilica, 2% nanoclay, 4% nanoalumina, and 0.2% CNT, respectively. For the purpose of characterizing dispersion, only the lower concentration of nanomaterials were used at this time.

The second rheological test performed was the multiple stress creep and recovery (MSCR) test. The MSCR test is typically used to measure the elastic recovery and plastic deformation of an asphalt binder, both of which are related to its ability to resist permanent defor-

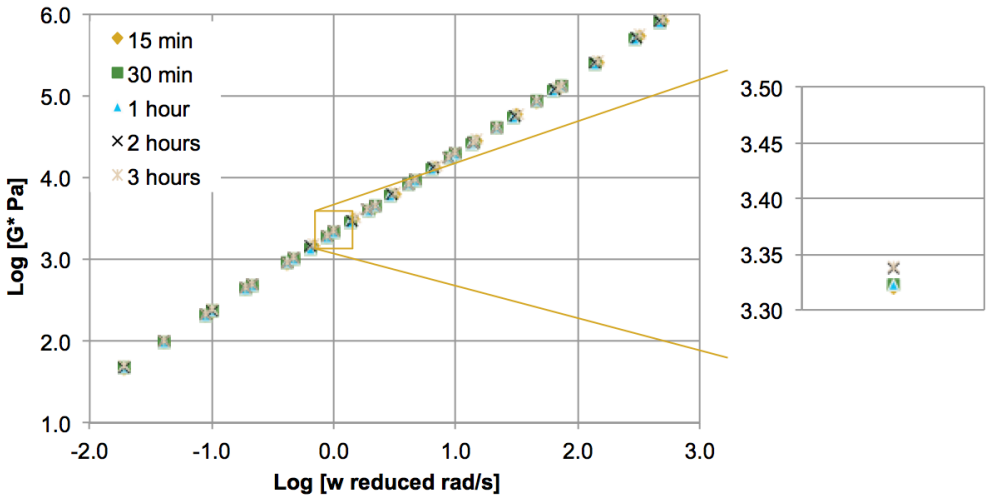

Figure 2.4. Master Curves For Neat Binder

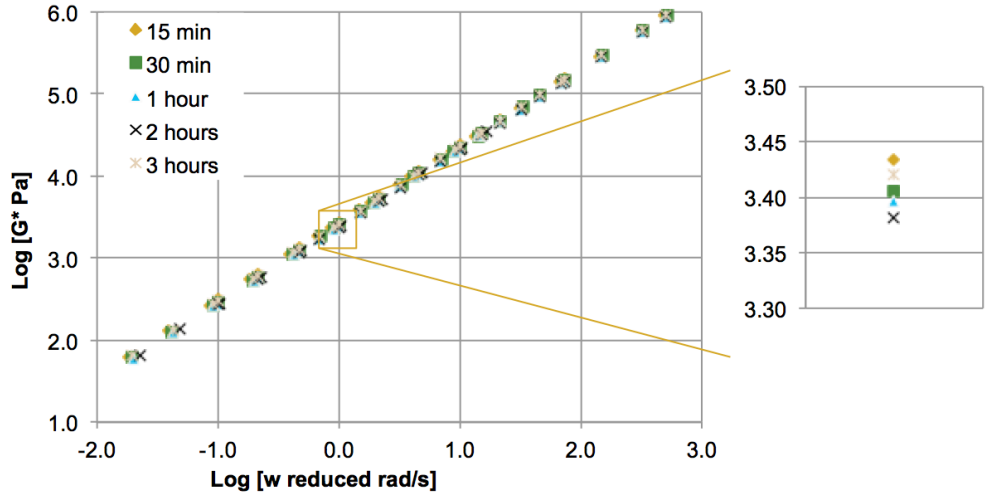

Figure 2.5. Master Curves For Binder + 4% Nanosilica

mation or rutting. The MSCR test consists of the successive application of load-recovery cycles on a sample of asphalt binder at two different stress levels. Thus, the asphalt binder's ability to recover part of the deformation caused by the applied stress is measured. Each cycle is performed over the course of 10 seconds in which a constant load is applied for 1 second followed by 9 seconds of recovery. A total of 20 cycles (load-recovery) are performed. The first 10 cycles are performed at a stress level of 0.1 kPa and the last 10 cycles at a stress level of 3.2 kPa. Within each load-recovery cycle, three significant deformations

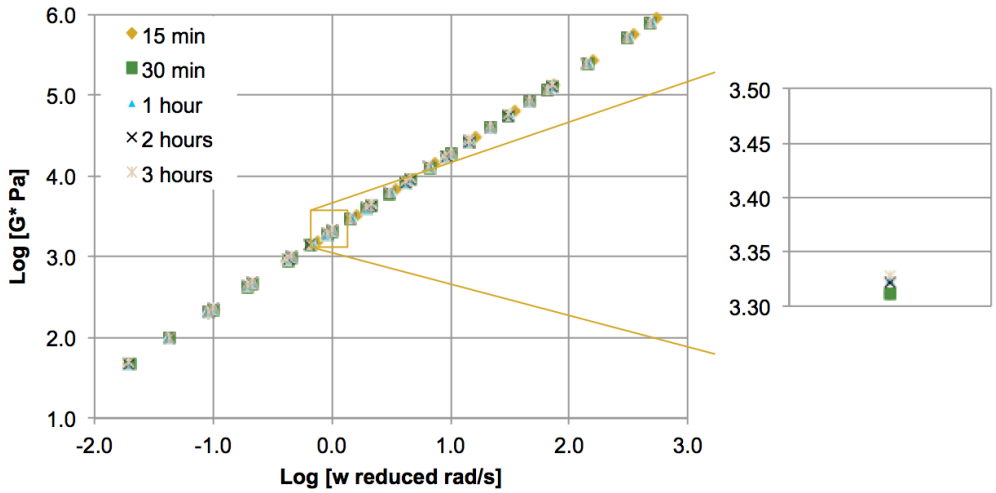

Figure 2.6. Master Curves For Binder + 2% Nanoclay

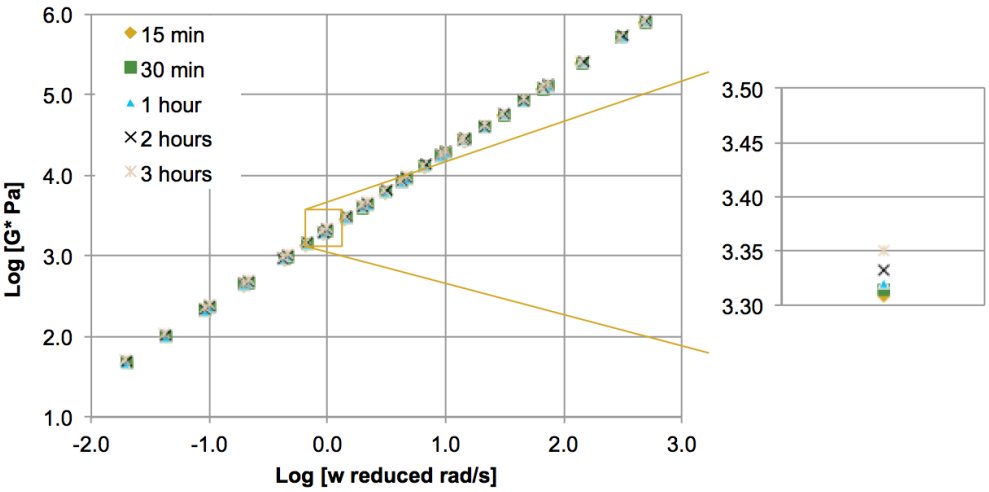

Figure 2.7. Master Curves For Binder + 4% Nanoalumina

are measured. Measurements are taken at the beginning of the load period (t = 0 seconds), at the end of the load period (t = 1 second), and at the end of the recovery period (t = 10 seconds). To characterize the properties of asphalt binders, two parameters are used. These parameters are the percent recovery ($R\%$) and the non-recoverable creep compliance (J_{nr}). The percent recovery is a measure of the deformation recovered during the rest period in each cycle. The non-recoverable creep compliance (J_{nr}) is defined as the permanent strain due to the application of the stress.

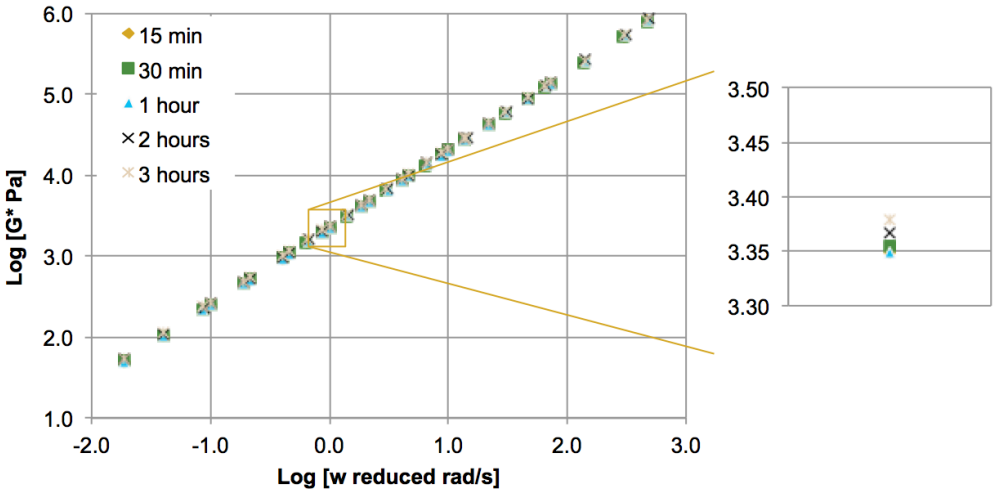

Figure 2.8. Master Curves For Binder + 0.2% CNT

Figure 2.9 shows the results from MSCR testing for the neat binder at a stress level of 0.1 kPa. Since the binder used for the test was unaged, only the lower stress level was considered. Figures 2.10, 2.11, 2.12, and 2.13 show the same results for binders modified with 4% nanosilica, 2% nanoclay, 4% nanoalumina, and 0.2% CNT, respectively.

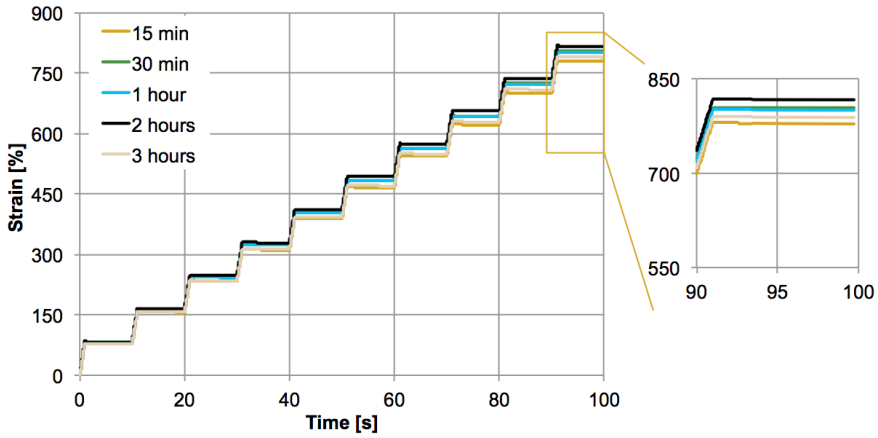

Figure 2.9. MSCR Results For Neat Binder

It must be emphasized here that the objective of these measurements was not to measure the rutting resistance or stiffness of the asphalt binder with and without any nanomaterials, but rather to investigate whether increased mixing time results in additional dispersion of the nanomaterial, which in turn reflects in terms of changes in observable mechanical

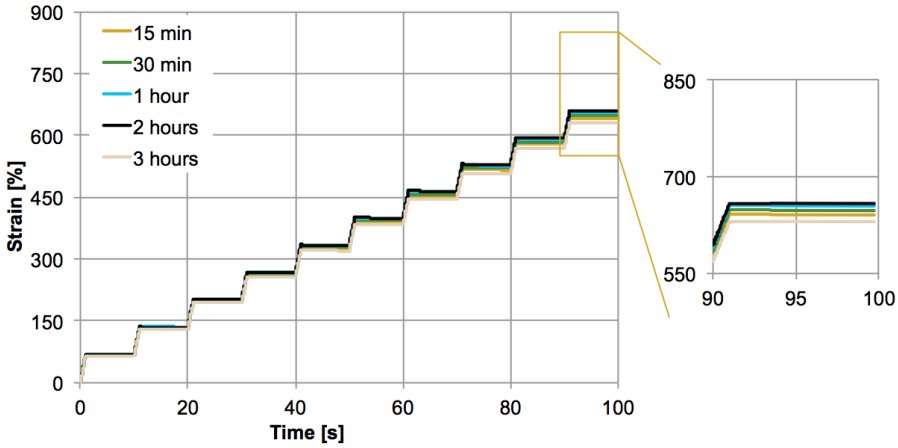

Figure 2.10. MSCR Results For Binder + 4% Nanosilica

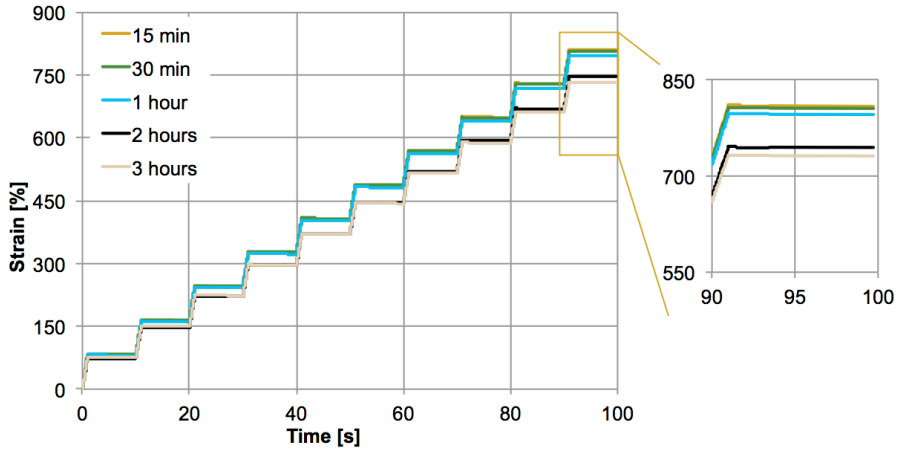

Figure 2.11. MSCR Results For Binder + 2% Nanoclay

properties. To this end, it was observed that in most cases, mixing beyond 2 hours did not result in any significant changes in the observable mechanical properties of the binder.

2.4.2 Results based on SEM

In order to evaluate the effects of mixing time of the nanomaterials with asphalt binder on the dispersion within the asphalt matrix, scanning electron microscopy (SEM) was also utilized as one of the tools. SEM provides high-resolution images at enhanced magnification, which can aid in observation of surface morphology and microstructure of the binder matrix.

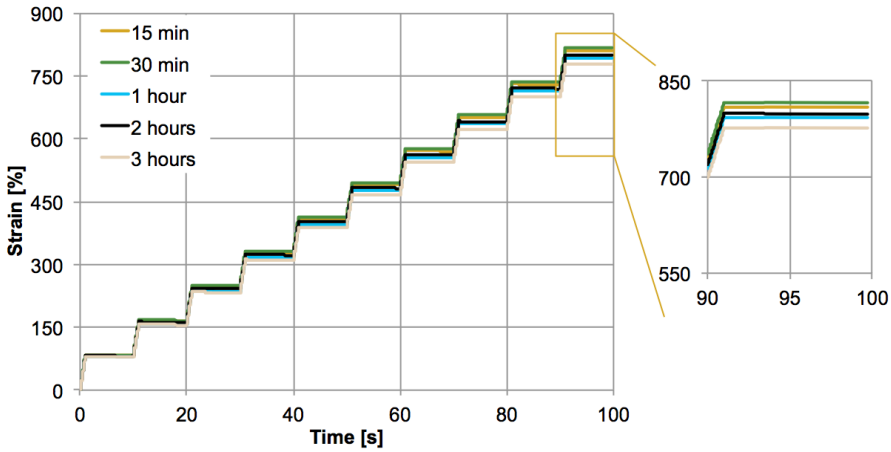

Figure 2.12. MSCR Results For Binder + 4% Nanoalumina

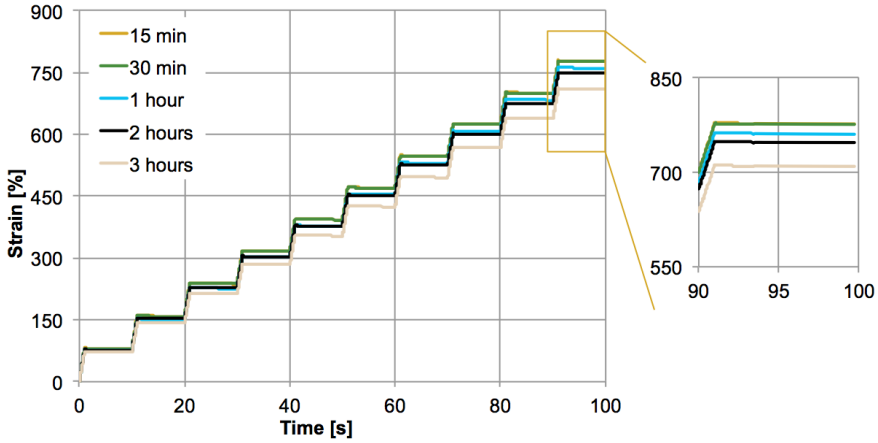

Figure 2.13. MSCR Results For Binder + 0.2% CNT

As mentioned before, CNTs were mixed with the binder at 2400 rpm with a high shear mixer for three hours with samples being collected for evaluation at predefined intervals of time (15, 30, 60, 120, and 180 minutes of mixing time). A small amount of the asphalt was removed at each time point and streaked on a smooth metal disk to create a flat surface for imaging. The metal disk was then attached to the SEM stub with a carbon tape to prevent detachment of the sample disk from the stub upon application of vacuum. The samples were analyzed by a FEI Quanta 650 SEM with a 5 kV beam.

While the SEM images do show a typical network structure of complex asphalt binder, the high-energy electron beam had likely altered surface morphology of the binder (e.g., evaporation of volatile organic compounds via localized heating). Figure 2.14 shows a

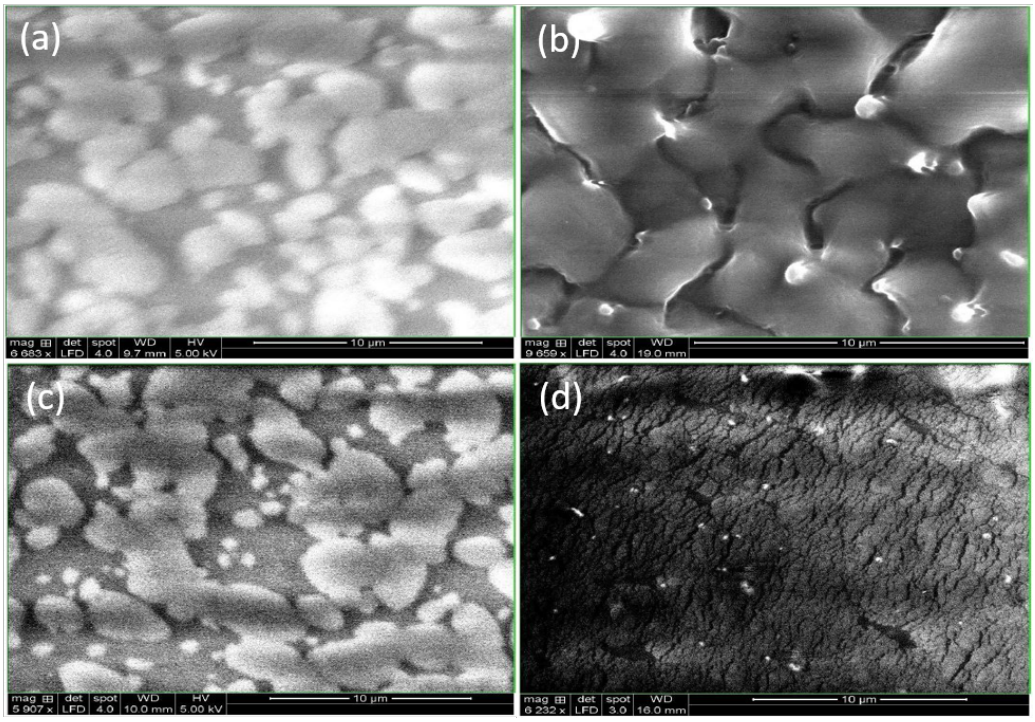

Figure 2.14. SEM micrograph of binder and binder + CNT at different mixing times: (a) binder only after 15 min, (b) binder + CNT after 15 min, (c) binder only after 3 h, and (d) binder + CNT after 3 h

typical SEM image of the binder with and without CNTs, sampled after 15 minutes and 3 hours of mixing. However, such topographical analysis of the binder, a complex mixture of organic molecules with a wide variation in chemical composition, was unable to discern differences in dispersion of nanomaterials within the binder.

2.4.3 Results based on AFM

The dispersion of nanomaterials in asphalt binder after different duration of mixing was also evaluated with atomic force microscopy (AFM, Bruker, Santa Barbara, CA). In this case, as before, nanoclay (2 wt. % of binder) and nanosilica (4 wt. % of binder) were mixed with the asphalt binder at 2400 rpm under shear mixing over 3 hours and at 150 °C. Samples for imaging were obtained after 15, 30, 60, 120, and 180 min of mixing. To prepare the samples, one drop of the viscous nanomaterial-binder mixture was placed on a 1 cm diameter metal disc (Bruker, Santa Barbara, CA) and spread evenly over the disc by smearing it with a glass slide. The same procedure was followed for samples for all

mixing times. AFM probes (Bruker, Santa Barbara, CA) with a spring constant of 6 N/m were used for imaging all samples. Representative images (Figure 2.15 and Figure 2.16) were taken using the ScanAsyst mode of the NanoScope 9.1 software.

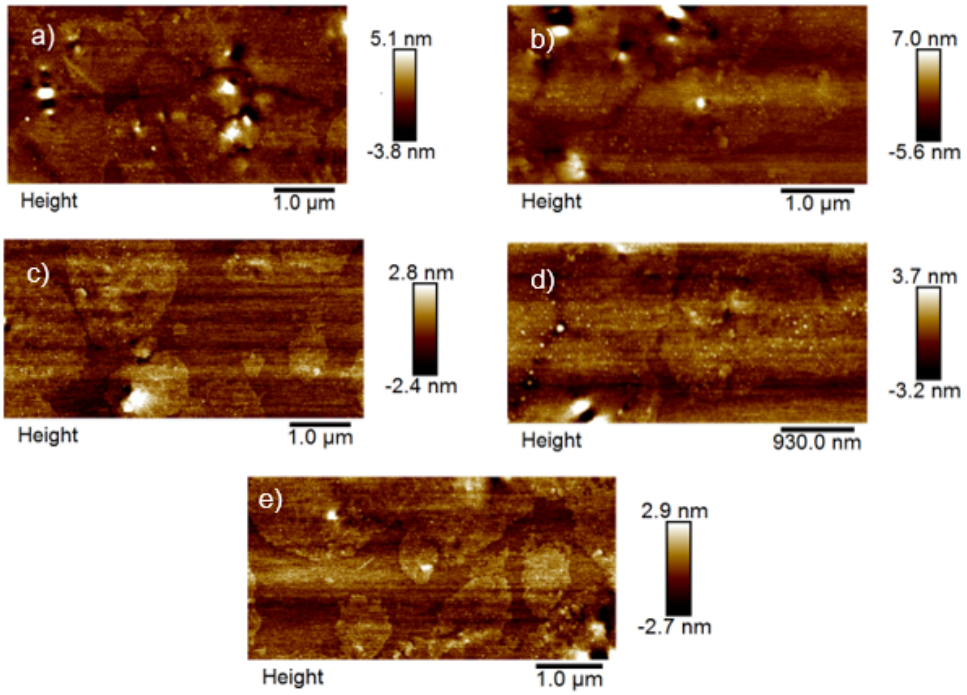

Figure 2.15. Nano-clay modified binder at a) 15 min, b) 30 min, c) 1 h, d) 2 h, and e) 3 h mixing times

At a lower magnification, AFM images of the neat binder and nanomaterial-enhanced binder appeared similar. But at higher magnification, the nanomaterial-enhanced binder images show distinct features with sizes in the nanometer to micrometer scale, which are likely agglomerates of the added nanoparticles. These features are evident in Figure 2.17 where the nanomaterial-modified binders show distinct spherical features that are not detectable in the neat binder images. The features displayed consistency, in terms of observable structure, in samples mixed for over 120 min. Based on this observation, a 2 hours mixing period was considered as appropriate for effectively dispersing the nanomaterials in the binder. The conclusion based on AFM imaging is consistent with the results obtained from dynamic shear rheometer (DSR) tests.

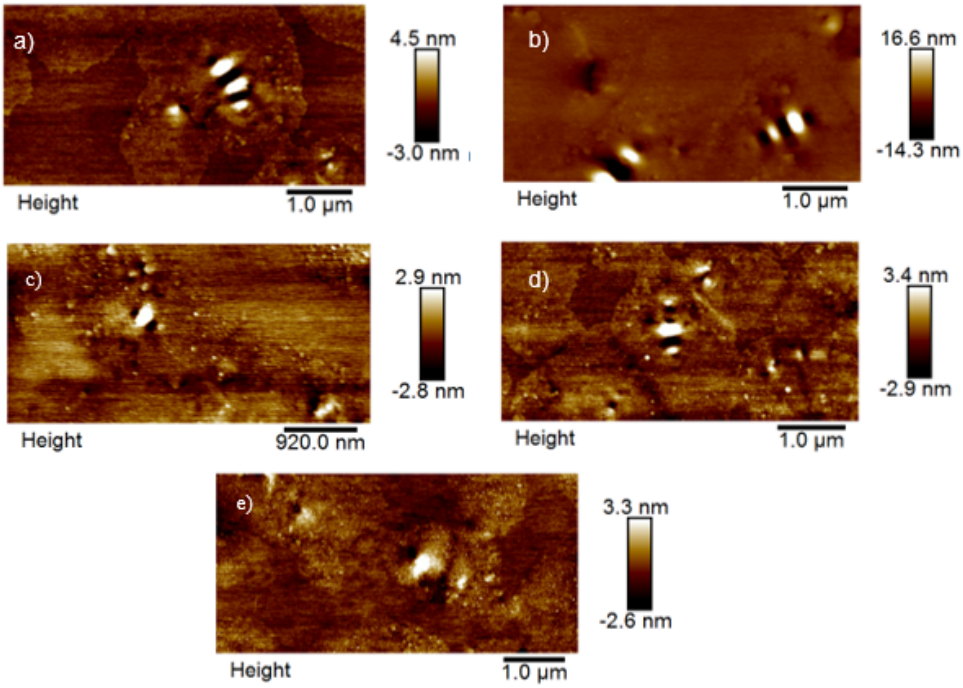

Figure 2.16. Nano-silica modified binder at a) 15 min, b) 30 min, c) 1 h, d) 2 h, and e) 3 h mixing times

2.4.4 Results based on DLS

The dark color of the asphalt binder makes it impractical to use any optical method to evaluate the dispersion of nanomaterials in the binder. In fact, the aforementioned methods based on rheological tests / parameters, SEM, and AFM (which relies on contact with the surface) were selected to avoid the use of optical methods and evaluate dispersion of nanomaterials in the binder. One other approach to directly evaluate the dispersion of nanomaterials using optical methods is by using a surrogate for asphalt binder. The dispersion of nanomaterials is dictated by the viscosity and polar character of the fluid or medium of dispersion. In order to find a surrogate to evaluate dispersion, several chemical solvents with similar polar character as the asphalt binder were considered. These solvents were then used as a medium to evaluate dispersion at room temperature. Although the viscosity of these solvents at room temperature is less than the viscosity of the binder even at its mixing temperature, this was considered as the best or ideal scenario to evaluate dispersion of nanomaterials.

To represent the polar character of the asphalt binder, five solvents were chosen based

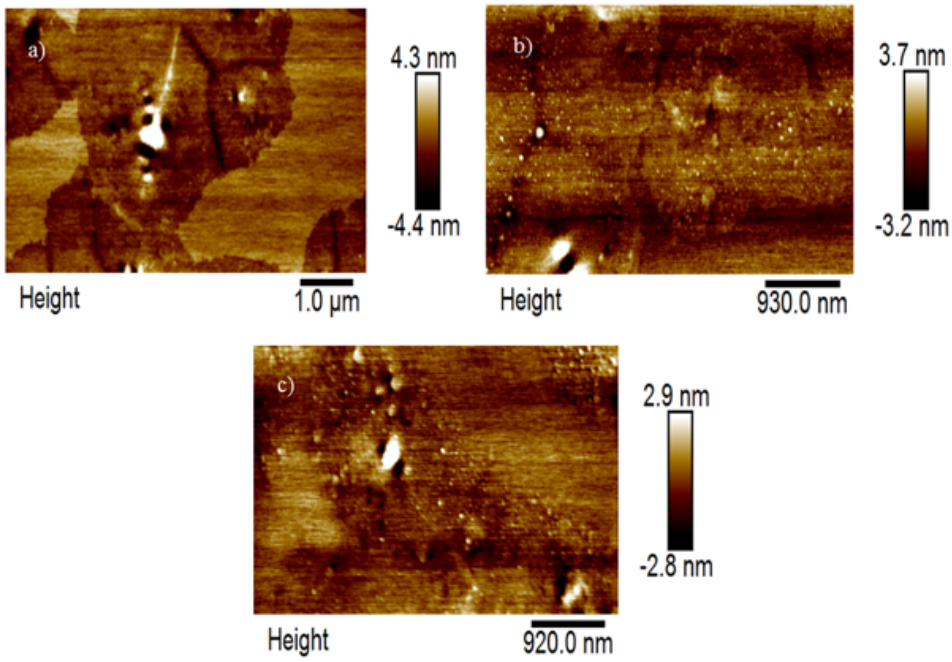

Figure 2.17. AFM images of a) neat binder, b) nanoclay modified binder, and c) nanosilica modified binder.

on American Society of Testing and Materials standard method (ASTM D4124-09). This method is used to obtain four defined fractions from petroleum asphalts based on their polarity. The four fractions are defined as saturates, naphthene aromatics, polar aromatics, and iso-octane insoluble asphaltenes. Solvents chosen are listed here:

1. iso-Octane or 2,2,4-trimethyl pentane (Sigma Aldrich, HPLC Grade)
2. n-Heptane (Sigma Aldrich, HPLC Grade)
3. Toluene (Sigma Aldrich, HPLC Grade)
4. Trichloroethylene (TCE) (Sigma Aldrich, ACS Grade)
5. Methanol (Sigma Aldrich, HPLC Grade, anhydrous)

As mentioned before, these solvents represent the best-case scenario for the dispersion of nanomaterials in asphalt. Since a suspension made up of 2% by weight of nanomaterials would result in an oversaturated condition for each of the cases, a 0.2% by weight suspension was prepared by addition of appropriate amount of nanomaterial to 50 mL of each of the solvents. These mixtures were dispersed by ultrasonication in a bath sonicator (Bransonic, Danbury, CT) for 1 hour. An aliquot of suspension was collected from 1 to 1.5 cm

below the top surface of the solvent and characterized using dynamic light scattering (DLS) with an ALV-CGS-3 goniometer system (ALV-GmbH, Langen, Germany), equipped with a 632.8 nm laser (ALV CGS-3 goniometer system, Langen, Germany). Scattered light was detected at 90°and converted to hydrodynamic radii (HDR) employing an auto-correlator and cumulant analysis. HDR data was collected every 15 s for a 25 min duration. Average HDR was plotted against time of measurement to observe evolution of particle size over time (Figure 2.18 to Figure 2.22.

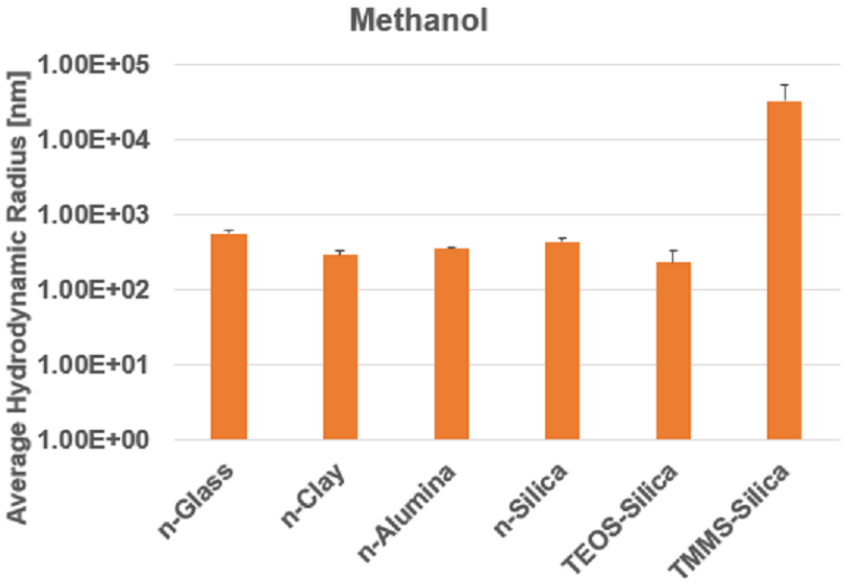

Figure 2.18. DLS Results for the various NM in Methanol

From the HDR data obtained, it is observed that nanoglass and modified-silica nanomaterials were dispersed better in the ideal fractions of the asphalt binder. These materials displayed an average HDR below 1000 nm in most of the solvents tested. It is worth noting that while the pristine nanomaterials can be below 100 nm in size, when mixed with the solvent, the HDR of the agglomerates can range from a few hundred nanometers to several microns. Such increase in size is typical for small particles with high diffusion characteristics in solvents. Furthermore, the uniformity of dispersion or solubility is dictated by the material properties and polarity of the solvent (Hansen and Beerbower, 1971). The aggregation tendency of nanoparticles composed of metals or metal oxides in nonpolar solvents is governed by strong van der Waals forces (Min et al., 2008). Aggregation can be potentially prevented by introducing steric or electrostatic stabilization (Aich et al., 2013;

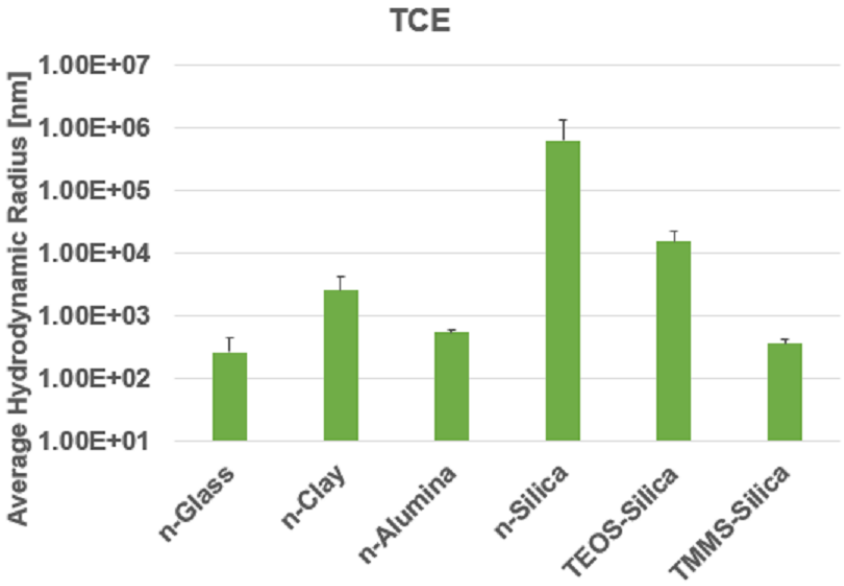

Figure 2.19. DLS Results for the various NM in TCE

Khan et al., 2015). The functionalization of nano silica with organosilanes are shown to be better dispersed than bare nano-silica in almost all the solvents, with average HDR below 1000 nm for all solvents except methanol. The conclusion from this analysis is that nanomaterials though are mixed as nano-scale particles when added to asphalt binder, due to inherent diffusion and surface properties, these particles aggregate and mostly do not remain at the nano-scale upon mixture. Thus mixing a particle which has nano-scale size may not necessarily lead to a uniformly dispersed nano-scale mixture when added to asphalt. Property enhancement due to addition of nanomaterials thus should consider size evolution as well as state of dispersion after addition to the binder and not based on pristine nano-scale properties. However, in conjunction with the rheological tests, it is postulated that a well-dispersed nanomaterial can possibly be more effective in enhancing the rheological properties of the binder.

2.5 SUMMARY

Based on the results seen above, it was determined that for the materials used in this study, a mixing time of two hours was appropriate. In the rheological tests, it was observed that for most of the materials, there was a significant change in properties between one and two hours of mixing. However, there was generally less change between two and three

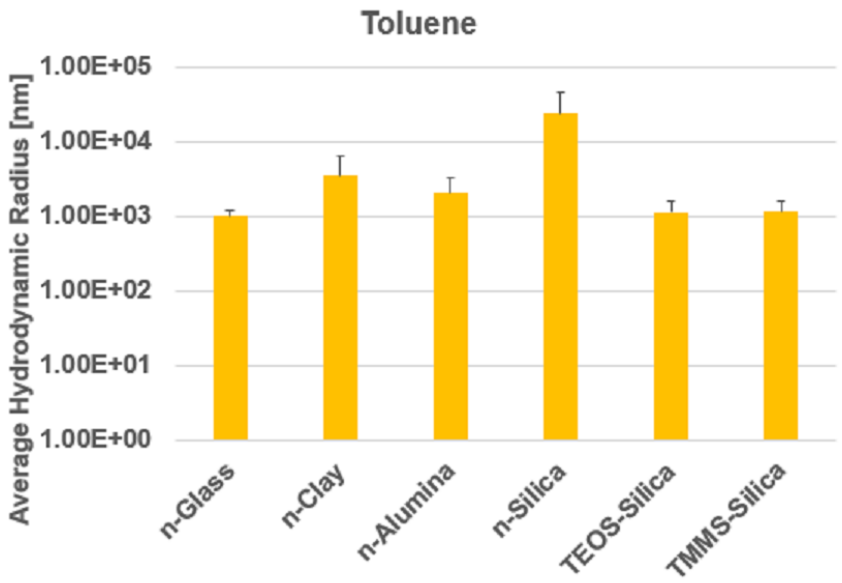

Figure 2.20. DLS Results for the various NM in Toluene

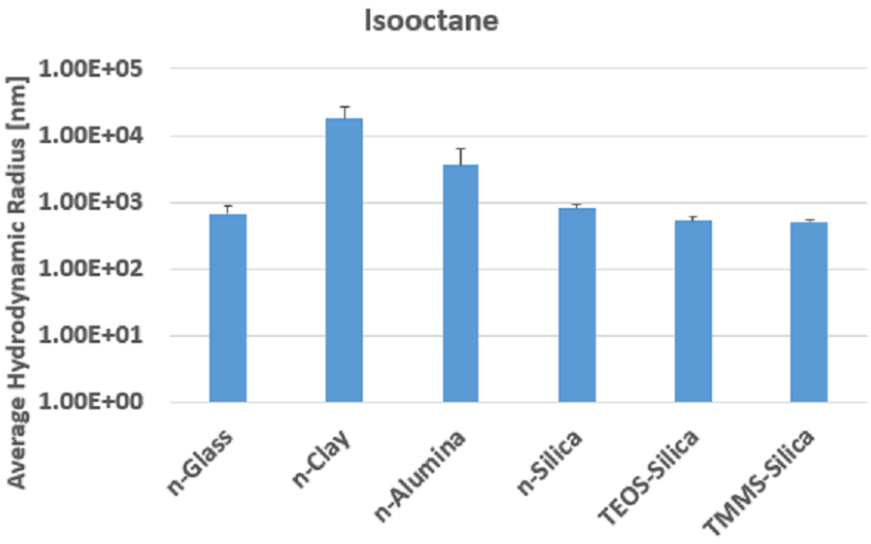

Figure 2.21. DLS Results for the various NM in Iso-octane

hours of mixing time. Therefore, it was recommended that for all tests moving forward, the nanomaterials would be blended with the binder in the high shear mixer for two hours.

Table 2.3 shows the final concentrations for the nanomaterials that were used in the

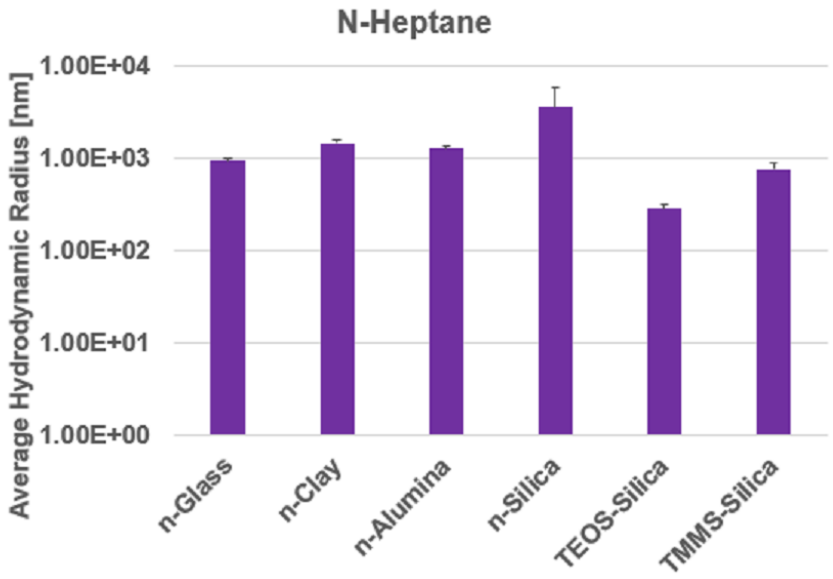

Figure 2.22. DLS Results for the various NM in n-Heptane

remainder of this study. For each of the four non-functionalized nanomaterials, two concentrations were selected, as stated before, while only one concentration was employed for the functionalized materials. Due to the high cost of not only the nanosilica particles, but also the added cost of functionalization, it was determined that only the lower percentage would be potentially cost-effective.

Table 2.3. Matrix of Nanomaterials Used in the Next Steps of This Study

Nanomaterial	Low Concentration	High Concentration
Nanosilica	4%	6%
Nanoclay	2%	7%
Nanoalumina	4%	6%
Nanoglass	3%	6%
Nanosilica (TEOS Modified)	4%	N/A
Nanosilica (TMMS Modified)	4%	N/A

CHAPTER 3. PROPERTIES OF BINDER MODIFIED USING NANOMATERIALS

3.1 OVERVIEW

This chapter provides an overview of the performance of the binders modified with nanomaterials as discussed in the previous chapter. Various rheological tests were performed on the modified binders as well as the original binder in different aging conditions. The tests performed included those specified by TxDOT as part of the characterization for asphalt binders and other tests that can provide information about the material properties of the binders. The following sections describe the tests that were performed and the results that were obtained for each modified binder.

3.2 MIXING OF NANOMATERIALS

As discussed before, the first task was to mix the nanomaterials with the asphalt binder in order to properly disperse these throughout the binder. In the previous chapter, the subject of mixing time was addressed. The optimum mixing time was determined to be two hours in the high shear mixer. First, the binder was heated to a temperature of 150 °C until it was viscous. The binder was then blended with the nanoparticles in the high shear mixer at 2400 rpm and at a temperature of 150 °C. After two hours, the modified binder was removed and allowed to cool.

3.3 AGING OF MODIFIED BINDERS

Two aging methods were used to determine the effects of nanomaterials in asphalt binder at different points in the binder's service life. Rolling Thin Film Oven (RTFO) aging simulates the short term aging caused by loss of volatiles that takes place during the mixing of the asphalt mixtures, transportation of asphalt mixtures from the plant to the construction site, and the placement process at the site. In this method, (AASHTO T 240) asphalt binder is placed in thin films into a cylindrical glass jar. The jars, on their side, are placed into an oven at a temperature of 163 °C and rotated at a speed of 15 rpm for 85 minutes.

The second aging method performed was done using a Pressure Aging Vessel (PAV). PAV aging simulates long-term aging that the asphalt binder will experience throughout its service life in the field due to oxidation. PAV aging can only be performed on binders that

have already been RTFO aged. The PAV aging process consists of placing the RTFO aged binder into a thin film in a small steel pan, and then placing the pan in the PAV for 20 hours. The temperature at which the binder is aged is 100 °C, and the vessel is pressurized to a pressure of 2.1 MPa.

3.4 RUTTING RESISTANCE OF MODIFIED BINDERS

3.4.1 Tests and parameters

In order to ensure that the binder is able to properly resist rutting, the Superpave criteria specifies two parameters that must be considered: the stiffness, and elasticity of the binder. Stiffness is represented by the complex shear modulus ($|G^*|$) while the elasticity is represented by the phase angle (δ). In order to resist rutting, a binder should have both a high stiffness and should be very elastic. Therefore, $|G^*|$ should be maximized and $sin(\delta)$ (representing the elastic portion of the material reponse) should be minimized. The final parameter to quantify rutting resistance is, therefore, $|G^*|/sin(\delta)$. This parameter can be measured in the Dynamic Shear Rheometer (DSR) using a frequency sweep test to generate the master curve. In order to measure this parameter, a 25 mm diameter plate is used in the DSR with a specimen of asphalt binder 1 mm in thickness. As in the previous chapter, the frequency sweep test was run at three temperatures, 35 °C, 45 °C, and 55 °C, with the reference temperature being 45 °C. The range of frequencies used included frequencies from 0.1 to 73 rad/s at a constant strain level of 0.5%.

Using this test, the neat binder and all nanomaterial-modified binders were assigned a true high grade. Following the AASHTO M320 standard and assuming a target asphalt binder PG 64, the dynamic modulus and the phase angle were calculated for the unaged binder at 58 °C, 64 °C, and 70 °C using the master curve that had been developed. Figure 3.1 shows a typical result from this test. In addition to the testing on unaged binder, the same test was performed with RTFO aged binder in order to determine the effects of aging.

In addition to the frequency sweep test, another test was performed to quantify rutting resistance of the binder, the Multiple Stress Creep and Recovery (MSCR) test. As discussed in the previous chapter, the MSCR test can predict the asphalt binder behavior with regards to permanent deformation. This test was developed with the purpose of better representing load conditions that cause this type of damage, due to problems in the Superpave parameter $|G^*|/sin(\delta)$. This method is specified in ASTM D7405. For the purposes of this study, the test was performed on RTFO aged binder, which simulates the binder at the beginning of

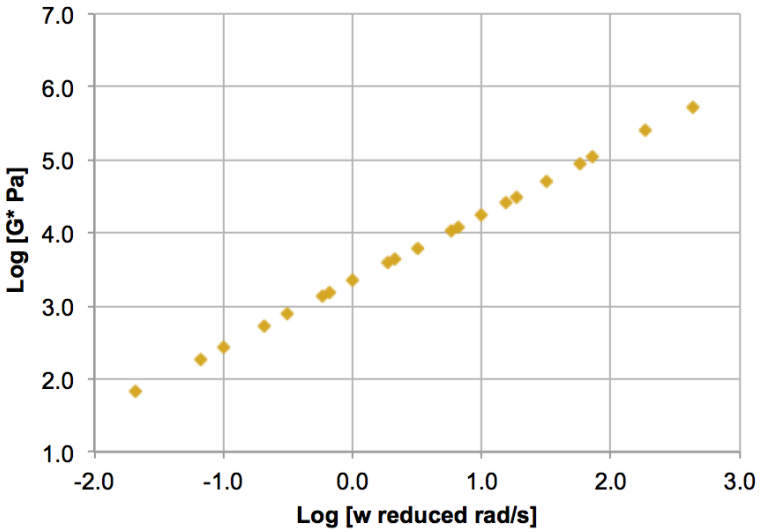

Figure 3.1. Typical Master Curve Produced Using Frequency Sweep

its service life, the most critical time for rutting in the field.

The test consists of the successive application of load-recovery cycles on a sample of asphalt binder at two different stresses levels. Thus, the asphalt binder's ability to recover part of the deformation caused by loads and permanent deformation, which is generated immediately after applying the stress, was measured. Each cycle was performed within 10 seconds in which a constant load is applied for 1 second followed by 9 seconds of recovery. A total of 20 cycles (load-recovery) were performed using the first 10 cycles at a stress level of 0.1 kPa and 10 cycles at a stress level of 3.2 kPa. Within each load-recovery cycle it was possible to obtain three notable deformations: at the beginning of the load period (t = 0 seconds), at the end of the load period (t = 1 second,) and at the end of the recovery period (t = 10 seconds).

To characterize the properties of asphalt binders two parameters are used. These parameters are the percent recovery ($R\%$) and the non-recoverable creep compliance (J_{nr}). The percent recovery is a measure of the deformation recovered during the rest period in each cycle (9 seconds without load). In other words, this is the difference between the deformation obtained immediately after applying the load and deformation obtained following 9 seconds rest. The non-recoverable creep compliance is defined as the permanent strain due to the application of a certain stress level.

For this portion of the study, the MSCR test was performed at three temperatures, 58 °C, 64 °C, and 70 °C. The results of $log(J_{nr})$ versus $log(T)$ were plotted, with a line of best

fit drawn through the three points. Finally, the temperature at which the J_{nr} value was 4.5 kPa^{-1} was considered to be the MSCR true high grade of the binder. A typical output from the MSCR test is shown in Figure 3.2.

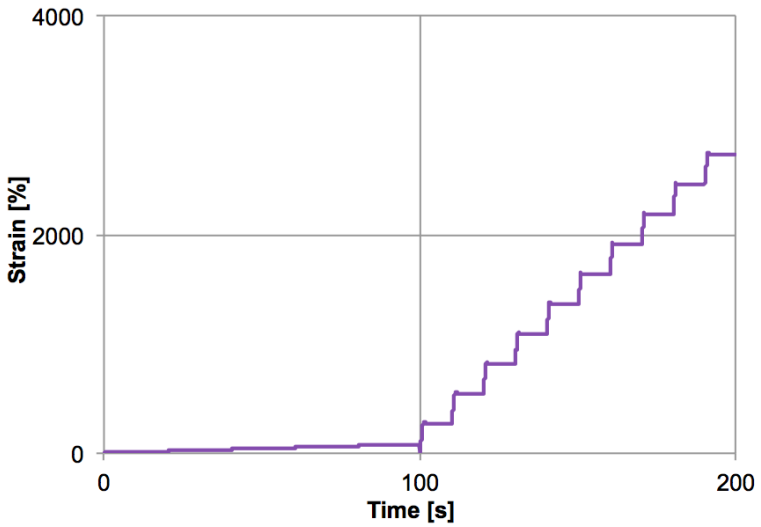

Figure 3.2. Typical Result of MSCR Test

To summarize, the following four parameters were measured and used to quantify the performance of each binder:

1. Complex Shear Modulus ($|G^*|$)
2. Phase Angle (δ)
3. Non-Recoverable Creep Compliance (J_{nr})
4. Percent Recovery ($\%R$)

3.4.2 Results

The results of the frequency test for rutting resistance in unaged binder at the reference temperature of 45 °C are shown in Figure 3.3. Figure 3.4 shows the change in the true high grade for each binder from that of the control binder based on the results of frequency sweep testing of the unaged binder. In order to calculate this value, the true high grade value of the unmodified control binder was subtracted from that of the modified binder.

While most of the binders showed little change in the true high grade in this test (less than 3 °C), the binders modified with nanoglass did change significantly in terms of performance. The binder modified with 3% nanoglass showed an improvement of more than

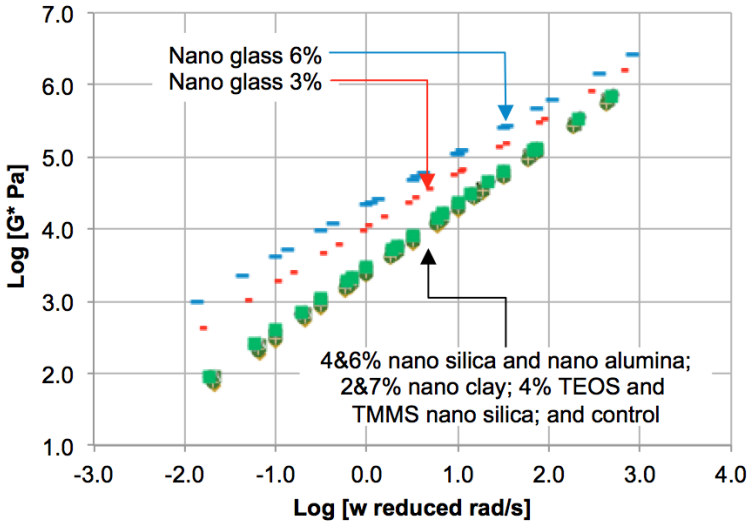

Figure 3.3. Results from Frequency Sweep Testing for All 11 Unaged Binders ($T_{ref} = 45^{\circ}C$)

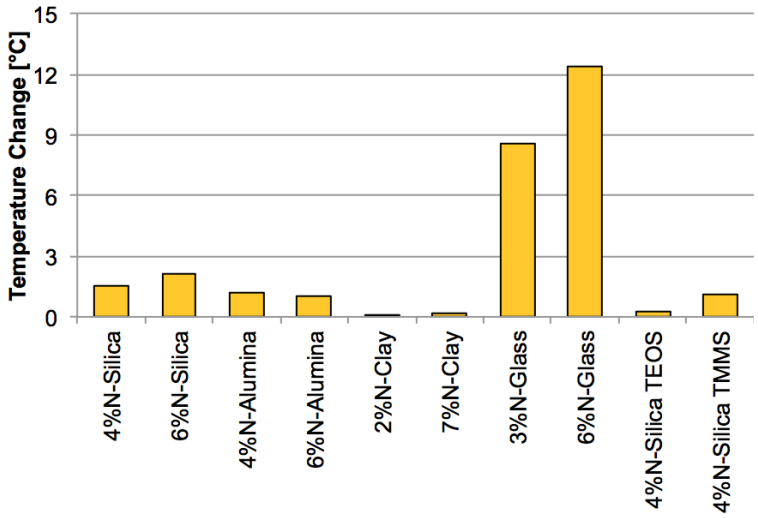

Figure 3.4. High Temperature Grade Change in Frequency Sweep Test due to Addition of Nanomaterials in Unaged Binder

8 °C, enough to shift the high grade from PG64 to PG70. Meanwhile, the binder modified with 6% nanoglass showed an even greater improvement of 12 °C, which was enough to shift the high grade from PG64 to PG76.

For the same test performed on RTFO aged binder, Figure 3.5 shows the results for

the master curves for all 11 binders. Figure 3.6 shows the change in high performance grade from the control binder's high grade after RTFO aging of the binder based on the frequency sweep test. Similar to the unaged results, most of the binders did not show much improvement over the control binder in terms of high temperature performance. However, the nanoglass-modified binder showed a large improvement.

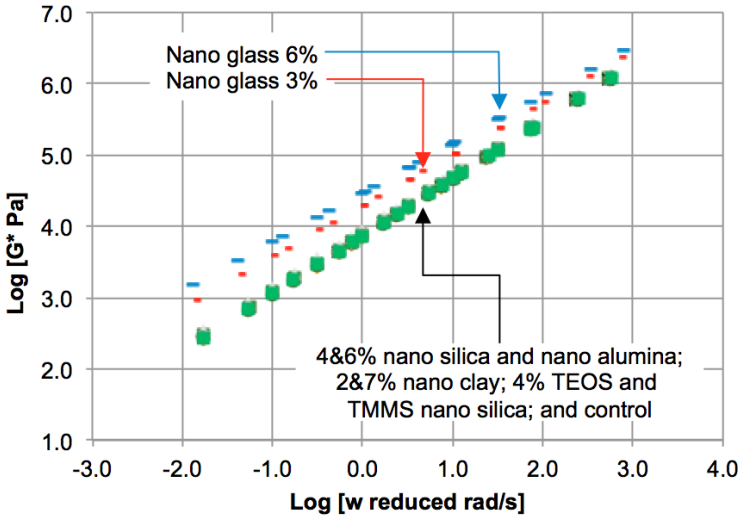

Figure 3.5. Results from Frequency Sweep Testing for All 11 RTFO Aged Binders ($T_{ref} = 45°C$)

In addition, the results for the MSCR testing at 58 °C are shown in Figure 3.7. The results for the MSCR test at 64 °C and 70 °C are shown in Figures 3.8 and 3.9, respectively. The change in MSCR true high grade assigned based on a J_{nr} of 4.5 kPa^{-1} to each binder, based on that of the control binder, is shown in Figure 3.10. The elastic recovery at the 58 °C testing temperature is shown in Figure 3.11. After being graded by the three methods (unaged frequency sweep, RTFO aged frequency sweep, and MSCR), the lowest of the three grades assigned to each binder is considered to be its high performance grade. The final high performance grade changes with regard to the control binder is shown in Figure 3.12.

3.4.3 Summary

A total of 11 binders were evaluated to determine the effects of adding nanoparticles to the rutting performance of the binders. Based on the results obtained, it is observed that the addition of nanoglass to the asphalt binder caused the biggest improvement in high tem-

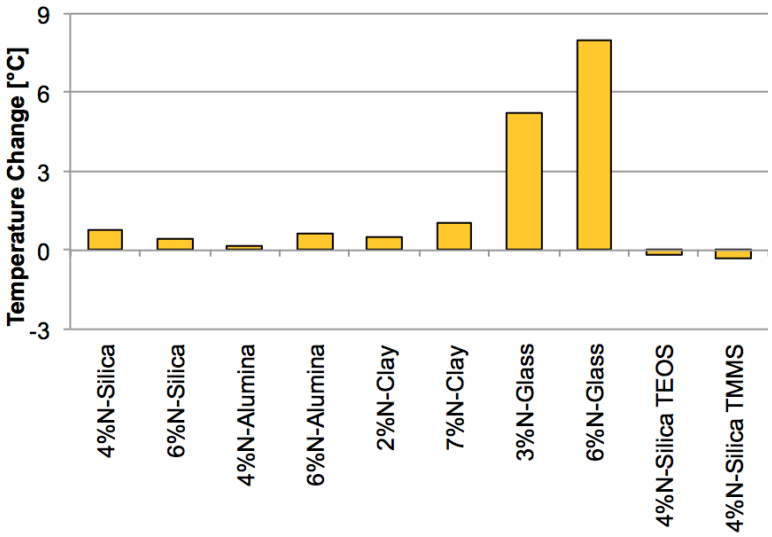

Figure 3.6. High Temperature Grade Change in Frequency Sweep Test due to Addition of Nanomaterials in RTFO Aged Binder

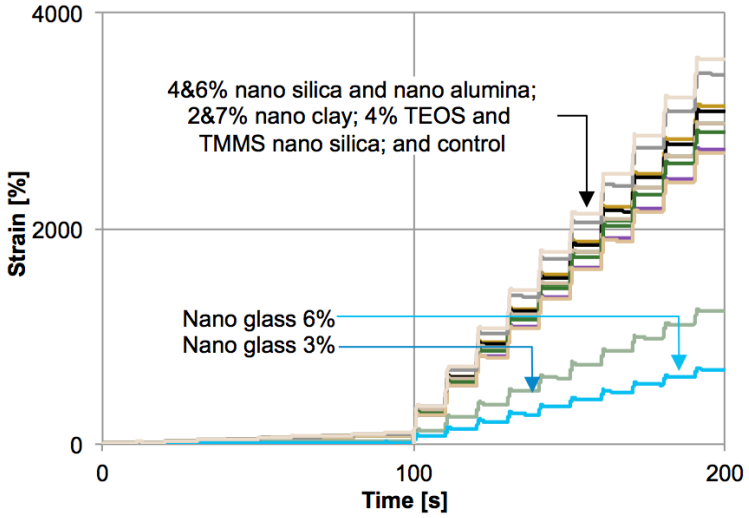

Figure 3.7. Results from MSCR Testing at 58 °C

perature properties. While other nanomaterials had a minimal effect on high temperature properties, the addition of nanoglass caused a grade change from PG64 to PG70 in both the high and low concentration cases. It was further observed that, in general, a higher concentration of nanoparticles has a tendency to enhance the high temperature properties of the binder.

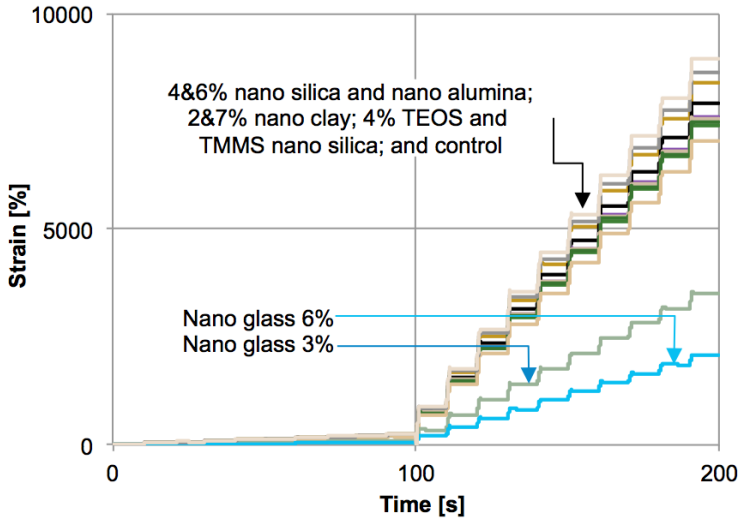

Figure 3.8. Results from MSCR Testing at 64 °C

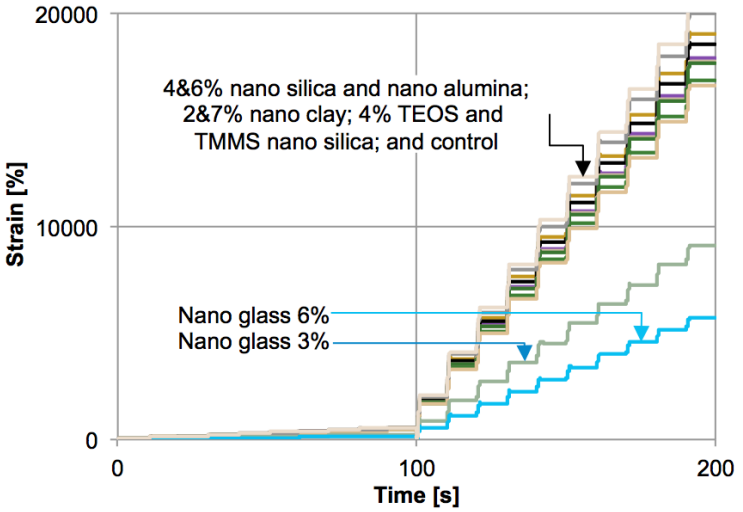

Figure 3.9. Results from MSCR Testing at 70 °C

3.5 FATIGUE CRACKING RESISTANCE OF MODIFIED BINDERS

3.5.1 Tests and parameters

Fatigue cracking is a primary form of pavement distress that occurs primarily after high traffic loading at intermediate temperatures. In order to evaluate the fatigue cracking resistance of the binders used in this study, a poker chip test (Figure 3.13) was used. The poker

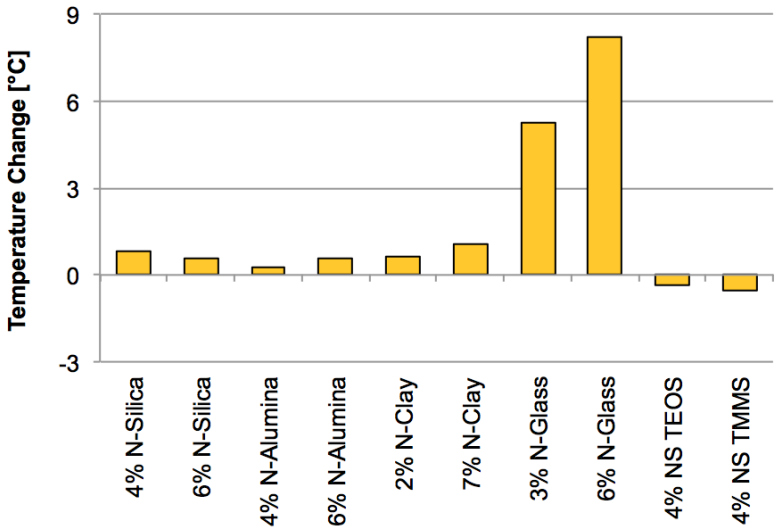

Figure 3.10. MSCR True High Grade Change From Control Binder

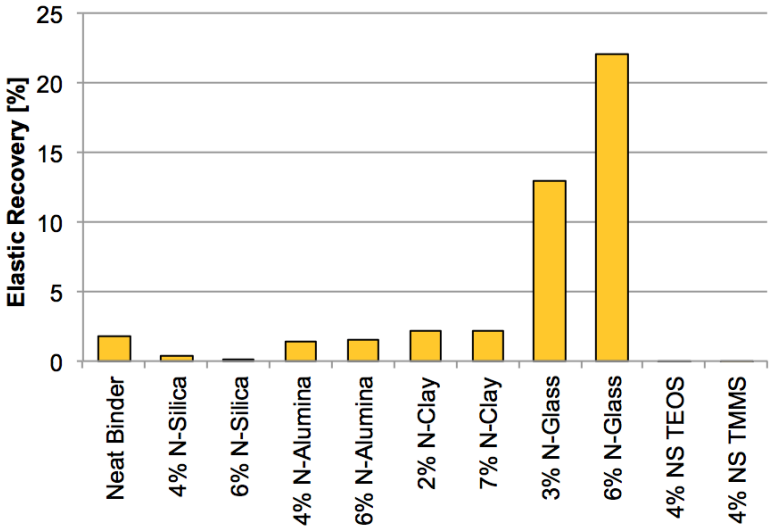

Figure 3.11. Elastic Recovery Based on MSCR Testing

chip test consists of a thin film of asphalt placed between two rigid steel substrates and loaded in uniaxial tension. For the purposes of this study, the films tested had a thickness of 300 micrometers and a diameter of 14.6 mm.

The test method involves heating the bottom plate to a temperature of 100 °C, then placing the binder sample on it. Then, the top plate is heated to the same temperature,

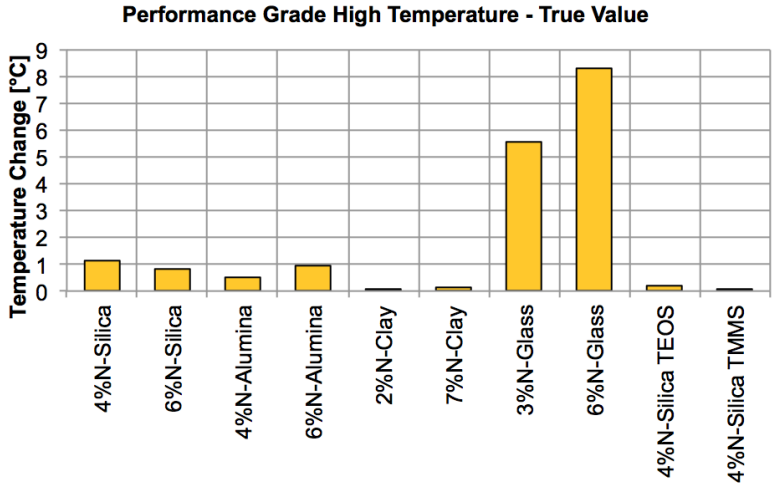

Figure 3.12. Change in High Performance Grade Assigned to Each Binder

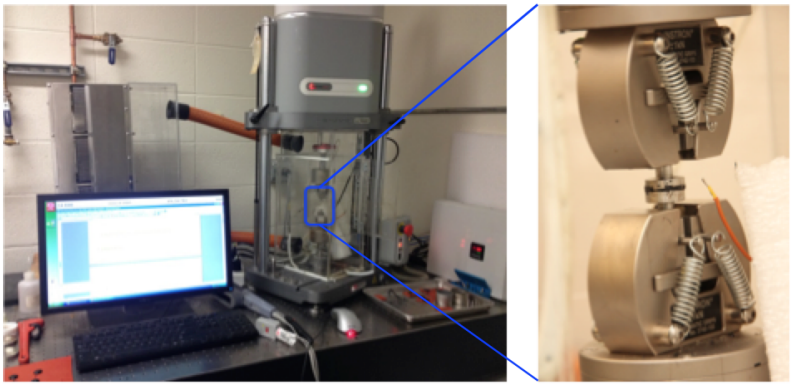

Figure 3.13. Testing Apparatus for the Poker Chip Test

and quickly lowered onto the bottom plate to create a thin film sample of thickness 370 microns. Over the next seven minutes, the sample is then lowered to a thickness of 330 microns. Then, the sample is set to the test thickness of 300 microns, and allowed to relax to that point over the next 8 minutes. Finally, any load is removed and the sample is allowed to condition for 15 additional minutes before the test is run. For this study, all tests were run in a load-controlled method at a loading rate of 1 N/s. The binders tested included both the unaged binders and the RTFO aged binders.

The output of this test is load versus displacement data, which can easily be converted to stress versus strain data. A typical poker chip test output is shown in Figure 3.14. The main output from a stress-controlled poker chip test is the peak tensile stress that the binder

was able to withstand in the test, referred to as the tensile strength.

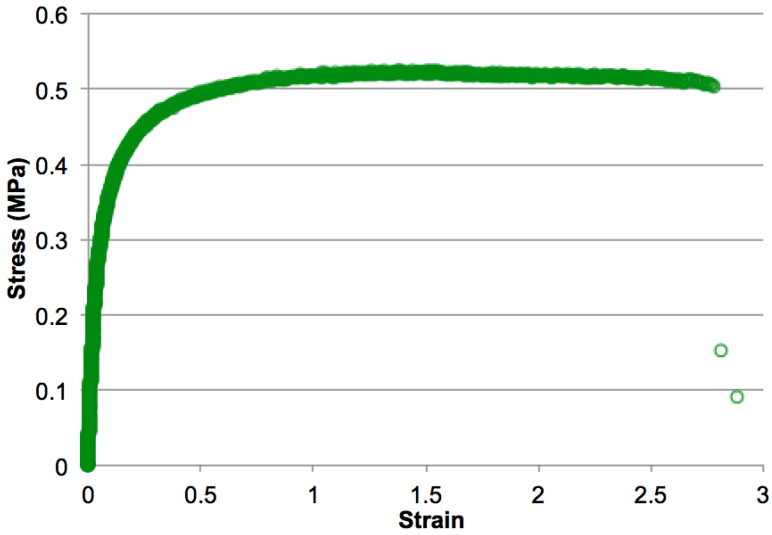

Figure 3.14. Typical Output From a Poker Chip Test

3.5.2 Results

Figure 3.15 shows the results from poker chip testing of all 11 unaged binders used in this study. In this chart, the maximum tensile strength of the binder is shown for each binder at each concentration used. Meanwhile, Figure 3.16 shows the same type of results for the poker chip testing of the RTFO aged binders that were studied.

3.5.3 Summary

For the unaged binders, each binder that was modified with nanomaterials showed a higher tensile strength in the poker chip test than the unmodified binder, with only the exception of 2% nanoclay (low percentage). Similar to the high temperature performance, binder modified with nanoglass showed the greatest improvement in terms of fatigue cracking performance based on the poker chip test. Another important note regarding the performance of the unaged binders is that the higher concentration of nanoparticles always led to a higher tensile strength.

For RTFO aged binder, it appears that the addition of nanomaterials had less effect at intermediate temperatures. When tested in the poker chip test, most of the binders showed negligible improvement, and in some cases even a slight decrease in tensile strength. Only

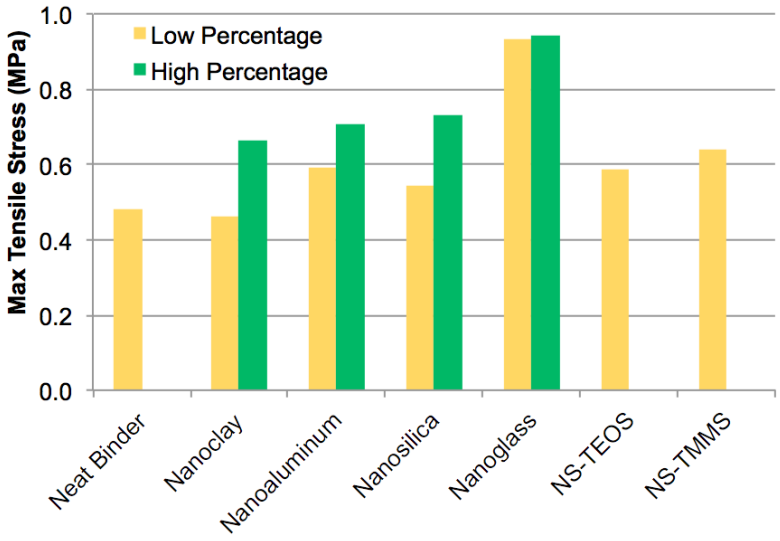

Figure 3.15. Results from Poker Chip Testing of Unaged Binders

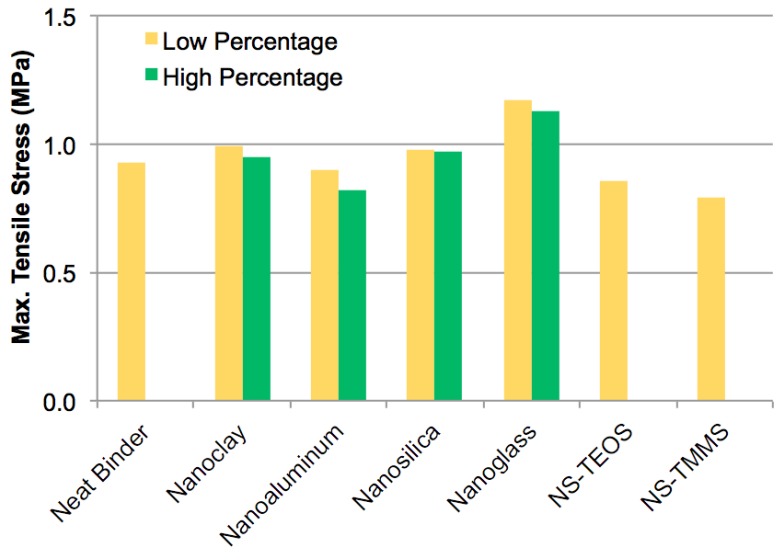

Figure 3.16. Results from Poker Chip Testing of RTFO Aged Binders

nanoglass showed significant improvement in tensile strength, but this was still much less of an improvement compared to the unaged condition. Considering that fatigue cracking typically occurs later in a pavement's service life, it appears that the nanomaterials studied here are not tremendously effective in terms of increasing fatigue cracking resistance.

3.6 LOW TEMPERATURE CRACKING RESISTANCE OF MODIFIED BINDERS

3.6.1 Tests and parameters

Low temperature cracking is a form of pavement failure that occurs at low temperatures and late in a pavement's service life. For the purposes of this study, two tests were performed to evaluate low temperature performance of the nanomaterial-modified asphalt binders. Since low temperature cracking occurs at the end of a pavement's service life, all tests for this portion of the study were performed on PAV aged binder.

The first test performed was the traditional Bending Beam Rheometer (BBR) creep test. This test, specified in AASHTO T 313, uses a beam made of asphalt binder with a length of 127 mm, a height of 12.5 mm, and a thickness of 6.25 mm. A traditional three point bending test was performed on the beam with a span length of 102 mm and a load was continuously applied at the center of the beam. The load applied had a magnitude of 980 mN. Upon application of the load, the deflection response of the beam was measured. For the purposes of this study, the test was performed at two temperatures: -12 °C and -18 °C.

Two parameters are measured in this test, the stiffness and m-value of the binder. The stiffness is a measure of the thermal stresses within the binder, and is measured as a function of time based on Equation 3.1. Because lower thermal stresses are preferred to resist cracking, a maximum stiffness was imposed on the binder. For a PG 64-22 binder like the original binder used for this study, the maximum allowable stiffness is 300 MPa at a test temperature of -12 °C. In order to find the m-value of the binder, stiffness values were plotted versus time on a log-log scale. The slope of this plot was considered to be the m-value of the binder. This value provides a measure of the binder's capability to relax stresses over time under constant deformation. Thus, a minimum m-value was specified. For a PG 64-22 binder the minimum m-value is 0.3 at a temperature of -12 °C. For other low PG grades, these parameters have the same value, but are measured at different test temperatures. For example, a PG 64-28 binder should have a maximum stiffness of 300 MPa and a minimum m-value of 0.3 at a test temperature of -18 °C. The test temperature should always be 10 °C higher than the assigned low temperature grade of the binder. Therefore, by testing at both -12 °C and -18 °C, the stiffness and m-values could be interpolated to the correct value to determine the true low grade of each binder.

$$S(t) = \frac{PL^3}{4bh^3\delta(t)} \tag{3.1}$$

The second test performed to evaluate low temperature performance was a strength test. This test was performed in a modified version of the BBR. This test involved the use of a sample of the same dimensions as the traditional BBR test, and used the same three point loading method. The difference here was that a monotonically increasing load was applied to the binder at a rate of 0.0833 N/s, rather than a constant load. The main parameter of interest that was calculated here is the maximum strain in the binder, which was calculated using beam theory and the deformation data recorded by the BBR. This test was also performed on PAV aged binder at a test temperature of -12 °C.

3.6.2 Results

Figure 3.17 shows the change in low temperature grade for each binder that was tested in the traditional BBR test based on the stiffness parameter, compared to the control binder. Figure 3.18 shows the same change but based on the m-value parameter only. It is important to note that in these two plots, a positive value represents an improvement in low temperature performance grade, meaning that a change of +1 actually signifies a true low grade 1 °C colder than the control binder. Figure 3.19 shows the change in low grade for each binder compared to the low grade of the control binder based on the most conservative case two parameters.

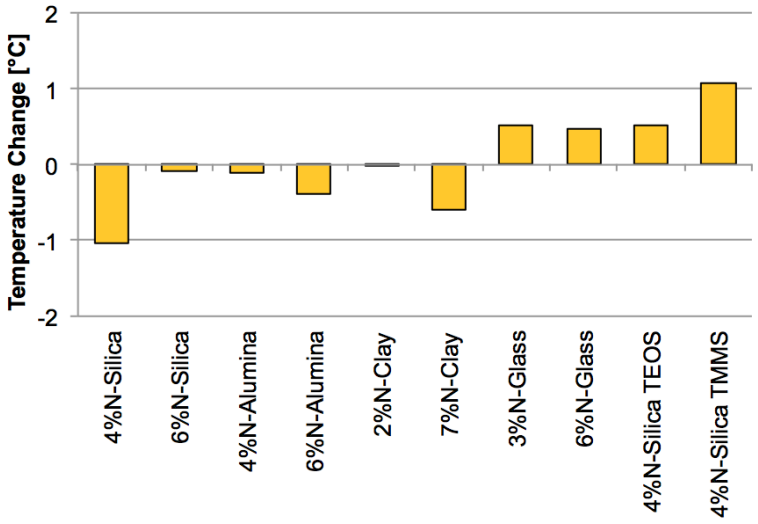

Figure 3.17. Low Temperature Grade Change Based on Stiffness Parameter for All Binders

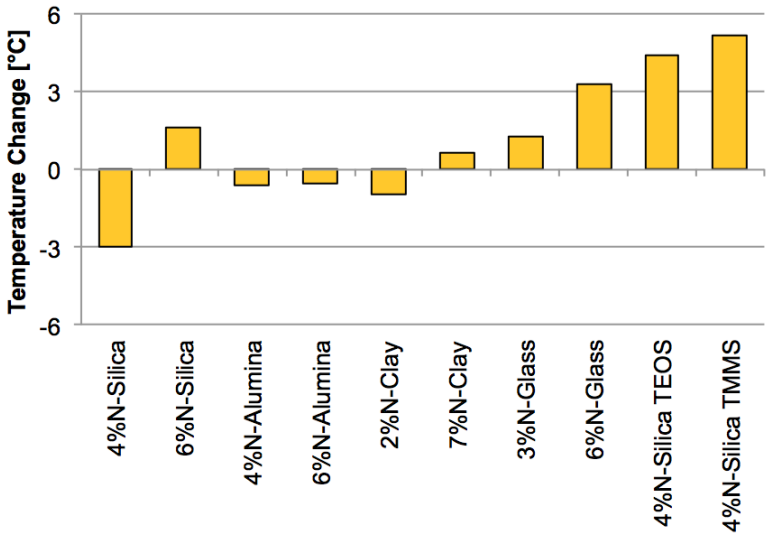

Figure 3.18. Low Temperature Grade Change Based on m-value Parameter for All Binders

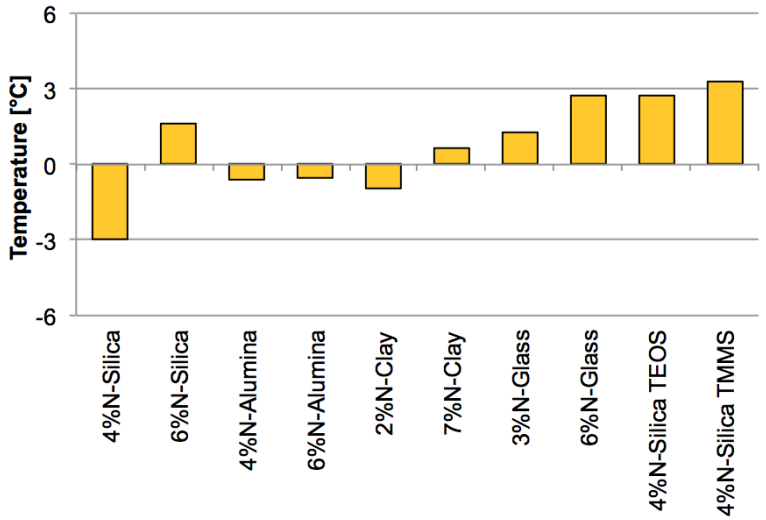

Figure 3.19. Low Temperature Grade Change Based on Both Parameters for All Binders

Figure 3.20 shows the results of the strength test. The maximum strain observed in each binder is shown.

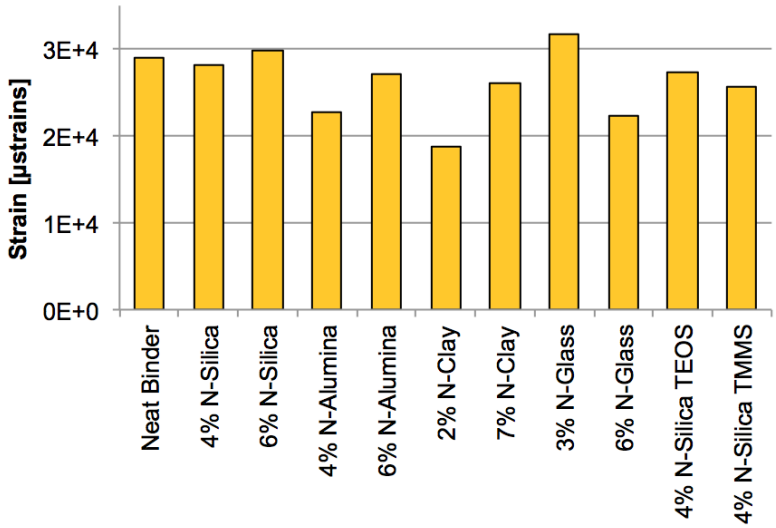

Figure 3.20. Failure Strain Observed in Strength Test for All Binders

3.6.3 Summary

Overall, most of the nanomaterials had minimal effects on the low temperature performance of the asphalt binders. Some increased the magnitude of the low temperature true grade by less than 2 °C, while others actually caused the low temperature true grade to become worse. However, it is notable that nanoglass did not cause any problem with regards to low temperature performance, although its benefits were not significant. The significance is that nanoglass can greatly increase rutting performance without compromising the lower temperature properties.

Another important observation was made regarding the functionalized nanosilica particles. Although the unmodified nanosilica barely showed an improvement at a concentration of 6%, and actually negatively impacted the binder's low temperature at a concentration of 4%, it was shown that this additive was more effective at low temperatures in its functionalized form. Both of the functionalization methods showed the best performance in terms of low temperature cracking performance and showed the best potential to improve the low temperature performance grade of asphalt binders.

3.7 MOISTURE RESISTANCE OF MODIFIED BINDERS

Moisture sensitivity of an asphalt mixture is a function of the surface properties of the binder and the aggregate. Previous studies (NCHRP Project 9-37 and TxDOT Project 4524)

have shown that surface free energy of asphalt binders and aggregates can be measured and used to assess the inherent moisture damage resistance of each asphalt binder-aggregate pair. Previous TxDOT project (4524) has produced an aggregate surface energy database for the aggregates most commonly used in the state of Texas. In this study the surface free energies of different asphalt binders were measured using the procedure recommended by TxDOT project 4524. Although the surface properties of the binder change significantly, those of the aggregate do not change significantly over time. In this study, the measured surface energies of different asphalt binders were used in combination with the surface energies of different aggregates from the database to assess the inherent moisture damage resistance of different modified and unmodified asphalt binders. This section describes the procedures used to accomplish this and the results of the testing.

3.7.1 Test and parameters

The surface free energy of the asphalt binder was measured using the contact angle method. Four different probe liquids were used as probes to measure the contact angle with each asphalt binder (control and nanomaterial modified). These contact angles were then used to back calculate the three surface free energy components of the asphalt binder. The following procedure was used to measure contact angles.

Contact angles between the binders (control and nanomaterial modified) and probe liquids were measured using a FTA200 contact angle goniometer (First Ten Angstroms, Inc., Portsmouth, VA). Figures 3.21 and 3.22 show this equipment and the software used.

The probe liquids used were water, formamide, diiodomethane, and ethylene glycol. The binder was heated to 140 °C to achieve a semi-liquid state. A few drops of the binder were placed and spread evenly on a glass slide. The glass slide was then allowed to cool and was placed on the platform of the goniometer. Using a syringe, the probe liquid was added dropwise on to the binder surface until an equilibrium angle between the solvent and the binder surface was formed. Such drops were placed on two different areas of the binder surface, and images were taken with a camera integrated with the goniometer system. The images were further analyzed to measure the contact angles on both sides of the solvent drops, the advancing and receding angle. The average of these four contact angles (2 drops on 2 sides) were reported as the average contact angle between each of the solvents and binder. Figures 3.23 through 3.26 summarize these results.

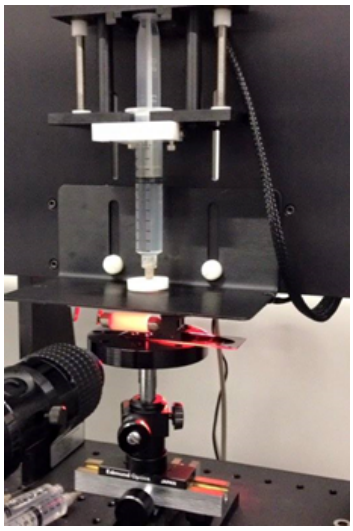

Figure 3.21. FTA200 Contact Angle Goniometer

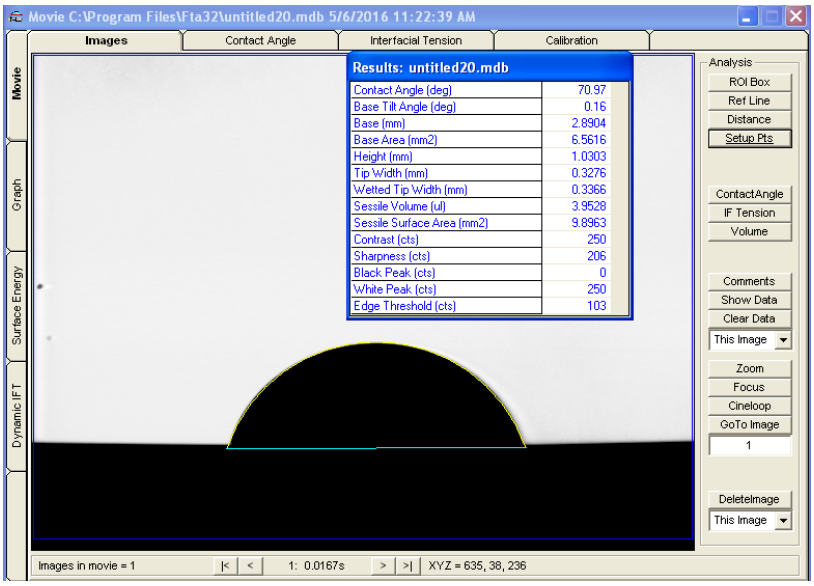

Figure 3.22. Software Contact Angle Goniometer

3.7.2 Results

In order to determine a parameter to gauge resistance to moisture damage, a bond energy parameter was determined as follows (this is based on the procedure developed and recommended in TxDOT Project 4524). The total adhesive bond energy between two solid surfaces denoted by suffixes “A” and “S” is given by equation 3.2.

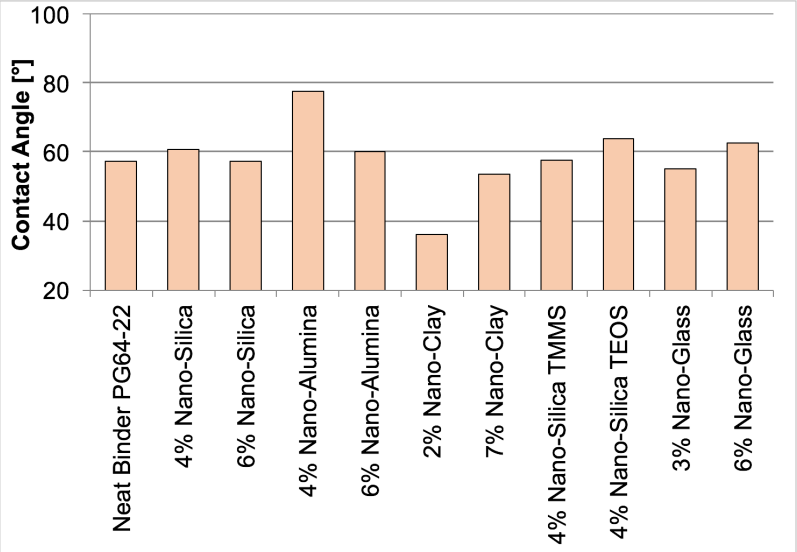

Figure 3.23. Contact Angle of Different Binders with Di-iodomethane

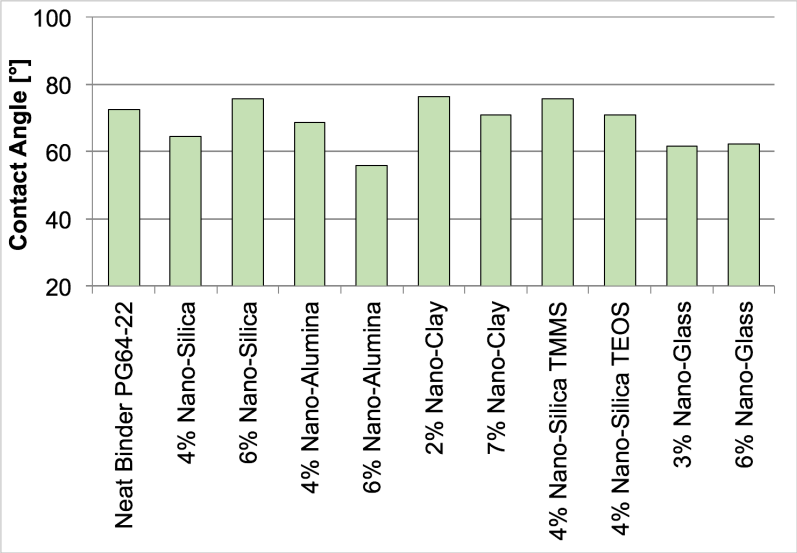

Figure 3.24. Contact Angle of Different Binders with Ethylene Glycol

$$\Delta G_{AS} = 2\sqrt{\gamma_A^{LW}\gamma_S^{LW}} + 2\sqrt{\gamma_A^{+}\gamma_S^{-}} + 2\sqrt{\gamma_A^{-}\gamma_S^{+}} \tag{3.2}$$

In equation 3.2, the superscripts LW, $+$, and $-$ denote the non-polar, acid, and base component of the surface free energies denoted by γ. Also, the interfacial energy between any two solid surfaces denoted by suffixes “A” and “S” is given by equation 3.3.

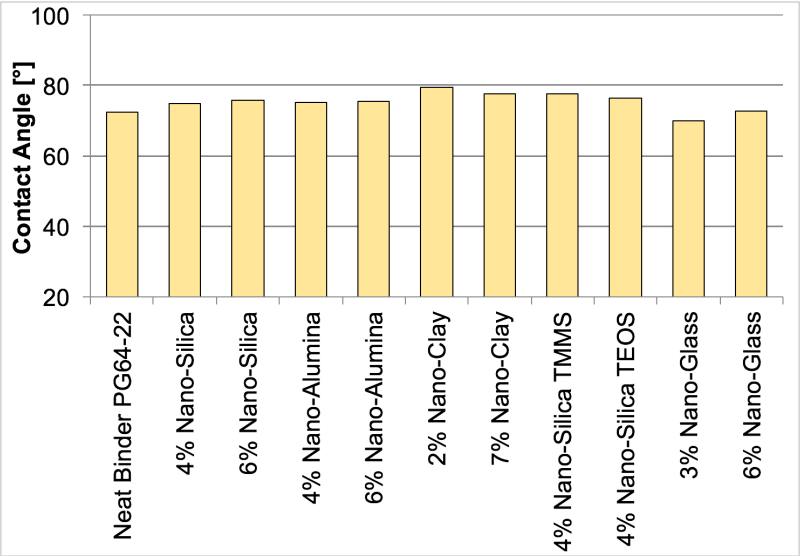

Figure 3.25. Contact Angle of Different Binders with Formamide

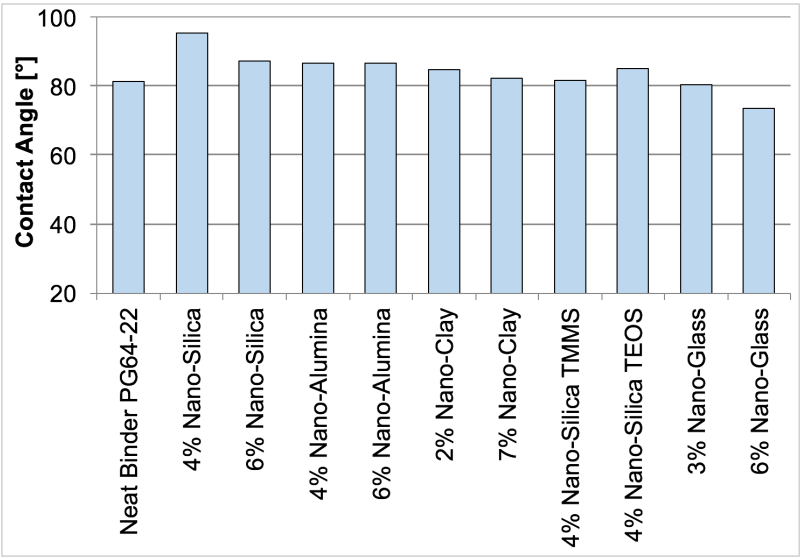

Figure 3.26. Contact Angle of Different Binders with Water

$$\gamma_{AS} = \gamma_A + \gamma_S - 2\sqrt{\gamma_A^{LW}\gamma_S^{LW}} - 2\sqrt{\gamma_A^{+}\gamma_S^{-}} - 2\sqrt{\gamma_A^{-}\gamma_S^{+}} \tag{3.3}$$

Equation 3.4 presents the net work done to displace a unit area of the asphalt-aggregate interface, “AS”, by water and create a unit area of the asphalt-water interface, “AW”, and the aggregate-water interface, “SW”, in terms of their respective interfacial surface energies.

Subscripts "S", "A", and "W" are used to represent the aggregate, asphalt, and water phases, respectively.

$$\Delta G_{WAS} = \gamma_{AW} + \gamma_{SW} - \gamma AS \tag{3.4}$$

The different interfacial surface energies in equation 3.4 can be calculated using expressions similar to equation 3.3. The value of ΔG_{WAS} is typically negative. This indicates that debonding of the asphalt-aggregate interface by water is associated with an overall reduction in free energy of the system and therefore, is thermodynamically favorable. A larger magnitude of ΔG_{WAS} implies a greater reduction in free energy of the system and a greater potential for water to displace asphalt from the aggregate-asphalt interface. Therefore, a low magnitude of reduction in free energy of the system is desirable and indicates better resistance to debonding in the presence of water. The negative value of work required to cause debonding can also be interpreted as the work done "by" the system favoring debonding, and therefore in presence of water, less external work is required to cause the same amount of damage.

The dry adhesive bond energy between asphalt and aggregate, ΔG_{AS}, and the reduction in free energy due to debonding of asphalt-aggregate interface by water, ΔG_{WAS}, are the two key bond energy parameters that can be used to assess moisture sensitivity of any asphalt-aggregate combination in an asphalt mixture. These two parameters are combined into a single indicator referred to as the energy ratio as shown in equation 3.5.

$$R^{Total} = \left| \frac{\Delta G_{AS}}{\Delta G_{WAS}} \right| \tag{3.5}$$

A high magnitude of dry adhesive bond strength and a low magnitude of reduction in free energy when water displaces asphalt from an aggregate surface are desirable in order to promote resistance to moisture induced damage. Therefore, a relatively high value of energy ratio, R^{Total} for an asphalt-aggregate pair suggests better resistance to moisture induced damage. Table 3.1 summarizes the results from these analysis.

Table 3.1. Energy Ratio of Different Asphalt Binders (Control and Nanomaterial Modified) with Different Aggregate Particles Showing Resistance to Moisture Induced Damage

Aggregates	Neat Binder	4% Nano-Silica	6% Nano-Silica	4% Nano-Alumina	6% Nano-Alumina	2% Nano-Clay	7% Nano-Clay	4% Nano-Silica TMMS	4% Nano-Silica TEOS	3% Nano-Glass	6% Nano-Glass
Limestone, Brownwood	0.85	0.74	0.98	0.85	0.87	2.18	1.15	0.99	0.63	0.67	0.72
Traprock, Knippa	0.15	0.10	0.21	0.22	0.21	0.67	0.28	0.23	0.06	0.06	0.11
Limestone, Odessa	0.71	0.61	0.82	0.73	0.74	1.86	0.97	0.83	0.52	0.54	0.59
R Gravel, Murphy	0.39	0.30	0.46	0.44	0.43	1.15	0.57	0.49	0.25	0.26	0.32
River Gravel-2, Murphy	0.57	0.48	0.67	0.61	0.61	1.56	0.80	0.68	0.40	0.42	0.47
Traprock-2, Knippa	0.21	0.14	0.26	0.27	0.25	0.77	0.34	0.29	0.10	0.10	0.16
Granite, Snyder,OK	0.73	0.47	0.77	0.70	0.67	1.69	0.93	0.87	0.52	0.56	0.71
Quartzite, Jones Mill,AK	0.80	0.63	0.89	0.78	0.79	1.99	1.06	0.93	0.59	0.62	0.70
Sandstone, Sawyer,OK	1.44	1.44	1.68	1.35	1.45	3.84	1.93	1.60	1.11	1.19	1.15
R Gravel, Prescott,AK	1.14	1.11	1.33	1.10	1.17	3.00	1.53	1.28	0.87	0.92	0.91
Granite-2, Snyder,OK	0.47	0.42	0.57	0.54	0.54	1.38	0.69	0.58	0.32	0.33	0.37
Sandstone, Sawyer,OK	0.99	0.90	1.14	0.98	1.02	2.52	1.33	1.14	0.75	0.79	0.82
Sandstone-2, Sawyer,OK	0.59	0.51	0.69	0.63	0.64	1.61	0.83	0.71	0.42	0.44	0.48
Limestone, New Braunfels	0.71	0.63	0.83	0.74	0.75	1.89	0.98	0.83	0.52	0.54	0.58

3.7.3 Summary

Previous TxDOT studies have demonstrated that a value of 0.5 or lower indicates a poor mixture performance. There were about four different aggregates (out of 14) that were rated as potentially having moisture damage problems with the control binder. The use of nanosilica at a lower percentage on an average reduced the energy ratio by 17%. While the energy ratios reduced in this case, 8 of the 10 binders that were flagged as acceptable in terms of moisture damage with the control continued to remain acceptable. On the other hand, the use of a higher percentage of nanosilica did show an improvement in the energy ratio. Similarly, the use of nanoalumina, nanoclay, and nanosilica-TEOS also showed an improvement (on an average) in terms of the energy ratio or moisture damage resistance. The only exception to this was nanosilica-TEOS at higher percentage. Finally, the use of nanoglass reduced the moisture damage resistance or energy ratio. However, even with this reduction, 8 out of 10 aggregates that were flagged as acceptable with the control binder continued to remain as acceptable.

CHAPTER 4. PERFORMANCE OF ASPHALT COMPOSITES MODIFIED USING NANOMATERIALS

4.1 OVERVIEW

The use of fine aggregate matrix (FAM) or the mortar portion of an asphalt mixture is to evaluate the properties of the binder as well as the binder-aggregate interaction. The FAM or mortar comprises of fine aggregate particles (passing #16 sieve and asphalt binder) in the same proportions as a typical full asphalt mixture. Since distresses such as fatigue cracking and moisture damage (due to the high surface area of finer particles and higher binder content) are more pronounced in the mortar portion of an asphalt mixture rather than in the coarse aggregate, it is advantageous to use the fine aggregate matrix to evaluate the influence of polymers modifiers, nanomaterials, or anti-stripping agents. The FAM can be tested using a dynamic shear rheometer similar to the asphalt binder. In fact, researchers from this team have developed this method for an implementation project for the TxDOT (4524).

4.2 MATERIALS

4.2.1 Mortar Fatigue Testing Using DSR

For the purpose of mortar testing, two of the 10 materials that had been evaluated previously using binder tests were selected for further evaluation. The first material that was selected was the asphalt binder modified with 6% nanoglass. This was because of the superior performance of nanoglass modified binder over other modified binders in terms of rutting performance and tensile strength at intermediate temperatures, while also slightly improving low temperature cracking resistance. Also, nanoglass is the most cost effective nanomaterial that was identified in this study. The second material that was chosen was the functionalized nanosilica modified with tetraethoxysilane (TEOS). This material showed a reasonable improvement in terms of rutting performance, but was shown to be the most effective nanomaterial modifier at lower temperatures. Low temperature properties (which also are indicators of intermediate temperature ductility and fatigue cracking resistance) are important characteristics desired in asphalt binders. Also in most cases, it is expensive to achieve high performance on the low temperature end. These two materials with a control

binder with no additives were used, for a total of three types of binders. The nanomaterial modified binders were produced by mixing the nanomaterials with the the binder at a concentration of 6% for two hours in the high shear mixer. This procedure was similar to the procedure discussed in Chapter 3. The aggregates used to prepare the mortar composites were obtained from a supplier in Texas. Two different binders were used with each nanomaterial, for a total of 6 materials (two different binder types x two nanomaterials + one unmodified control).

4.2.2 Hamburg Wheel Tracking Device and Overlay Test

In addition to mortar testing, conventional TxDOT laboratory mixture tests were also performed. The Hamburg Wheel Tracking Device (HWTD) was used to assess the rutting resistance and moisture damage resistance of asphalt mixtures, according to the procedure specified in Tex-242-F. This test was performed for asphalt mixtures using the PG 70-22 binder modified with 6% of nanoglass; as this was the most promising scenario in terms of rutting resistance of the asphalt binder based on the MSCR test as well as cost. A mixture with the same PG 70-22 binder was also evaluated using the HWTD, without any nanomaterial to serve as a control for the comparison of mixture performance.

The Overlay Test (OT) was also used to assess the fatigue resistance or reflective cracking of asphalt mixtures, according to the procedure specified in Tex-248-F. Nanoglass was chosen as the modifier for the OT since it showed the best performance in terms of fracture resistance based on the poker chip test. The two mixtures used with the HWTD were also used with the OT.

The control asphalt mixture used for both tests was a 9.5 mm SMA Gap Graded mix, also referred to as a Stone Matrix Asphalt (SMA) mix. One reason to select the SMA type asphalt mixture is because it is typically being used for both structural and surface applications.

Class A aggregates were used for the coarse aggregates (material retained on the No. 8 sieve) and Class B aggregates were used for the fine aggregates. The aggregates were primarily dolomitic in nature. These were obtained from two different sources: Capital Aggregates at the Bolm Road plant and Capital Aggregates Delta at Marble Falls.

4.3 SPECIMEN FABRICATION

4.3.1 DSR FAM Specimens

The gradation used for the mortar specimens was a typical gradation for the fine aggregate component of an asphalt mixture in the state of Texas. This gradation is shown in Table 4.1. All mortars used an asphalt binder content of 8%.

Table 4.1. Gradation Used For Mortar Specimens

Sieve Size	Percent Passed	Percent Retained
No. 16	100	0
No. 30	63.4	36.6
No. 50	37.2	26.2
No. 200	12.5	24.7
Pan	0	12.5

Aggregate samples obtained from the field were sieved and recombined in the proportions indicated in Table 4.1. The aggregates were then heated at 150 °C in a convection oven overnight prior to specimen fabrication to ensure that theese were moisture free. These aggregates were then mixed with the binder at 150 °C, and the loose mixture was left in the oven for 2 hours to simulate short-term aging. After this step, the mixture was placed in the Superpave Gyratory Compactor (SGC), and compacted at the compaction temperature of 120 °C until it was no longer possible to compact the specimen any more, resulting in an approximate air void content of nearly 0%. This was mostly in accordance to Specification (TxDOT Tex-241-F) with the exception of the compaction termination criterion. The compaction termination criterion (compaction until maximum density is reached) was intended to achieve a near 0 percent air voids in the mortar since this is the matrix phase of the asphalt mixture. Approximately 20 specimens were obtained from each specimen generated in the Superpave Gyratory Compactor (SGC). Figure 4.1 shows a typical FAM test specimens cored out of an SGC specimen.

The cylindrical specimens that were cored from the inner core of the SGC specimen were used in this study. The cylindrical specimens had a diameter of 12.5 mm. After coring, the specimens were cut to the target height of 50 mm. Figure 4.2 shows the finished test specimens that were evaluated using the DSR.

After the FAM specimen was fabricated, the ends of each specimen were glued with

Figure 4.1. Typical FAM Test Specimens Cored Out of a Superpave Gyratory Compacted Specimen

Figure 4.2. Typical FAM Test Specimens Cored Out of a Superpave Gyratory Compacted Specimen

a strong epoxy resin to metal plates to ensure proper adhesion between the specimen and the steel plates. These plates served to attach the specimen to the DSR device. Figure 4.3 represents the final configuration of the specimen inside the DSR device.

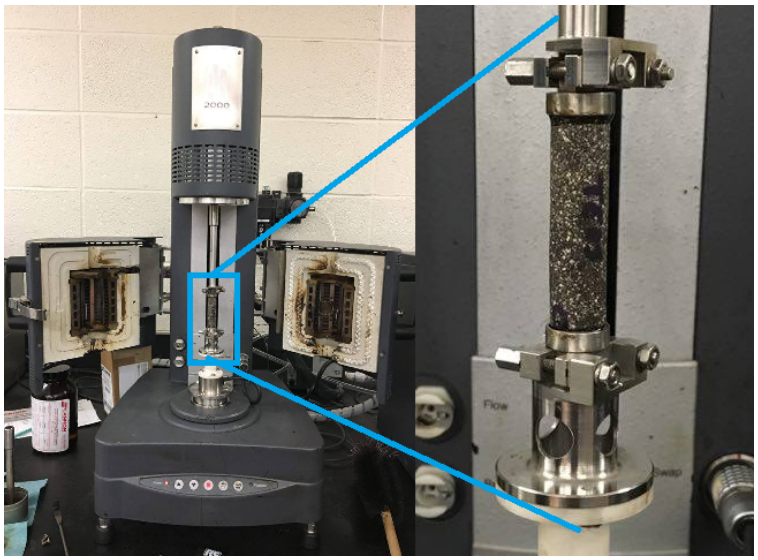

Figure 4.3. FAM Specimen Configuration in the DSR

4.3.2 Hamburg Wheel Tracking and Overlay Specimens

The 9.5 mm SMA Gap Graded mix used for the Hamburg Wheel Tracking (HWTD) and Overlay (OT) specimens was a typical gradation designed for use as a surface mix on a flexible pavement according to TxDOT specifications. This gradation is shown in the Table 4.2 and Figure 4.4.

Table 4.2. Gradation Used For Hamburg Wheel Tracking and Overlay Specimens

Sieve Size	Percent Passed	Percent Retained
1/2 in	100	0
3/8 in	95.0	5.0
No. 4	43.0	52.5
No. 8	24.0	19.0
No. 16	17.0	7.0
No. 30	15.0	2.0
No. 50	13.5	1.5
No. 200	12.5	4.5
Pan	0	9.0

In order to avoid raveling and bleeding in the field, it is crucial to use the optimum binder content in an asphalt mixture. As per TxDOT 2014 Specifications, Item 347 speci-

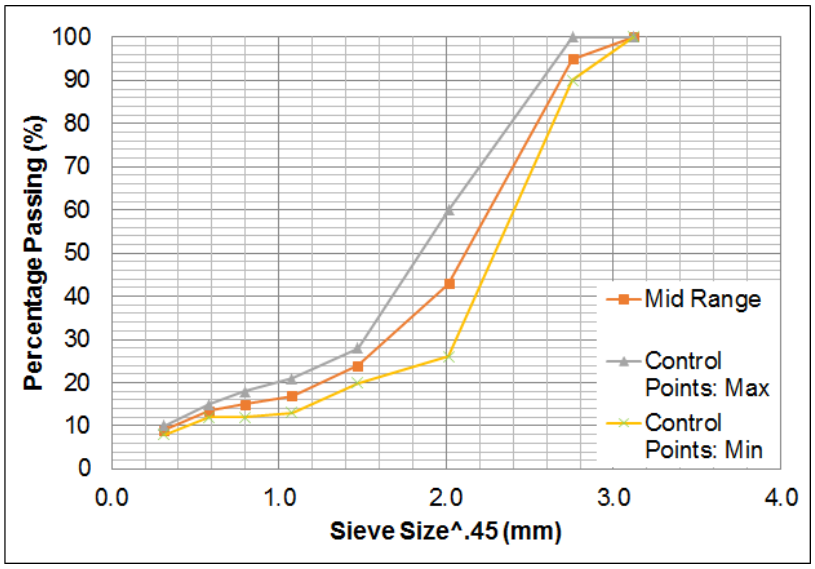

Figure 4.4. Gradation Used For Hamburg Wheel Tracking and Overlay Specimens

fies the criteria to establish the optimum asphalt binder content. For this task, the optimum asphalt binder content was determined using the aforementioned specification. The procedure used to determine the optimum binder content is briefly described below:

1. The asphalt binder was heated inside the oven at 150 °C until the binder was workable and of consistent viscosity throughout the container. This temperature was based on the PG of the asphalt binder (TxDOT Tex-241-F).
2. The aggregates sampled from the field were from different stock piles. For this task, researchers did not use the stock pile gradations to prepare aggregate blends. Instead, aggregates from each stock pile were sieved into different size fractions and recombined following the gradation outlined Table 4.4. Also, aggregate samples obtained from the field had a high dust content. For this study, all aggregates were washed and then used in the mixture design.
3. The washed aggregates were heated overnight inside the oven at 150 °C. This was to ensure that the moisture was removed from the aggregates.
4. The aggregates in their predetermined proportions were mixed with the asphalt binder in the mixer until all the aggregate particles were coated by the asphalt binder.
5. The mixture was placed inside the oven at 135 °C for 2 hours. This temperature simulated short-term aging during mixing, transportation, and compaction in the field. The temperature was selected based on the PG of the asphalt binder (TxDOT Tex-

241-F).

6. After two hours, the mixture was remixed for about 2 minutes to avoid segregation between the aggregates and asphalt binder. During this process it was also ensured that all the aggregate particles were coated by the asphalt binder.
7. Two specimens were prepared at each binder content in the Superpave Gyratory Compactor (SGC). The specimens were used to measure the volumetric bulk specific gravity (G_{mb}) of the asphalt mixture (TxDOT Tex-207-F). The height of each SGC sample was between 110 and 120 mm at N_{design} of 50 gyrations.
8. Two loose mixture samples were also set aside at each binder content in order to obtain the theoretical maximum specific gravity (G_{mm}) of the asphalt mixture (TxDOT Tex-227-F).
9. The air void content was then calculated using the values for G_{mm} and G_{mb}. The air void content vs. binder content was plotted and this plot was used to determine the optimum binder content, which was defined as the binder content at 4% air voids.

The optimum binder content for this 9.5 mm SMA Gap Graded asphalt mixture was determined to be 6.3% by weight. Test specimens for the HWTD and OT were prepared using a similar procedure. The aggregates were heated at 150 °C in a convection oven overnight prior to specimen fabrication to ensure that there was no moisture. The prescribed gradation of aggregates (Table 4.2) was then mixed with the optimum asphalt binder content at 150 °C, and then left in the oven for two hours to simulate short-term aging. The mixture was placed in the SGC as specified in Tex-241-F, and compacted at the compaction temperature of 120 °C until it achieved a target of 7% of air void content for both tests.

As shown in Figure 4.5, the specimens were cut to the correct dimensions following the Specifications Tex-242-F for HWTD and Tex-248-F for OT. Figure 4.6 and Figure 4.7 show the test specimens obtained for HWTD and OT, respectively.

Figure 4.5. Saw Used For Hamburg Wheel Tracking and Overlay Specimens

Figure 4.6. Specimen Used For Hamburg Wheel Tracking Test

Figure 4.7. Specimen Used For Overlay Test

4.4 DESCRIPTION OF THE TEST METHODS

4.4.1 Mortar test using DSR

Although testing a FAM mixture does not provide a direct measurement of the mixture properties, it does present several advantages particularly when the objective of the study is to investigate the effect of different modifiers and/or fillers on the performance of the composite. First, it is faster and is cost efficient to fabricate and test FAM specimens as compared to full asphalt mixtures. Second, the FAM specimens are designed to incorporate fine aggregate particles (typically passing No. 16 ASTM sieve) from the same source and in a relative proportion similar to that of the intended full asphalt mixture. The linear viscoelastic properties and resistance of the test specimens to fatigue cracking were measured at 25 °C using the dynamic shear rheometer (DSR). A frequency sweep was conducted where shear oscillations following a sinusoidal wave form at a low stress amplitude of 25 kPa were applied at different frequencies from 30 to 0.01 Hz to determine the undamaged complex modulus $|G^*|$ and phase angle δ of the FAM specimens. Also a time sweep was conducted in shear oscillation following a sinusoidal waveform with a high stress amplitude of 350 kPa. The time sweep or fatigue test was conducted at a frequency of 10 Hz until specimen failure to determine the fatigue cracking resistance of the mortar specimens.

4.4.2 Hamburg Wheel Tracking

The Hamburg Wheel Tracking Device (HWTD) was used to evaluate premature failure susceptibility of the mixtures due to weakness in the aggregate structure, inadequate binder stiffness, moisture damage, and other factors including inadequate adhesion between the asphalt binder and aggregate of the asphalt mixture. This Test, as described in Tex-242-F, uses a wheel tracking device. It applies a load of 158 lb via a steel wheel that passes over the laboratory compacted test specimens at a constant rate of 50 passes per minute. Following the standard test method, the test was run under water at a constant temperature of 50 °C. Rut depth measurements were taken every 100 passes of the wheel, allowing a maximum rutting of 12.5 mm to be set as a failure criterion for a maximum of 20000 passes of the wheel.

After the HWTD specimens were fabricated using the method described earlier, four specimens were used to create the configuration presented in the Figure 4.8. This configuration simulates two slabs using four specimens, where the wheel load can pass on top of

it. The samples are 6.2 cm in depth and 15.0 cm in diameter and they are cut on the sides to simulate a slab.

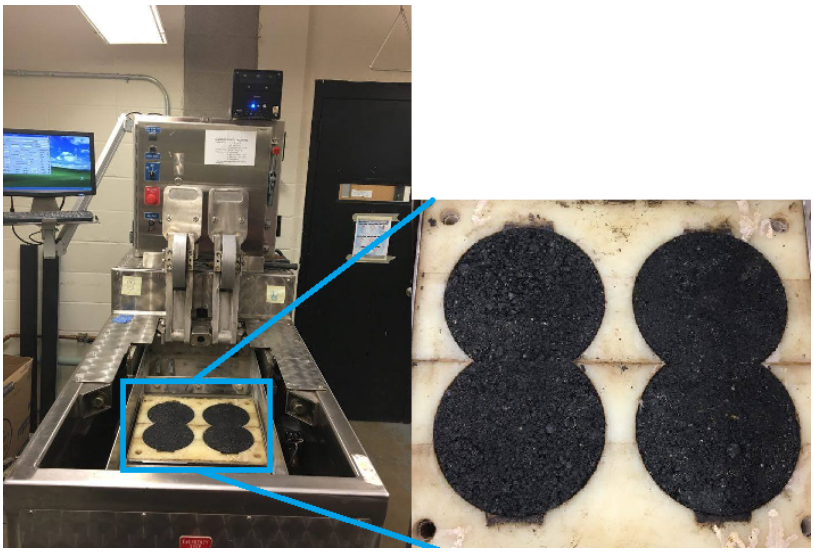

Figure 4.8. HWT Specimen Configuration in the HWTD

4.4.3 Overlay Test

The Overlay Test (OT) was chosen to evaluate the susceptibility of asphalt mixtures to fatigue or reflective cracking. This Test, as described in Tex-248-F, involves using an electro-hydraulic system that applies repeated direct tension loads to specimens. More specifically, this load is applied in a cyclic triangular waveform with a constant maximum displacement of 0.06 cm to asphalt mixtures fabricated in the lab. A sliding block, onto which the specimen is glued, reaches the maximum displacement and then returns to its initial position in 10 second (one cycle).

After the OT specimens were fabricated using the method described earlier, one of the sample faces was glued with a strong epoxy resin to metal plates to ensure proper adhesion between the sample face and the steel plates. The plates with the glued specimen were then attached to a feedback controlled servo hydraulic loading frame as shown in Figure 4.9.

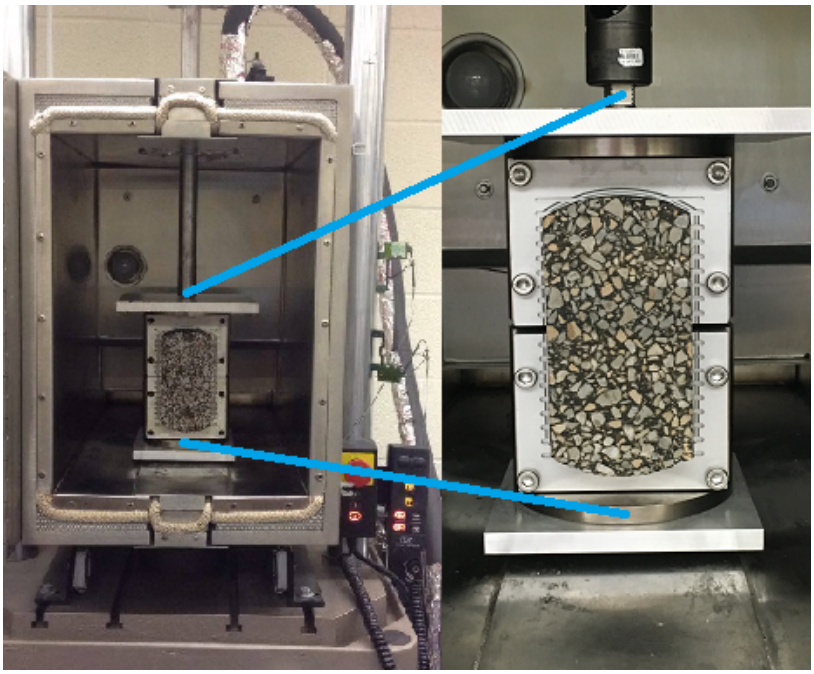

Figure 4.9. Overlay Specimen Configuration in the Servo-Hydraulic Machine

4.5 RESULTS

4.5.1 Results from mortar test using DSR

Frequency sweep testing was performed for all specimens tested in the Dynamic Shear Rheometer. The complex shear modulus of each specimen ($|G^*|$) was measured at frequencies between 0.01 and 30 Hz. The amplitude used to measure this property was 25 kPa. The relationship between complex shear modulus and frequency for the PG 64-22 binder, both as a control and when modified with both nanomaterials, is shown in Figure 4.10. The same plot for the PG 70-22 binder is shown in Figure 4.11.

The complex shear modulus values at 10 Hz are shown for the PG 64 and 70 binders, respectively (Figures 4.12 and 4.13). The phase angles measured at 10 Hz for the same binders are shown in Figures 4.14 and 4.15.

In addition to the frequency sweep testing, a time sweep test was performed on each specimen as well. Between the two tests, the specimen was conditioned at the testing temperature for at least 30 minutes in order to reduce the influence of time history on the frequency sweep test. The time sweep test was used to determine the fatigue life of the specimen. This test involved loading the specimen at a stress amplitude of 350 kPa and at

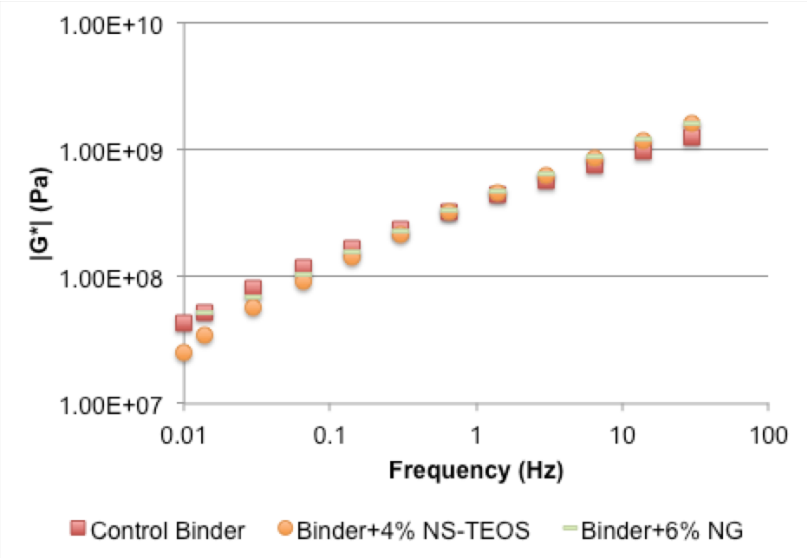

Figure 4.10. Complex Shear Modulus versus Frequency for PG 64-22 Binder

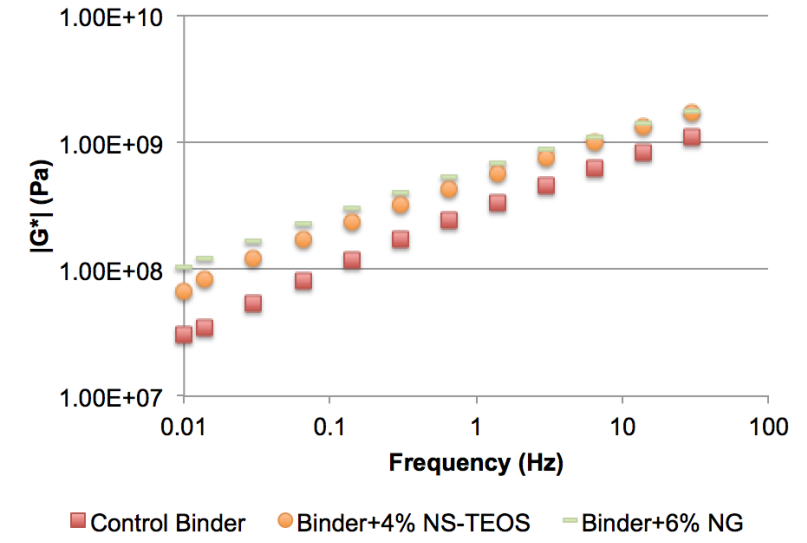

Figure 4.11. Complex Shear Modulus versus Frequency for PG 70-22 Binder

a frequency of 10 Hz. The test continued until the specimen showed a 50% reduction in complex shear modulus from the control value as measured in the frequency sweep test. A typical result of the test is shown in Figure 4.16. The fatigue lives of the PG 64 and PG 70 binders, respectively are shown in Figures 4.17 and 4.18.

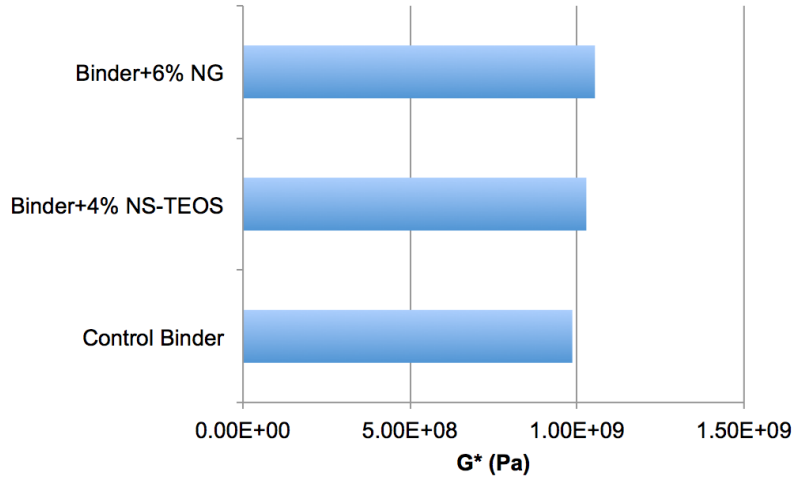

Figure 4.12. Complex Shear Modulus at 10 Hz for PG 64-22 Binder

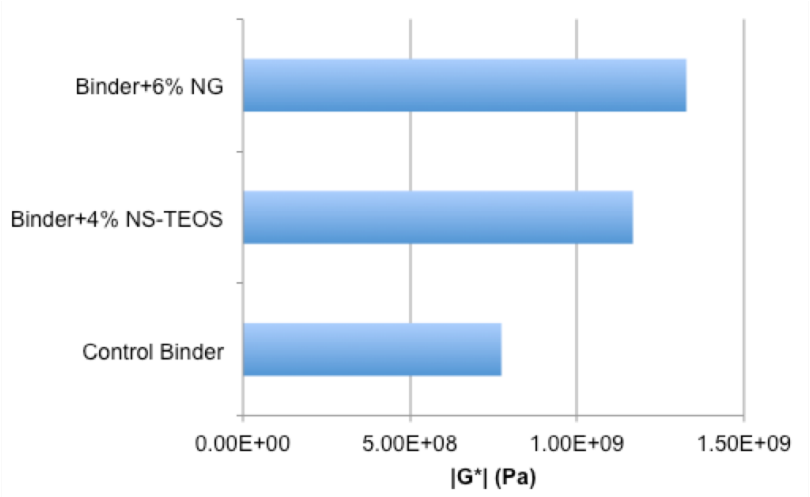

Figure 4.13. Complex Shear Modulus at 10 Hz for PG 70-22 Binder

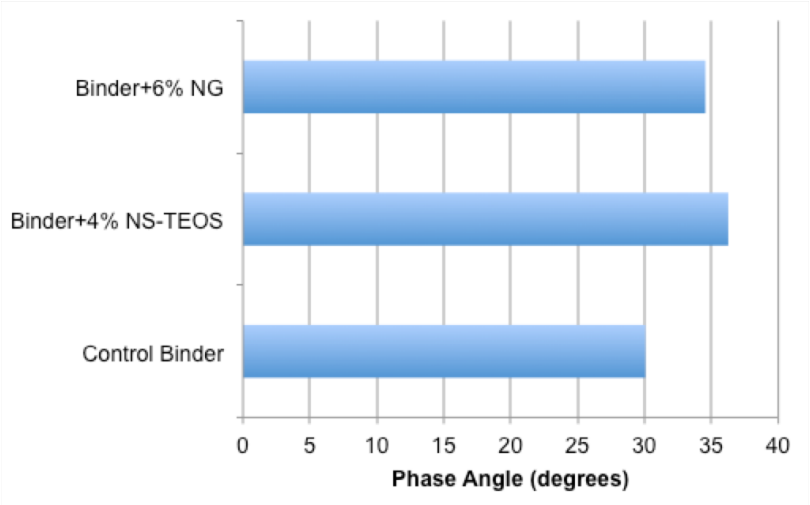

Figure 4.14. Phase Angle at 10 Hz for PG 64-22 Binder

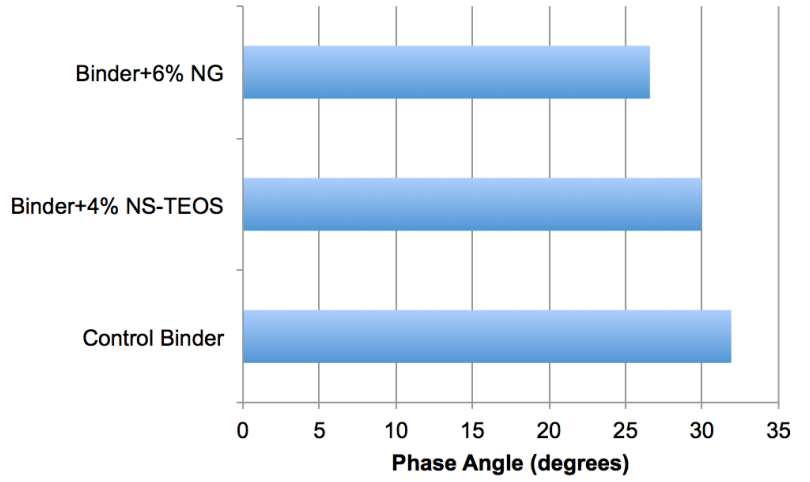

Figure 4.15. Phase Angle at 10 Hz for PG 70-22 Binder

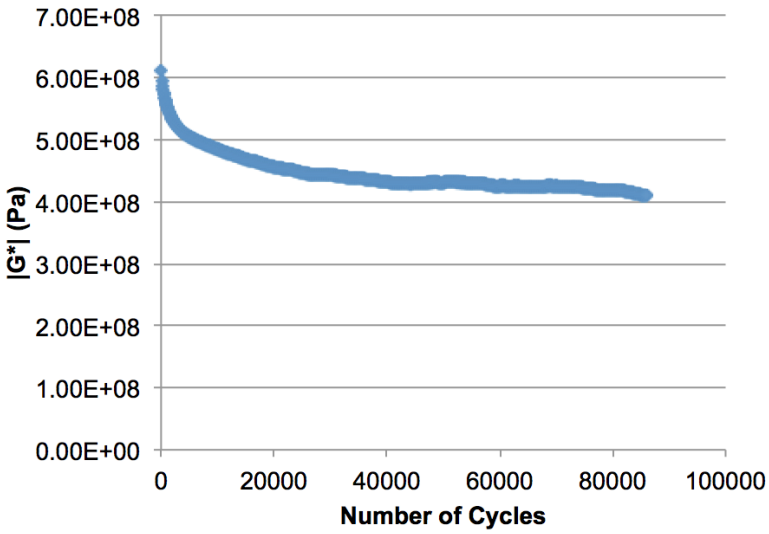

Figure 4.16. Typical Result From Time Sweep FAM Test

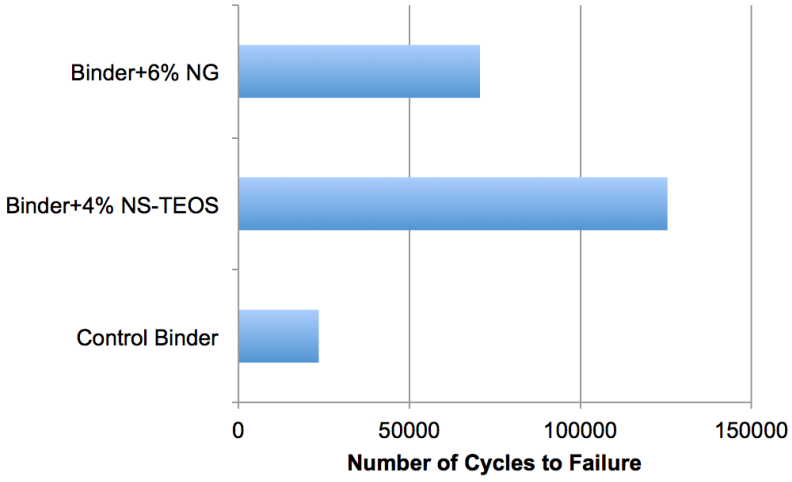

Figure 4.17. Fatigue Life at 10 Hz for PG 64-22 Binder

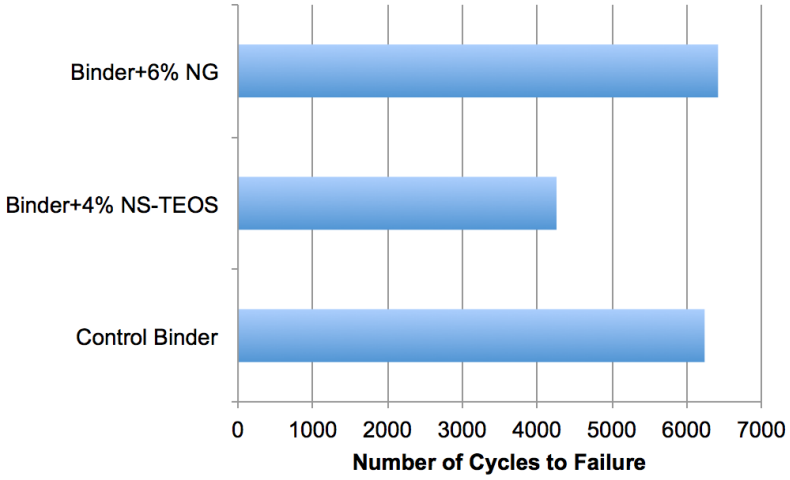

Figure 4.18. Fatigue Life at 10 Hz for PG 70-22 Binder

4.5.2 Results from Hamburg Wheel Tracking Device

As described earlier, HWTD was used to evaluate two mixtures with the same gradation and binder content (9.5 mm SMA Gap Graded mixes) using the control binder PG 70-22 and the same binder modified using 6% nanoglass. Figure 4.19 shows the results obtained.

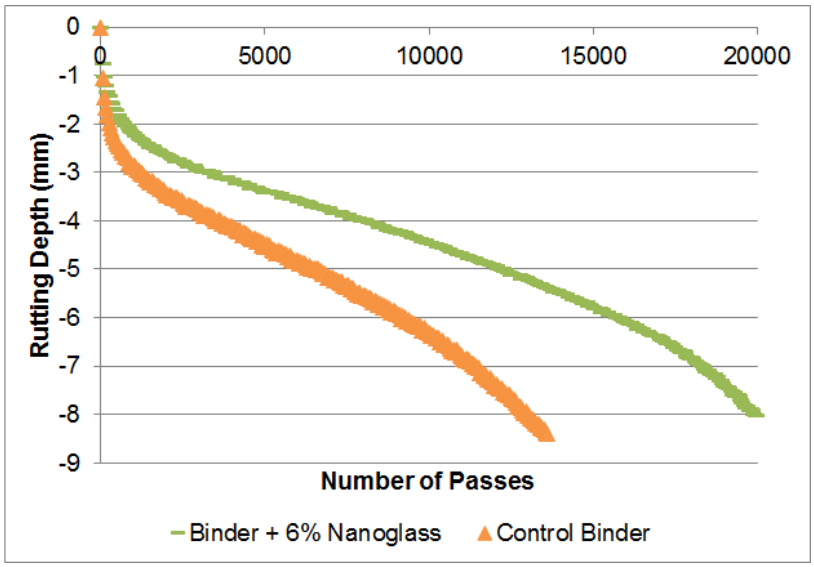

Figure 4.19. Hamburg Wheel Tracking Results

Furthermore, a bar graph is generated to compare the number of load cycles to reach 8.0 mm of rutting. Figure 4.20 shows the number of passes for the asphalt mixture using the base PG 70-22 binder and the asphalt mixture using the same gradation, binder, and binder content but with the binder modified using 6% of nanoglass.

Based on the results from the HWTD it can be concluded that the adhesion between the asphalt binder and aggregate was improved with the addition of 6% of nanoglass. The mixture with the base binder reached a rutting of 8.0 mm at 13,000 cycles and the mixture that used the same binder mixed with 6% of nanoglass achieved that same level of rutting at 19,900 cycles. This shows an improvement of 35% with the nanoglass.

4.5.3 Results from Overlay Test

While the HWTD revealed a significant improvement in regard to rutting performance of the asphalt mixture with nanoglass, less improvement was observed in terms of fatigue cracking resistance, as measured with the OT. In this test, the first cycle is critical, as it

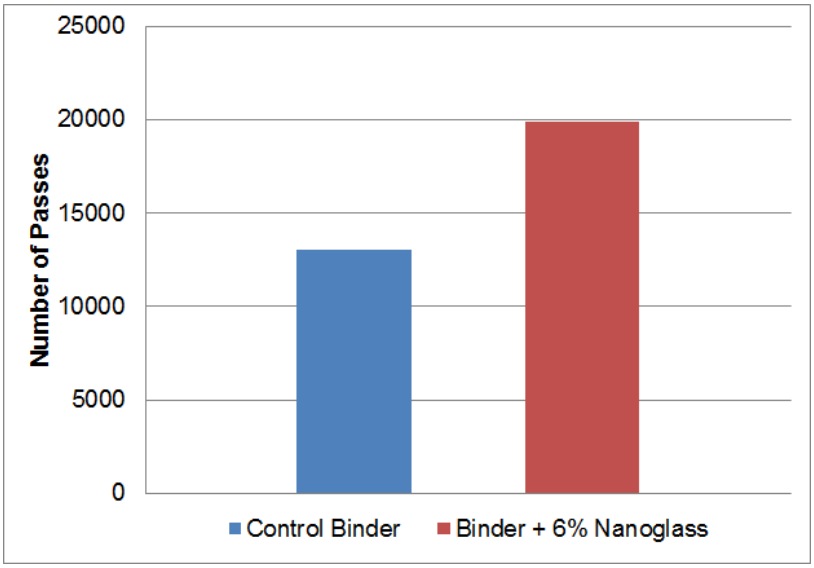

Figure 4.20. Number of Cycles to Reach 8 mm Rutting

provides a measure of the initial behavior of the material before any damage has occurred.

Throughout the course of the test, all four specimens (two replicates of each) lasted the entire 1000 cycles that are specified by TxDOT as the criteria to pass the specification. None of the specimens had any observable cracking. Figure 4.21 shows both the initial and final stiffness indicators for both the control sample and the mixture with nanoglass added to the binder.

Overall, the difference between the two binders in the fatigue cracking resistance based on this test method was observed to be minimal.

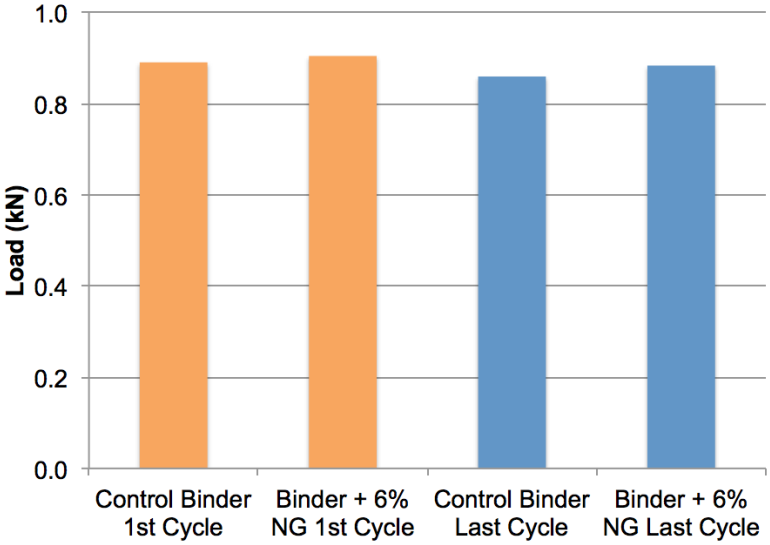

Figure 4.21. Initial and Final Stiffness Indicators as Measured in the Overlay Test

4.6 SUMMARY

Based on the tests performed on asphalt mortars and full asphalt mixtures, the following conclusions are drawn:

1. Nanoglass showed significant improvement in the rutting resistance of the binder. This was confirmed by the binder testing, which showed an improvement in the high temperature grade of the binder upon addition of the nanoglass. Considering these were two different binders, this improvement is further validated.
2. Fatigue cracking resistance was less affected by the addition of both nanomaterials. At high frequencies, minimal change in the fatigue cracking parameter, $|G^*|sin(\delta)$, was observed based on frequency sweep testing. Additionally, the overlay test showed a minimal change in the load reached by the mixture, and the change in load throughout the test, confirming that nanoglass has a small positive effect on fatigue cracking resistance.

CHAPTER 5. COST ANALYSIS, USAGE GUIDE, AND SUMMARY

5.1 COST ANALYSIS

Based on a review of the literature, various nanomaterials were chosen as potential candidates for binder modification. The initial objective of this project was to investigate carbon nanotubes (CNTs) as a modifier for asphalt binders. However, owing to the high price of CNTs ($450/kg), only a small amount i.e., 0.2% by weight of the binder, could be justified. To put this into perspective, modifying 1 MT of asphalt binder using 0.2% CNT would require 2 kg of CNT costing about $900. Given that the current cost of asphalt binder (as of this writing) is in the range of $400 /MT, addition of CNT even at such small doses can double or triple the cost of the binder. As such, even with future price reductions or use of lower quality CNT, the cost of the CNT modified binder is likely to remain very high compared to traditional modifiers.

Owing to the aforementioned fiscal constraint and based on inputs from the Project Monitoring Committee at TxDOT, additional lower cost nanomaterials were considered for evaluation. These nanomaterials were selected based on a detailed review of the literature, as summarized in a previous chapter. Four additional nanomaterials were selected, and each one was evaluated at two concentrations: a high concentration and a low concentration. The high and low concentration for each nanomaterial was determined based on a review of the literature.

Table 5.1 presents the approximate cost of the different nanomaterials considered in this study. The cost of asphalt mixtures produced using these nanomaterial modified binders was also computed and compared to the cost of a mix using unmodified binder. The following assumptions were used in this cost analysis:

- The cost of nanomaterials when used in bulk quantities is expected to be much less than cost typically associated with smaller procurement; as such the cost of the nanomaterials was assumed to be 50% of the cost listed in Table 5.1.
- A typical asphalt mix was assumed with 5% binder content.
- The cost of asphalt binder was assumed at $450 per ton.
- The cost of aggregate was assumed to be $15 per ton.
- Additional production costs associated with handling and mixing are not accounted for.

Table 5.2 presents a summary from the above analysis. This table summarizes the

percentage increase in cost of an asphalt mixture with the use of the nanomaterial as a modifier compared to the cost the same mixture without any nanomaterial.

Table 5.1. Nanomaterials cost (in USD) per kilogram

Nanomaterial	Cost ($/kg)
CNT	450
Nanoclay	126
Nanosilica	166
Nanoalumina	179
Nanoglass	1.11
TEOS-modified silica	192
TMMS-modified silica	196

Table 5.2. Cost estimates (in USD) per ton of nano-modified hot mix asphalt (HMA) at low and high percentages of Nanomaterials

Nanomaterial	Percentage	Percent increase in cost of HMA at low %	Percent increase in cost of HMA at high %
CNT	0.2%, and 1.5%	60	450
Nanosilica	4%, and 6%	443	664
Nanoalumina	4%, and 6%	477	716
Nanoclay	2%, and 7%	168	588
Nanoglass	3%, and 6%	2	4
TEOS-modified silica	4%, and 6%	512	768
TMMS-modified silica	4%, and 6%	523	784

Results from rheological and dispersion studies conducted concluded that nano-glass and TEOS-modified silica showed improved properties for the asphalt mix. Based on this and the percent increase in cost of the nanomaterial modified asphalt mixture shown in Table 5.2, it appears that nanoglass as developed and produced at UT-Pan American is affordable and results in significant enhancement.

5.2 A GUIDE FOR FUTURE RESEARCH OR PRACTICAL IMPLEMENTATION OF NANOMATERIAL-MODIFIED BINDERS

This section is intended to serve as a general guide for preparation, handling, and use of nanomaterials to modify asphalt binders. It must be emphasized that these steps are not exhaustive in terms of all safety precautions that must be taken while handling nanomaterials or asphalt binders. Users are encouraged to carefully understand the safety and health risks through material safety data sheets and other relevant documentation prior to handling nanomaterials and asphalt binders.

5.2.1 Method to add nanomaterials to asphalt binder through carrier fluids: A few critical considerations

As discussed earlier, one of the main challenges of using nanomaterials in asphalt binder is to properly disperse the nanoparticles throughout the binder. Various dispersion mediums can be considered as carriers, e.g., water, flux oil and kerosene. Nanomaterials can also be directly added and dispersed in the binder.

5.2.1.1 Water

Foamed asphalt binder production is a common method to produce warm mix asphalt. Nanomaterials can be effectively dispersed in water and therefore it is possible to use such a concentrate of water to blend nanomaterials with the asphalt binder during the production of foamed asphalt. A critical aspect to consider this approach is the concentration of the target nanomaterial in the water-nanomaterial concentrate. Based on the results from existing literature as well as the tests conducted in this study, it appears that in almost all cases the concentrations of nanomaterials required to make a significant impact on the performance of are too high to result in a low viscosity workable aqueous medium. For example, addition of 5% by weight of nanomaterial to the asphalt binder and use of 2% water by weight of the binder would imply that the nanomaterial-water concentrate be prepared using a nanomaterial concentration that is over 70% by weight of water. At such high concentrations, the water-nanomaterial concentrate will cause trouble in foam production with spray nozzles. Furthermore, the spraying process produces aerosol droplets, which can carry the nanomaterials into the air. Most nanoparticles have been identified with health hazards from inhalation, and thus it would require adequate precautions to prevent vapors from escaping into the open atmosphere. For these stated reasons, the use of water as a

dispersant was ultimately discarded in this study and may not be a feasible mode of adding nanoparticles unless a nanoparticle that can significantly improve binder performance at extremely low concentrations can be discovered in the future.

5.2.1.2 Flux Oil

In order to ensure dispersion of nanomaterials in the asphalt binder, flux oil can also considered as a possible carrier or dispersant. The dispersion method involves mixing CNTs or other nanomaterials with flux oil using a high-shear mixer for two hours at elevated temperatures. Based on the findings from this study, flux oil up to 10% by weight of the binder may be required. Depending on the target concentration of the nanomaterial in the asphalt binder, appropriate nanomaterial to flux oil concentration must be determined to prepare the concentrate. In this study, the flux oil blend would contain about 30 to 50% by weight of the nanomaterial. Once this flux oil blend is prepared, it can then be added to the virgin asphalt binder to prepare a nanomaterial modified asphalt binder. It must be noted that different types and sources of flux oils will result in different levels of dispersion and resulting binder performance. Irrespective of the source and type, the flux oil selected to serve as a dispersant must have a similar (low) viscosity to enable dispersion and delivery of nanomaterials. Based on the experience from the materials included in this study, the influence of flux oil on the binder properties was more significant compared to the benefits of dispersing the nanomaterials. However, this may not be universally true for all flux oil - nanomaterial - binder combinations.

5.2.1.3 Kerosene

Kerosene has a low viscosity at room temperature and easy to use as a dispersant for nanomaterials at room temperature. It also has a low boiling point, which would make it possible to remove it from the binder-nanomaterial blend after dispersion. However, it was determined that this method would not be suitable due to safety concerns and is generally not recommended for use with asphalt binders. Specifically, kerosene has a low flash point (38 to 72 °C) and autoignition point (220 °C). Any mixing with asphalt binder will have to take place at temperatures higher than 150 °C, which is much higher than the flash point. Therefore, kerosene was ruled out as a potential carrier of nanomaterials.

5.2.2 Direct mixing of nanomaterials in the asphalt binder

As discussed above, flux oil, water, and kerosene are generally unsuitable or unsafe for use as a dispersant for nanomaterials. However, it is possible that flux oil or water may be used as dispersing agents if highly effective nanomaterials were to become available in the future. Direct dispersion of the nanomaterials in the binder was found to be most practical, cost-effective, and safe. The direct dispersion of nanomaterials can be achieved by blending the materials with binder in a high shear mixer at 2400 rpm at 150 °C. This temperature may be adjusted based on the mixing temperature of the specific base binder that is being used.

5.2.3 A screening tool to evaluate ability of nanomaterials to disperse in asphalt binders

Asphalt binders are primarily comprised of hydrocarbons with complex and varying molecular composition. The key to the successful use of a nanomaterial is its ability to effective disperse in the medium. The dispersion of nanoparticles in the asphalt binder is dependent on the physico-chemical interaction between the binder and the nanoparticles. Nanoparticles that do not disperse and form micrometer sized agglomerates are not as effective in improving binder properties. In such cases, these particles at best play the role of an active filler (albeit an expensive one). In other words, as a first step it is important to ensure that effective dispersion of these particles is achieved in the asphalt binder. As evidenced from the research documented in this study, evaluating the dispersion of nanoparticles in a dark soft medium such as asphalt binders is extremely challenging. To overcome this challenge, this research also developed a rapid technique to evaluate the ability of a nanomaterial to disperse in the asphalt binder matrix. This technique is summarized in this section and can be employed with other nanomaterials in the future.

The potential for dispersion of any given nanomaterial in asphalt binder can be evaluated using surrogate solvents that mimic the physico-chemical environment of the asphalt binder. Although the viscosity of these surrogate solvents at room temperature is less than the viscosity of the binder even at its mixing temperature, this was considered as the best or ideal scenario to evaluate dispersion of nanomaterials in the viscous and complex binder material. To represent the polar character of the asphalt binder, five solvents were chosen based on American Society of Testing and Materials standard method (ASTM D4124-09). This method is used to obtain four defined fractions from petroleum asphalts based on their polarity. The four fractions are referred to as saturates, naphthene aromatics, polar aromat-

ics, and iso-octane insoluble asphaltenes. The solvents used in this method to separate the four fractions of asphalt are listed below:

- Methanol
- Iso-octane
- Toluene
- TCE
- n-Heptane

Note that of these five solvents, methanol is extremely polar and does not necessarily represent the physico-chemical environment of any typical asphalt binder. The use of methanol is only to evaluate the extreme case of dispersion of nanomaterials in asphalt binders. The procedure to evaluate the best case scenario for the dispersion of nanomaterials in an asphalt binder "like" environment is as follows.

Prepare a 0.2% by weight suspension by adding the nanomaterial of interest to 50 ml of each of the solvents. Disperse the mixtures in an ultrasonication bath (e.g. Bransonic, Danbury, CT) for one hour. Collect an aliquot of the suspension from 1 to 1.5 cm below the top surface of the solvent and characterize it using dynamic light scattering (DLS) system (e.g. ALV-CGS-3 goniometer system, ALV-GmbH, Langen, Germany) equipped with a 632.8 nm laser (ALV CGS-3 goniometer system, Langen, Germany). In such systems, scattered light is typically detected at 90° and converted to hydrodynamic radii (HDR) employing an auto-correlator and cumulant analysis. Collect the HDR every 15 seconds for a 25 minute duration. The HR in the solvents (other than methanol) provides the best case scenario for the dispersion of nanomaterials in the asphalt binder. For example, in some cases observed in this study, nanoparticles did not fully disperse in the solvents (except methanol) and formed agglomerates that were several micrometers in size, approaching the size of typical filler particles.

Safe handling of nanomaterials

Exposure to nanomaterials may pose health risks via direct and indirect contact and exposure. Protective measures, e.g., technical, organizational, and personal protection measures could be applied to control and minimize exposure. Other important tools for risk management include occupational exposure limits for nanomaterials and classification and labeling of nanomaterials. The low solubility of many nanomaterials (e.g., particles, tubes and their agglomerates and aggregates) in water and biological fluids may prove to be an additional hazard in occupational environments. Engineering controls, including enclosure, local ex-

haust ventilation (LEV), and general ventilation are important instruments to preventing exposure. If the nanomaterial sources cannot be enclosed, LEV with different types of hoods, depending on the requirements of the process can be used. Local ventilation has to be assisted by general ventilation systems. Maintenance of such systems is also an important consideration. An appropriate filtration system has to be used to remove NMs from the exhaust air, preferably with multi-stage filters having high-efficiency particulate air filter (HEPA) or ultra-low penetration air filters (ULPA). Personal protective equipment (PPEs), including gloves, masks, and coats, are also important to minimize exposure to nanomaterials. PPEs like respirators should demonstrate high filtration efficiency, chemical resistance, good fit, easy maintenance, and long wear time. Administrative controls can be wide ranging. NM health and safety should be incorporated into the occupational safety plan and usage protocols. Nanomaterial handling training should be provided to the personnel involved. Control banding for assessing the risks from nanomaterials with unknown exposure levels should be considered.

5.3 CONCLUDING REMARKS

This study evaluated the feasibility of effectively dispersing several different types of nanomaterials to modify asphalt binders in an effort to improve the performance of the resulting asphalt mixtures. Initially the study was focused on the use of carbon nanotubes. However, owing to the cost of these nanomaterials and based on a review of the literature, the study was expanded to include other nanomaterials. These were nanosilica, nanoclay, nanoalumina, and nanoglass. In an effort to improve dispersion, nanosilica was also surface functionalized using two different agents. Several techniques were used to evaluate the mixing conditions required to disperse nanomaterials as well as to assess the extent of dispersion of these nanomaterials. Direct observations with SEM, AFM and mechanical tests, as well as indirect observations in reference solvents showed that in most cases nanomaterials do not disperse as nanometer sized particles but rather form agglomerates that are several micrometers in size. Under such circumstances, the benefits of using nanomaterials are rather limited. Amongst the nanomaterials used in this study, nanoglass was the only material that could achieve the highest degree of dispersion with aggregates not exceeding nanometer length scale, was cost-effective, and demonstrated improvement in mechanical properties as observed using the binder, mortar, and mixture tests. This study also presented procedures to rapidly evaluate whether dispersion can be achieved by the nanomaterials in an asphalt binder as a screening tool before subscribing to the use of such

materials for material property enhancement.

REFERENCES

Aich, N., Boateng K., L., Flora, J. R. V., and Saleh, N. B. 2013. Preparation of non-aggregating aqueous fullerenes in highly saline solutions with aÂ biocompatible non-ionic polymer. *Nanotechnology*, 24(39):395602.

Al-Adham, K. H. and Arifuzzaman, M. D. 2014. Moisture damage evaluation in carbon nanotubes reinforced asphalts. *Sustainability, Eco-efficiency, and Conservation in Transportation Infrastructure Asset Management*, page 103.

Björnström, J., Martinelli, A., Matic, A., Börjesson, L., and Panas, I. 2004. Accelerating effects of colloidal nano-silica for beneficial calcium silicate hydrate formation in cement. *Chemical Physics Letters*, 392(1):242–248.

Campillo, I., Guerrero, A., Dolado, J. S., Porro, A., Ibáñez, J. A., and Goñi, S. 2007. Improvement of initial mechanical strength by nanoalumina in belite cements. *Materials Letters*, 61(8-9):1889–1892.

Cao, L., Sahu, S., Anilkumar, P., Bunker, C. E., Xu, J., Fernando, K. A. S., Wang, P., Guliants, E. A., Tackett, K. N., and Sun, Y.-P. 2011. Carbon Nanoparticles as Visible-Light Photocatalysts for Efficient CO2 Conversion and Beyond. *Journal of the American Chemical Society*, 133(13):4754–4757.

Cheng, J., Shen, J., and Xiao, F. 2011. Moisture susceptibility of warm-mix asphalt mixtures containing nanosized hydrated lime. *Journal of Materials in Civil Engineering*, 23(11):1552–1559.

Crudden, J. J., Lazzaro, J. V., and Welch, E. K. 2011. Antimicrobial cements and cementitious compositions.

Diab, A., You, Z., and Wang, H. 2013. Rheological Evaluation of Foamed WMA Modified with Nano Hydrated Lime. *Procedia-Social and Behavioral Sciences*, 96:2858–2866.

Fakhim, B., Hassani, A., Rashidi, A., and Ghodousi, P. 2015. Preparation and microstructural properties study on cement composites reinforced with multi-walled carbon nanotubes. *Journal of Composite Materials*, 49(1):85–98.

Fang, C., Yu, R., Liu, S., and Li, Y. 2013. Nanomaterials Applied in Asphalt Modification: A Review. *Journal of Materials Science & Technology*, 29(7):589–594.

Gao, D., Sturm, M., and Mo, Y. L. 2009. Electrical resistance of carbon-nanofiber concrete. *Smart Materials and Structures*, 18(9):95039.

Ge, Z. and Gao, Z. 2008. Applications of nanotechnology and nanomaterials in construction. *First Inter. Confer. Construc. Develop. Countries*, pages 235–240.

Gkikas, G., Barkoula, N.-M., and Paipetis, A. S. 2012. Effect of dispersion conditions on the thermo-mechanical and toughness properties of multi walled carbon nanotubes-reinforced epoxy. *Composites Part B: Engineering*, 43(6):2697–2705.

Han, B., Yu, X., and Kwon, E. 2009. A self-sensing carbon nanotube/cement composite for traffic monitoring. *Nanotechnology*, 20(44):445501.

Hansen, C. M. and Beerbower, A. 1971. Solubility parameters. *Kirk-Othmer Encyclopedia of Chemical Technology*, 2:889–910.

Huang, Y. Y. and Terentjev, E. M. 2012. Dispersion of carbon nanotubes: mixing, sonication, stabilization, and composite properties. *Polymers*, 4(1):275–295.

Jahromi, S. G. and Khodaii, A. 2009. Effects of nanoclay on rheological properties of bitumen binder. *Construction and Building Materials*, 23(8):2894–2904.

Jayapalan, A. R., Lee, B. Y., and Kurtis, K. E. 2009. Effect of nano-sized titanium dioxide on early age hydration of Portland cement. In *Nanotechnology in Construction 3*, pages 267–273. Springer.

Jo, B.-W., Kim, C.-H., Tae, G.-h., and Park, J.-B. 2007. Characteristics of cement mortar with nano-SiO< sub> 2</sub> particles. *Construction and Building Materials*, 21(6):1351–1355.

Kemp, K. C., Seema, H., Saleh, M., Mahesh, K., Chandra, V., and Kim, K. S. 2013. Environmental applications using graphene composites: Water remediation and gas adsorption. *Nanoscale*.

Khan, I. A., Flora, J. R. V., Afrooz, A. R. M. N., Aich, N., Schierz, P. A., Ferguson, P. L., Sabo-Attwood, T., and Saleh, N. B. 2015. Change in chirality of semiconducting single-walled carbon nanotubes can overcome anionic surfactant stabilisation: a systematic study of aggregation kinetics. *Environmental Chemistry*, 12(6):652–661.

Khattak, M. J., Khattab, A., Rizvi, H. R., and Zhang, P. 2012. The impact of carbon nano-fiber modification on asphalt binder rheology. *Construction and Building Materials*, 30:257–264.

Konsta-Gdoutos, M. S., Metaxa, Z. S., and Shah, S. P. 2010. Highly dispersed carbon nanotube reinforced cement based materials. *Cement and Concrete Research*, 40(7):1052–1059.

Kordkheili, H. Y., Shehni, S. E., and Niyatzade, G. 2015. Effect of carbon nanotube on physical and mechanical properties of natural fiber/glass fiber/cement composites. *Journal of Forestry Research*, 26(1):247–251.

Lee, J., Mahendra, S., and Alvarez, P. J. J. 2010. Nanomaterials in the construction industry: a review of their applications and environmental health and safety considerations. *ACS nano*, 4(7):3580–3590.

Li, G. Y., Wang, P. M., and Zhao, X. 2005. Mechanical behavior and microstructure of cement composites incorporating surface-treated multi-walled carbon nanotubes. *Carbon*, 43(6):1239–1245.

Li, G. Y., Wang, P. M., and Zhao, X. 2007. Pressure-sensitive properties and microstructure of carbon nanotube reinforced cement composites. *Cement and Concrete Composites*, 29(5):377–382.

Li, H. and Zhang, X. 2015. Research on Properties of Graphite Oxide Nano-fine Particles Modified Asphalt. *International Journal of engineering Research and Applications*, 5(6):119–121.

Li, Z., Wang, H., He, S., Lu, Y., and Wang, M. 2006. Investigations on the preparation and mechanical properties of the nano-alumina reinforced cement composite. *Materials Letters*, 60(3):356–359.

Liu, C. H., Zhang, H. L., Li, S., and Zhu, C. Z. 2014. The Effect of Surface-modified Nano-titania on the Ultraviolet Aging Properties of Bitumen. *Petroleum Science and Technology*, 32(24):2995–3001.

Liu, X., Chen, L., Liu, A., and Wang, X. 2012. Effect of nano-CaCO3 on properties of cement paste. *Energy Procedia*, 16:991–996.

Liu, Y., Wang, X., Yang, F., and Yang, X. 2008. Excellent antimicrobial properties of mesoporous anatase TiO< sub> 2</sub> and Ag/TiO< sub> 2</sub> composite films. *Microporous and Mesoporous Materials*, 114(1):431–439.

Ma, W., Liu, L., Zhang, Z., Yang, R., Liu, G., Zhang, T., An, X., Yi, X., Ren, Y., and Niu, Z. 2009. High-strength composite fibers: realizing true potential of carbon nanotubes in polymer matrix through continuous reticulate architecture and molecular level couplings. *Nano letters*, 9(8):2855–2861.

Metaxa, Z. S., Konsta-Gdoutos, M. S., and Shah, S. P. 2009. Carbon nanotubes reinforced concrete. *ACI Special Publication*, 267.

Metaxa, Z. S., Konsta-Gdoutos, M. S., and Shah, S. P. 2013. Carbon nanofiber cementitious composites: effect of debulking procedure on dispersion and reinforcing efficiency. *Cement and Concrete Composites*, 36:25–32.

Min, Y., Akbulut, M., Kristiansen, K., Golan, Y., and Israelachvili, J. 2008. The role of interparticle and external forces in nanoparticle assembly. *Nat Mater*, 7(7):527–538.

Musso, S., Tulliani, J.-M., Ferro, G., and Tagliaferro, A. 2009. Influence of carbon nanotubes structure on the mechanical behavior of cement composites. *Composites Science and Technology*, 69(11):1985–1990.

Nazari, A. 2011. The effects of curing medium on flexural strength and water permeability of concrete incorporating TiO2 nanoparticles. *Materials and Structures*, 44(4):773–786.

Nazari, A. and Riahi, S. 2011a. Improvement compressive strength of concrete in different curing media by Al2O3 nanoparticles. *Materials science & engineering. A, Structural materials: properties, microstructure and processing*, 528(3):1183–1191.

Nazari, A. and Riahi, S. 2011b. The effects of zinc dioxide nanoparticles on flexural strength of self-compacting concrete. *Composites Part B: Engineering*, 42(2):167–175.

Nazari, A., Riahi, S., Riahi, S., Shamekhi, S. F., and Khademno, A. 2010a. Embedded ZrO2 nanoparticles mechanical properties monitoring in cementitious composites. *Journal of American Science*, 6:86–89.

Nazari, A., Riahi, S., Riahi, S., Shamekhi, S. F., and Khademno, A. 2010b. The effects of incorporation Fe2O3 nanoparticles on tensile and flexural strength of concrete. *Journal of American Science*, 6(4):90–93.

Nazari, A., Sh, R., Shamekhi, S. F., and Khademno, A. 2010c. Benefits of Fe2O3 nanoparticles in concrete mixing matrix. *Journal of American Science*, 6(4):102–106.

Nazari, A., Sh, R., Shamekhi, S. F., and Khademno, A. 2010d. Influence of Al2O3 nanoparticles on the compressive strength and workability of blended concrete. *Journal of American Science*, 6(5):6–9.

Nazari, A. H. and Riahi, S. 2011c. Effects of CuO nanoparticles on microstructure, physical, mechanical and thermal properties of self-compacting cementitious composites. *Journal of Materials Science & Technology*, 27(1):81–92.

Pillai, S., Catchpole, K. R., Trupke, T., and Green, M. A. 2007. Surface plasmon enhanced silicon solar cells. *Journal of applied physics*, 101:93105.

Quercia, G., Spiesz, P., Hüsken, G., and Brouwers, J. 2012. Effects of amorphous nanosilica additions on mechanical and durability performane of SCC mixtures.

Saleh, N. B., Pfefferle, L. D., and Elimelech, M. 2008. Aggregation kinetics of multiwalled carbon nanotubes in aquatic systems: measurements and environmental implications. *Environmental science & technology*, 42(21):7963–7969.

Saleh, N. B., Pfefferle, L. D., and Elimelech, M. 2010. Influence of biomacromolecules and humic acid on the aggregation kinetics of single-walled carbon nanotubes. *Environmental Science & Technology*, 44(7):2412–2418.

Santagata, E., Baglieri, O., Tsantilis, L., and Dalmazzo, D. 2012. Rheological characterization of bituminous binders modified with carbon nanotubes. *Procedia-Social and Behavioral Sciences*, 53:546–555.

Sedaghat, A., Ram, M. K., Zayed, A., Kamal, R., and Shanahan, N. 2014. Investigation of physical properties of graphene-cement composite for structural applications. *Open Journal of Composite Materials*, 2014.

Sobolev, K., Flores, I., Hermosillo, R., and Torres-Martínez, L. M. 2006. Nanomaterials and nanotechnology for high-performance cement composites. *Proceedings of ACI Session on Nanotechnology of Concrete: Recent Developments and Future Perspectives, Denver, USA*.

Sun, W., Jiang, H., and Wang, C. 2014. Effects of carbon nanotubes on mechanical and 2D-3D microstructure properties of cement mortar. *Journal of Wuhan University of Technology-Mater. Sci. Ed.*, 29(3):513–517.

Xiao, F., Amirkhanian, A. N., and Amirkhanian, S. N. 2010. Influence of carbon nanoparticles on the rheological characteristics of short-term aged asphalt binders. *Journal of Materials in Civil Engineering*, 23(4):423–431.

Yao, H., You, Z., Li, L., Goh, S. W., Lee, C. H., Yap, Y. K., and Shi, X. 2013a. Rheological properties and chemical analysis of nanoclay and carbon microfiber modified asphalt with Fourier transform infrared spectroscopy. *Construction and Building Materials*, 38:327–337.

Yao, H., You, Z., Li, L., Lee, C., Wingard, D., Yap, Y., Shi, X., and Goh, S. 2013b. Rheological Properties and Chemical Bonding of Asphalt Modified with Nanosilica. *Journal of Materials in Civil Engineering*, 25(11):1619–1630.

Yao, H., You, Z., Li, L., Lee, C. H., Wingard, D., Yap, Y. K., Shi, X., and Goh, S. W. 2012. Rheological properties and chemical bonding of asphalt modified with nanosilica. *Journal of Materials in Civil Engineering*, 25(11):1619–1630.

You, Z., Adhikari, S., and Emin Kutay, M. 2009. Dynamic modulus simulation of the asphalt concrete using the X-ray computed tomography images. *Materials and Structures*, 42(5):617–630.

You, Z., Mills-Beale, J., Foley, J. M., Roy, S., Odegard, G. M., Dai, Q., and Goh, S. W. 2011. Nanoclay-modified asphalt materials: Preparation and characterization. *Construction and Building Materials*, 25(2):1072–1078.

Zaib, Q., Khan, I. A., Yoon, Y., Flora, J. R. V., Park, Y.-G., and Saleh, N. B. 2012. Ultrasonication study for suspending single-walled carbon nanotubes in water. *Journal of nanoscience and nanotechnology*, 12(5):3909–3917.

Zhang, X., Fujishima, A., Jin, M., Emeline, A. V., and Murakami, T. 2006. Double-layered TiO2-SiO2 nanostructured films with self-cleaning and antireflective properties. *The Journal of Physical Chemistry B*, 110(50):25142–25148.

APPENDIX

Provided as an appendix is Product P1, Learning Materials to Promote Use of CNT Modified Binders.

THE UNIVERSITY OF TEXAS AT AUSTIN
CENTER FOR TRANSPORTATION RESEARCH

0-6854-P1

LEARNING MATERIALS TO PROMOTE USE OF CNT MODIFIED BINDERS

Research Supervisor:
Navid Saleh

TxDOT Project 0-6854: Engineering the Properties of Asphalt Mixtures Using Carbon Nanotubes

FEBRUARY 2017; PUBLISHED SEPTEMBER 2018

Performing Organization:	**Sponsoring Organization:**
Center for Transportation Research The University of Texas at Austin 1616 Guadalupe, Suite 4.202 Austin, Texas 78701	Texas Department of Transportation Research and Technology Implementation Office P.O. Box 5080 Austin, Texas 78763-5080
Performed in cooperation with the Texas Department of Transportation and the Federal Highway Administration.	

Helpful tips to modify asphalt binders with nanomaterials

PROJECT 6854

Organization

This learning material is organized in two parts:

PART 1: General safety considerations while handling nanomaterials

PART 2: Procedures to modify binders with nanomaterials

PART 1
General Safety Considerations

NOTE: This is an overview of safety considerations and are not intended to serve as a comprehensive safety guide. Personnel handling and using nanomaterials must carefully review the MSDS for such materials and be familiar with instructions provided by the producers of these materials before attempting to use these materials in the lab.

Overview of nanomaterials

- **Nanoparticles (NPs)**: Particles with one or more dimensions in the 1 to 100 nanometers (nm) size range.
- Include metals or metal oxides, carbonaceous materials like carbon nanotubes (CNTs), fullerenes and carbon black, silicate, organic nanoparticles or nano composites among others.
- Unique physical and chemical properties attributed to their large surface area to volume ratio.
- Increasing production and use of nanoparticles → increased number of workers and consumers exposed to nanoparticles.

Safety and handling

- The low solubility of many NMs and their tendency to agglomerate in water, air, and biological fluids may prove to be an additional hazard.
- Protective measures should be applied to control and minimize exposure (technical, organizational and personal protection measures).

Nanomaterial Exposure

- Inhalation
- Ingestion
- Skin Contact

Safety and handling

- Consideration to be given to the occupational exposure limits (OELs) for NMs and classification of hazardous NMs.
- Characteristics of the NM should be known before undertaking work, and factored into selecting PPEs and equipment:
  - Composition
  - Size
  - Morphology
  - Functionality
  - Toxicity
  - Surface area

Safety and handling

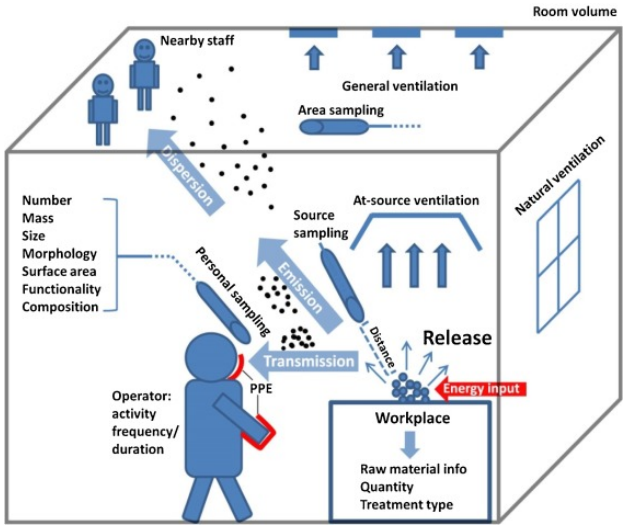

Ding, Yaobo, et al. "Airborne engineered nanomaterials in the workplace—a review of release and worker exposure during nanomaterial production and handling processes." *Journal of hazardous materials* 322 (2017): 17-28.

Safety and handling – Engineering controls

- Engineering controls, including enclosure, local exhaust ventilation (LEVs), and general ventilation are important instruments.
- Local ventilation can be assisted by general ventilation systems.
- Must be maintained regularly.
- Filtration systems to remove NMs from the exhaust air.
- Multi-stage filters having high-efficiency particulate air filter (HEPA) or ultra-low penetration air filters (ULPA).
- Transfer or mixing of NM should be conducted in a fume hood to prevent exposure to aerosolized NMs.

Safety and handling – Engineering controls

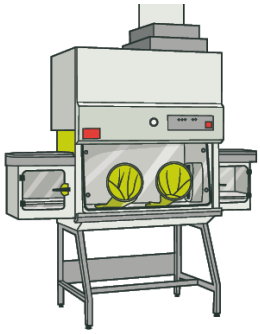

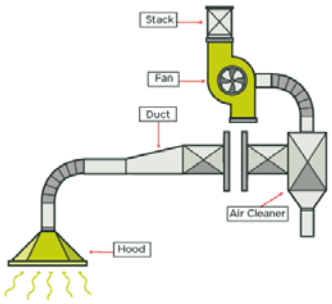

http://www.worksafe.govt.nz

Hamilton Scientific Mistral Fume Hoods

Safety and handling – Admin. and Org. controls

- Administrative controls: NM health and safety should be incorporated into the occupational safety plan.
- Appropriate NM handling training should be provided to the personnel.
- Training should address transportation, handling, spilling incidents for NMs.
- Material Safety Datasheets (MSDS) for materials selected should be referred for information on hazards and appropriate measures.
- Control banding or risk classification for assessing the risks from nanomaterials with unknown exposure levels should be considered.

Safety and handling – Admin. and Org. controls

Worker/Environmental Hazard	Release/Exposure Probability: Unlikely (1)	Low (2)	Likely(3)	Probable (4)
Very High or Unknown (D)	Control Level III	Control Level III	Control Level IV	Control Level IV
High (C)	Control Level II	Control Level II	Control Level III	Control Level IV
Medium (B)	Control Level I	Control Level I	Control Level II	Control Level III
Low (A)	Control Level I	Control Level I	Control Level I	Control Level II

Control Level	Guidelines
I	Minimum control, general area ventilation, work on a bench top
II	Work within an approved laboratory ventilation hood required; air cleaning recommended (e.g., HEPA filtration for particulates should be considered for environmental protection)
III	Containment, such as a glove box, required to prevent loss to the work environment. Particulate effluent from the glove box should be evaluated
IV	Review by a specialist required; full containment of the operation and air-cleaning devices (e.g., HEPA filtration for particulates) required on ventilation for environmental protection

Bunker, K., et al. "Evaluation of Unbound Engineered Nanoparticles from a Worker Exposure and Environmental Release Perspective." AGU Fall Meeting Abstracts. Vol. 1. 2009.

Safety and handling – PPEs

- Personal protective equipment (PPEs), including gloves, masks, and coats, are also important to minimize exposure.

- Characteristics for PPEs to be considered:
  - high filtration efficiency,
  - chemical resistance,
  - good fit,
  - easy maintenance, and
  - long wear time

Gloves and Eyewear

Lab Coat

Safety and handling – PPEs

- Non-woven materials for lab coats have been shown to be more effective against NMs.
- Double-gloving while working with small nanomaterials is recommended.
- Safety goggles may be more appropriate as eyewear while aerosolized NMs.
- Risk of aerosolizing NMs should be minimized where possible.
  - Inhalation being a major route for unwanted exposure, airborne NMs more likely to pose health risk.
  - Use of PPEs and wet wiping while weighing dry nano-powders and sanitization of nanomaterials in open containers recommended.

Safety and handling – Summary

Identify

- Understand likely exposure and efficacy of protective measures utilized.
- Consider the composition, physico-chemical characteristics and toxicity level.

Assess Risk

- Risk assessment to be based on current state of knowledge of toxicity and exposure pathways.

Train and Plan

- Train personnel, identify practical handling guidelines handling NMs in the workplace.
- Select appropriate PPE and safe transportation/transfer measures.
- Prevent inhalation exposure - use respirators, fume hoods and glove boxes in conjunction with general exhaust ventilation.
- Label work areas, indicate hazards, work procedures and PPEs required.

PART 2
Modifying Binders

NOTE: Methods to evaluate modified binder are not unique to nanomaterial modified binders; current standards and methods can be used.

Carriers and mixing models

NMs can be delivered or incorporated in different carriers or mixed directly in dry state; following are potential carriers and limitations

- Water (generally not recommended):
  - NMs dispersed in water cannot be added to hot or warm mix asphalt
  - The only exception to above is warm mix asphalt produced using foaming in which can the water+NM concentrate can be added to the foaming agent
  - When used as a foaming agent the NM concentration in the binder cannot be more than 0.1 to 0.2% (water is generally 2% w/w of binder and this would imply the NM be about 10% w/w in water); the NMs in this study did not meet performance requirements at such low concentrations
  - It may be possible to use NMs with water as a carrier in asphalt emulsions used in the production of cold asphalt mixes

Carriers and mixing models

NMs can be delivered or incorporated in different carriers or mixed directly in dry state; following are potential carriers and limitations

- Kerosene (not recommended):
  - Kerosene can serve as a good carrier for NMs but it is not recommended due to low flash point temperature, safety and environmental considerations
- Flux oil (generally not recommended):
  - NMs can be effectively dispersed in flux oil and used as a carrier
  - Flux oil is generally not recommended for use as a carrier; based on the NMs used in this study the softening due to flux oil did not offset the beneficial affects of using NMs

Carriers and mixing models

NMs can be delivered or incorporated in different carriers or mixed directly in dry state; following are potential carriers and limitations

- Direct mixing / no carrier (recommended):
  - This involves directly mixing the NMs in the asphalt binder at elevated temperatures (150 to 160 °C)
  - Direct dispersion of the nanoparticles in the binder was deemed to be the most practical, cost effective, and safe approach (with safe handling and use of proper and safe equipment)

Nanomaterial Asphalt Binder

Mixing

1. Determine the NM and weight concentration to be used to modify the asphalt binder.
2. Weigh the required amount of nanomaterial using a scale taking into consideration safety and appropriate handling procedures. The weight of nanomaterial used is a percentage by weight of asphalt binder (typically 300 g of binder for binder testing)

Mixing

3. Heat 300 grams of asphalt binder inside a quart gallon can at 150 °C using a conventional oven. The time required is the sufficient time to make workable the asphalt binder in the mixing process.

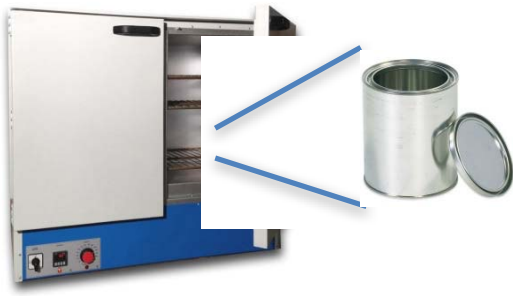

Mixing

4. Add the appropriate amount of nanomaterial (% wt) into the can with hot asphalt binder. Take into consideration safety and handling procedures.
5. Start mixing under a fume hood using a high shear mixer at 2,400 rpm for two hours. Use a heating mantle to maintain a constant temperature of 150 °C during mixing.

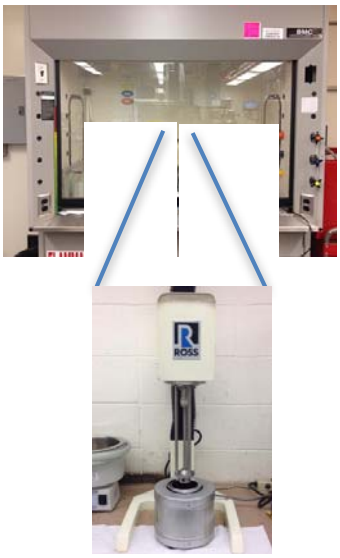

Mixing

6. Ensure that the target mixing temperature is maintained during the blending and dispersion for the two hour duration.
7. After two hours, remove the mixer blade from the can containing the asphalt binder blended with the nanomaterial.

Mixing

8. Take into consideration safety and handling procedures to remove the can from the heating mantle and let the material cool.
9. The NM modified binder can now be used with any typical binder or mixture tests.
10. The binder must not be subsequently subjected to solvent extraction without appropriate precautions.